PUBLIC HEALTH-RELATED IMPACTS OF CLIMATE CHANGE

DRAFT

A Report From:
California Climate Change Center

Prepared By:
Deborah M. Dreschler and Nehzat Motallebi,
California Air Resources Board

Michael Kleeman, University of California, Davis

Dan Cayan, Scripps Institution of Oceanography, UC San Diego

Katharine Hayhoe[1,2], Laurence S. Kalkstein[4], Norman Miller[3], Scott Sheridan[5], and Jiming Jin[3]

[1]Dept. of Geosciences, Texas Tech University, Lubbock, Texas; [2]ATMOS Research and Consulting, Lubbock, Texas; [3]Atmosphere and Ocean Sciences Group, Earth Sciences Division, Lawrence Berkeley National Laboratory, California; [4]Center for Climatic Research, Dept. of Geography, University of Delaware, Delaware; [5] Dept. of Geography, Kent State University, Ohio.

R. Tony VanCuren, California Air Resources Board

WHITE PAPER

Arnold Schwarzenegger, *Governor*

December 2005
CEC-500-2005-197-SD

Acknowledgements

The authors wish to acknowledge the following for their contributions to this report: Mimi Sogutlugi and Jonathan Taylor for running the emission computer model-EMFAC; Dr. Eileen McCauley, Doug Thompson , Larry Hunsaker, and Hector Maldonado for review of the report; and Mary Tyree (UCSD), Martha Coakley (UCSD), and Josh Schriffin (UCSD) for their development of the GCM statistical downscaling method.

Preface

The Public Interest Energy Research (PIER) Program supports public interest energy research and development that will help improve the quality of life in California by bringing environmentally safe, affordable, and reliable energy services and products to the marketplace.

The PIER Program, managed by the California Energy Commission (Energy Commission), annually awards up to $62 million to conduct the most promising public interest energy research by partnering with Research, Development, and Demonstration (RD&D) organizations, including individuals, businesses, utilities, and public or private research institutions.

PIER funding efforts are focused on the following RD&D program areas:

- Buildings End-Use Energy Efficiency
- Energy-Related Environmental Research
- Energy Systems Integration
- Environmentally Preferred Advanced Generation
- Industrial/Agricultural/Water End-Use Energy Efficiency
- Renewable Energy Technologies

The California Climate Change Center (CCCC) is sponsored by the PIER program and coordinated by its Energy-Related Environmental Research area. The Center is managed by the California Energy Commission, Scripps Institution of Oceanography at the University of California at San Diego, and the University of California at Berkeley. The Scripps Institution of Oceanography conducts and administers research on climate change detection, analysis, and modeling; and the University of California at Berkeley conducts and administers research on economic analyses and policy issues. The Center also supports the Global Climate Change Grant Program, which offers competitive solicitations for climate research.

The California Climate Change Center Report Series details ongoing Center-sponsored research. As interim project results, these reports receive minimal editing, and the information contained in these reports may change; authors should be contacted for the most recent project results. By providing ready access to this timely research, the Center seeks to inform the public and expand dissemination of climate change information; thereby leveraging collaborative efforts and increasing the benefits of this research to California's citizens, environment, and economy.

For more information on the PIER Program, please visit the Energy Commission's website at www.energy.ca.gov/pier/ or contact the Energy Commission at (916) 654-5164.

Table of Contents

List of Figures

List of Tables

Abstract

Summer temperatures in California under scenarios of future climate change are projected to increase by 2° to 7°C, depending on the emission scenario used and the sensitivity of the climate model. Increases will be accompanied by longer, more frequent, and more severe extreme heat conditions. These increases are expected to affect human health through both indirect effects on air pollution and direct effects on heat-related mortality. Here, we analyze the potential impacts of rising temperature on California heat and heat-related mortality based on projections from three atmosphere-ocean general circulation models (AOGCMs)—HadCM3, GFDL (no mortality estimates), and PCM—forced with the IPCC SRES with higher (A1fi), mid-high (A2), and lower (B1) emission scenarios.

Both mean seasonal and 90th percentile temperatures indicate consistent increases in summer heat, both statewide and for five urban centers (Los Angeles, Sacramento, Fresno, San Francisco, and San Bernardino). Proportionally larger increases are projected for the currently more moderate coastal cities in comparison with inland cities. By end-of-century, increases in extreme heat are 2 to 2.5 times greater than the 1971–2000 average under the B1 scenario, and 2.5 to 4 times greater under the higher A1fi/A2 scenarios.

For an increasingly urbanized population, extreme heat waves create a significant risk of adverse health effects and heat-related mortality. Using observed correlations between apparent temperature thresholds and heat-related excessive mortality for each of the five cities, we next estimate the projected change in heat-related mortality for each urban center. The largest increases in absolute values as well as the largest proportional increases (when acclimatization is taken into account) are projected for Los Angeles, where end-of-century acclimatized mortality is projected to increase by 3 times under B1 and 4-8 times under A1fi/A2. San Bernardino shows similar increases to Los Angeles, but efficient acclimatization by inland cities (Sacramento, Fresno) lowers their projected increases significantly. For Sacramento, a 40% reduction in projected mortality due to acclimatization reduces projected increases to 2.75 times historical values for B1 and 3 to 4 times under A1fi/A2. The benefits of acclimatization are even stronger for Fresno, where historical response to hot summers suggests a net reduction in heat-related mortality by end-of-century, even under the A1fi/A2 scenarios, on the order of 5% to 30% when acclimatization is included. In general, the inland population appears less susceptible to heat than those of coastal cities, and acclimatization also appears to be more effective. Similar to extreme heat, projected changes in heat-related mortality also display significant inter-scenario differences, although the influence of the coastal/inland gradient is stronger here due to the characteristics of the populations in those regions.

Californians experience the worst air quality in the nation, with annual health and economic impacts estimated at 7000 deaths and $50 billion per year. Ozone and particulate matter (PM) are the pollutants of greatest concern (maximum levels are about double California's air quality standards), and the current control programs for motor vehicles and industrial sources cost about $10 billion per year. Two recent reports from the National Research Council of the National Academies (NRC 2001, 2004) note that climate change could exacerbate air pollution. In general, the findings from this study support this conclusion, but public health impacts related to air pollution are difficult to predict for several reasons.

Higher temperature will increase the rate at which atmospheric chemical reactions proceed, thereby increasing concentrations of ozone and particulate matter (PM) precursors, but more nitrate (a major component of $PM_{2.5}$) will volatilize. In addition, the analysis indicates that other factors that affect air pollutant levels—such as relative humidity, wind speed, and mixing height—could also change in response to climate change and interact with the temperature effects. The analysis indicates that changes in the concentrations of ozone and PM are unlikely to be uniform across an air basin, and will have a differential effect on the populace. In addition, climate change occurs in the context of the faster time scale of emission control efforts to attain the ambient air quality standards for ozone and PM. Consequently, the magnitude of health impacts attributable to ozone and PM in the future will be proportional to the degree to which ambient air quality standards are not attained.

The number of days meteorologically conducive to pollution formation may rise by 75%–85% in the high ozone areas of Los Angeles (Riverside) and the San Joaquin Valley (Visalia) by the end of the century under a medium-high emissions/temperature scenario (A2), but only 25%–35% under the lower emissions/temperature path (B1). In addition, global background ozone (primarily formed from the greenhouse gas methane and nitrogen oxides from fuel combustion) is projected to increase by 4%–10% (low scenario) to 25% (high scenario) at 2100. If the latter were to occur, the ozone targets would be impossible to attain in much of California, even with near-zero local emissions. The future trend for PM is not as clear—particles are reduced by increasing temperature but also affected by rainy days, wildfires, global dust storms, humidity, and other factors—and is the subject of ongoing study.

Existing air pollution control programs do not consider the impact of climate change even though it could slow progress toward attainment of the ambient air quality standards and increase control costs by boosting emissions, accelerating chemical processes, and raising inversion temperatures during summertime stagnation episodes. The NRC (2004) recommended that "the air quality management system will need to ensure that pollution reduction strategies remain effective as the climate changes, because some forms of air pollution, such as ground-level ozone, might be exacerbated." Air pollution control agencies should build climate change considerations, which are expected to be significant for at least ozone, into efforts to attain the health-based ambient air quality standards.

In addition to temperature, climate change may also alter historical rainfall patterns, although future trends for California are inconclusive. If altered rainfall patterns could lead to an increased number of instances where water and sewage treatment facilities fail, exposing the public to contaminated water. It is not possible to forecast the likely incidence of resulting diseases. Outbreaks of waterborne illness are related to complex interactions between the water contamination potential of discrete rainfall events, the capabilities of water and sewage treatment facilities, the effectiveness of public health programs designed to minimize exposure of the public to contaminated water, and the public's compliance with these programs and recommendations.

Mosquitoes and vector-borne diseases appear to be temperature sensitive. However, transmission and maturation of the viruses depend on many factors in addition to ambient temperature, including the specific organism, and the interaction of the various aspects of climate change (temperature, humidity, rainfall) on the ecology, development, behavior, and

survival of both the organism and its host. Consequently, rising temperature may or may not increase the rate of transmission of these diseases, depending on the outcome of interactions between aspects of climate, the organism itself, the insect host, the effectiveness of vector control programs, and the public's compliance with recommended protective behaviors, such as staying indoors during times of greatest mosquito activity, and use of insect repellent. The small number of cases of vector-borne diseases reported in California is likely related to the effectiveness of state and county surveillance and control programs.

Our review suggests that fire smoke can increase various indices of public health, including mortality, hospitalization, emergency room visits, and respiratory symptoms, in a manner and magnitude similar to that reported for PM_{10} and $PM_{2.5}$. However, the actual magnitude of future fire impacts cannot be estimated due to the unique nature of each fire, and the necessity that the smoke plume cover an inhabited area. The literature consistently suggests that the people most at risk are those with existing cardiopulmonary disease, and that risk seems to increase with advancing age. In addition, the literature suggests that in terms of actual number of cases, wildfire impacts are likely to be modest.

It is clear that those living in poverty and in inner city areas will need greater assistance than other segments of the community in coping with various potential impacts associated with climate change. The particular vulnerabilities of environmental justice communities will require consideration in developing mitigation and adaptation actions. Although there will be costs involved, the literature suggests that the most effective adaptation would be to ensure that all housing units have functional air conditioners. This measure will reduce risk of not only heat-related mortality, but also exposure to air pollution and vector-borne diseases. In addition, means to assist the poor with increased electricity costs will be required to ensure that the benefit of this intervention accrues to this segment of the population. Communities should also consider developing protocols for distribution of bottled water to disadvantaged areas to minimize human illness in the event of water contamination events.

1.0 Introduction

Considerable evidence suggests that the average ambient temperature is increasing worldwide, that temperatures will continue to increase into the future, and that global warming will result in changes to many aspects of climate, including temperature, humidity, and precipitation. It is expected that California will experience changes in both temperature and precipitation under current trends. Many of the changes in climate projected for California could have ramifications for public health (IPCC 2001), and this document summarizes the most likely impacts, including mortality and morbidity related to temperature, air pollution, vector and waterborne diseases, and wildfires. Where possible, estimates of the magnitude and significance of these impacts are also discussed, along with possible adaptations that could reduce climate-related health impacts.

In the context of this review, weather refers to meteorological conditions at a specific place and time over a relatively short time frame, such as up to a year or two. Climate, on the other hand, refers to the same meteorological conditions, but over a longer time frame, such as decades or centuries.

2.0 Heat-Related Effects

It is well known that extreme temperatures, both high and low, increase the risk of death. Annually in the United States, an average of about 400 deaths are directly attributable to heat (CDC 2001, 2005b), and an average of nearly 700 deaths are directly attributable to cold (CDC 2005a). There has been a decline in the number of deaths attributed to heat and cold over the past 30 years (Davis et al. 2003a,b; CDC 2005a,b; Donaldson et al. 2003), primarily due to the increasing number of households with central heating and air conditioning. Results from analyses of various global climate change scenarios suggest that the future is likely to have fewer extremely cold days and a greater number of extremely hot days. Consequently, looking forward, heat-related mortality is a public health impact of great concern.

Analyses of temperature-related mortality are complicated by the fact that there is no uniform standard for classifying temperature-related deaths, and while ambient temperature may contribute to death, it is not always listed on the death certificate as causing or contributing to death (Basu and Samet 2002). Some investigators believe that temperature-related deaths are underreported, based on analyses of observed deaths during high- and low-temperature periods compared to the number expected during a similar time period not impacted by either high or low temperatures (Mirabelli and Richardson 2005; Basu and Samet 2002). However, the results of these statistical analyses are rarely validated against observed cases.

While both high and low temperatures can be direct causes of death, as noted above, the annual number of cases directly attributable to temperature in the United States is small and has declined since the late 1970s (Davis et al. 2003a,b; CD 2005a,b; Donaldson et al. 2003). Analyses of deaths and their relationship to ambient temperature have consistently reported that deaths from preexisting cardiovascular and respiratory diseases increase with both low and high temperatures, and mainly in the elderly (Kunst et al. 1993; Basu and Samet 2002). This is likely related to age- and disease-related impairment of thermoregulatory capacity in this population (Basu et al. 2004). Thermoregulation is also adversely affected by some common medications used to treat cardiovascular disease and mental health disorders, increasing the risk of adverse outcomes in these populations (CDC 2002; Kaiser et al. 2001), and there is evidence that medications in these classes increase risk of temperature-related mortality.

Identified risk factors for both heat- and cold-related death include age above 65 years, chronic cardiovascular or respiratory disease, mental impairment, substance abuse, lack of air conditioning or heating, poverty, and residence in an urban area (CDC 2005a,b; Kilbourne 2002; Kaiser et al. 2001). Lower socioeconomic status has also been identified as a risk factor for temperature-related mortality (O'Neill et al. 2003; Curriero et al. 2002; Michelozzi et al. 2005). Other identified risk factors for temperature-related include social isolation, not leaving the home daily, and for heat-related mortality, living on the upper floors of multistory buildings (Naughton et al. 2002).

2.1. Shape of the Temperature-Mortality CR Function

In many geographical areas there appears to be a threshold temperature range above and below which heat- and cold-related mortality, respectively, increase. This results in a "J" or

"U" shaped relationship between temperature and mortality, although the threshold temperature and the steepness of the slopes of both tails of the regional functions vary according to the region's typical temperature pattern (Curriero et al. 2002; Kunst et al. 1993; Davis et al, 2003; Kysely 2004). Threshold temperature varies by latitude and is influenced by local climate conditions (Curriero et al., 2002; Keatinge et al., 2005; Donaldson et al. 2003; McGeehin and Mirabelli 2001). For example, the threshold temperature for increased heat-related mortality is lower in the central and northern United States, compared to the southeastern part of the country, meaning that high heat days have less impact in the hotter southeastern United States than in parts of the country that more rarely have high temperatures (Curriero et al. 2002; Basu and Samet 2002; Donaldson et al. 2002). Similarly, cold weather has a lesser effect in parts of the country that frequently have cold weather (Curriero et al. 2002; Keatinge et al. 2000). This is thought to be related to physiological, social, and behavioral adaptation by populations (Keatinge et al. 2005; Donaldson et al. 2003). However, Kovats et al. (2004) found that the relationship between temperature and hospitalizations, and temperature and mortality are not parallel.

Curriero et al. (2002) found that an increase in cold weather mortality is evident within three days of the onset of a period of extreme cold, and within one day of the onset of a period of extreme heat. Kunst et al. (1993) reported that a large portion of cold-related mortality occurred within one week of the onset of a cold snap, and that heat-related mortality was associated with high temperature on the same day, and the following two days, in agreement with Michelozzi et al. (2005). These results suggest that temperature-related mortality is principally related to temperatures either on the day of death, or within a few days preceding death. In addition, mortality is greater for heat waves early in the summer, compared to later in the season, suggesting biological adaptation (Kysley 2004). Several studies (Kunst et al. 1993; Kalkstein et al. 1997; Kysely 2004) point to harvesting, suggested by a reduced death rate in days following an extreme temperature event. This suggests that a portion of those most vulnerable to temperature-related mortality were already near the end of life, and that the amount of life lost was relatively small.

2.2. Relation to Air Pollution

Ambient concentrations of both ozone and PM are affected by ambient temperature, humidity, and precipitation (Bernard et al. 2001; CARB 2005). Since ambient temperature, ozone, and PM all affect public health, there is concern as to whether ambient temperature and air pollution interact in their effects, and whether or not their individual effects can be separated. A review by Basu and Samet (2002) of epidemiologic studies investigating the relationship between air pollutants, temperature, and mortality concluded that results were conflicting, and that it was uncertain whether air pollutants were confounders, effect modifiers, or whether they had no effect with temperature. However, the majority of epidemiologic studies of air pollution include controls for temperature, thus to the extent these controls are successful, confounding between temperature and air pollution should be minimal. Keatinge and Donaldson (2001) found that cold-related mortality in London was not related to concurrent patterns in ambient sulfur dioxide, carbon monoxide, or smoke (surrogate for PM).

During the summer of 2003, Europe was impacted by a severe heat wave that persisted for two weeks. Fischer et al. (2004) and Stedman (2004) estimated the contribution of air pollution to heat mortality for the Netherlands and the United Kingdom, respectively. Both analyses were based on statistical modeling using existing concentration response functions relating air pollution to mortality, and concluded that a larger number of deaths were related to air pollution, and fewer to heat, than previous analyses had reported. Unfortunately, both analyses were based on statistical estimations of past and future mortality, and neither was validated against actual mortality data. In addition, both the Netherlands and the United Kingdom rarely have elevated temperatures. Consequently, the local populations would be more vulnerable to heat due to lack of physiological adaptation, as well as lack of adaptive infrastructure, such as availability of air conditioning and heat emergency plans. Although the relevance of these results to the considerably different climate of California is uncertain, the results suggest that future studies should more carefully investigate the relative contribution of air pollution in studies of temperature-related mortality.

2.3. Analysis of Climate Impacts on Extreme Heat and Heat-Related Mortality in California

2.3.1. Introduction

As global temperatures rise, California will also experience increases in mean, daytime, and nighttime temperatures. Increases in the frequency, intensity and duration of extreme heat events are expected, with a greater number of consecutive hot days. Higher temperatures, particularly in summer months, will strain many of California's resources, including its electricity supply for industrial and residential cooling. Extreme heat and oppressive heat events are also known to impact human health and result in heat-related mortality (Martens 1998; McGeehin and Mirabelli 2001; Schär et al. 2004; McMichael et al. 2001). In particular, summer mortality from extreme heat and extended heat events is expected to rise—spatial, intra-seasonal, socioeconomic, behavioral, and physiological acclimatization notwithstanding.

With several large metropolitan centers, California is now home to 34.5 million people (U.S. Census Bureau 2001)—more than 200 per square mile—and its population is projected to double within the next 30 years, as well as becoming more and more urbanized. Prior studies have estimated heat-related mortality for California metropolitan areas (Chestnut et al. 1998; Kalkstein 1987, 1989, 1993; Kalkstein and Valimont 1986; Oechsli et al. 1976), using different methods with a range of theoretical foundations, including empirical observation, modeling based on temperature thresholds, heat stress indices, and synoptic methods identifying "offensive air masses." Synoptic approaches have revealed that California locations historically have experienced relatively few "offensive air mass" conditions, which cause marked increases in heat-related mortality (Kalkstein and Greene, 1997). This may be one of the reasons why California has yet to invest in the heat-watch-warning systems currently operational in many cities in other parts of the United States.

Table 1. Heat-related mortality projections for the 1990s, 2050s and 2090s for five California cities, as calculated by Hayhoe et al. (2004).

	1990s	2050s		2090s	
	Acc	UnAcc	Acc	UnAcc	Acc
Los Angeles					
Actual	165	-	-	-	-
PCM B1	158	357	304	394	319
PCM A1	158	818	719	948	790
Had B1	153	351	275	667	551
Had A1	153	432	339	1429	1182
San Francisco					
Actual	41	-	-	-	-
PCM B1	35	84	84	134	134
PCM A1	35	146	146	447	447
Had B1	39	92	92	153	153
Had A1	38	75	75	271	271
San Bernardino/Riverside					
Actual	32	-	-	-	-
PCM B1	28	50	50	83	83
PCM A1	28	57	57	104	104
Had B1	28	60	60	82	82
Had A1	33	73	73	135	129
Sacramento					
Actual	10	-	-	-	-
PCM B1	14	18	11	29	17
PCM A1	14	25	15	86	52
Had B1	15	43	26	51	31
Had A1	25	42	25	148	89
Fresno					
Actual	13	-	-	-	-
PCM B1	10	19	5	30	7
PCM A1	10	26	6	72	17
Had B1	12	14	4	18	5
Had A1	14	42	10	74	18

Only three studies to date have modeled excess heat-related mortality under various climate change projections. Two of these used older models and now-outdated emissions scenarios

for selected California metropolitan areas, rendering the compatibility of their results with this study questionable. However, for completeness we summarize them here. Projected increases in mortality for Los Angeles and San Francisco for a study using the GISS model (Kalkstein and Valimont 1987; Kalkstein 1993) were found to vary substantially with the climate scenario and degree of acclimatization (no, partial, or full acclimatization). Resulting mortality figures for Los Angeles, for example, varied between a 100% decrease and a 20-fold increase. The second study used three climate models (GFDL89, UKMO, and ECHAM; Kalkstein 1989) run out to 2050 on unspecified "business-as-usual" emissions scenarios and assuming full acclimatization. Mortality rates varied between a 35% decrease and a 275% increase by 2050 (relative to 1997 rates for various California cities).

In Hayhoe et al. (2004), we first estimated the impact of projected changes in temperature and humidity—as simulated by the HadCM3 and PCM models for the SRES A1fi (higher) and B1 (lower) emission scenarios—on the frequency of oppressive heat events that have demonstrated historical correlations with elevated mortality rates. This was done for five urban centers in California: Los Angeles, San Francisco, San Bernardino/Riverside, Fresno, and Sacramento. We then estimated the impact of projected changes in temperature and humidity on heat-related deaths that would occur in these five major urban centers. As shown in Table 1, these results indicated large increases in unacclimatized heat-related mortality, smaller increases in acclimatized mortality estimates, and significant inter-scenario differences and coastal/inland distinctions. Although increases in the frequency and severity of extreme heat and heat wave events were found to be greater inland relative to coastal cities, when the potential for acclimatization was included, inland populations (Sacramento, Fresno) demonstrated a greater ability to cope with the projected increases than those of coastal cities (Los Angeles, San Francisco). This outcome is similar to many other hot, semi-arid cities such as Phoenix, Arizona, where the population and general urban structure are already well adapted to frequent and extreme heat (Kalkstein, 2003). Finally, the results for San Bernardino/Riverside surprisingly indicated no potential for acclimatization based on current-day population response to extreme heat. Explanations for this result are currently being investigated, including taking greater account of socioeconomic factors (such as the penetration of air conditioning and the housing stock) that might explain these non-intuitive results.

Here we expand upon the heat-mortality analysis from Hayhoe et al. (2004), the results of which are shown in Table 1, to calculate projected changes in mean daily maximum and minimum summer temperatures, 90th percentile temperature exceedances, and the frequency and intensity of oppressive heat events that display historical correlations with heat-related mortality for 2035–2065 and 2070–2099 relative to 1971–2000 for the same five California urban centers (Los Angeles, San Francisco, San Bernardino/ Riverside, Fresno, and Sacramento). Heat projections are now based on simulations from three atmosphere-ocean general circulation models: the HadCM3, PCM and GFDL2.1 models, and for three of the SRES scenarios: A1fi (higher), A2 (mid-high), and B1 (lower) emission scenarios. Mortality estimates are based on HadCM3 and PCM only. Heat-related mortality estimates are determined by projections of threshold meteorological conditions for each city beyond which mean mortality has been observed to display a statistically significant increase. Estimates of heat-related mortality are produced for two cases: first, assuming no acclimatization by the population to extreme heat, and second, assuming acclimatization

occurs as estimated by the procedures outlined in Section 2.4 of this report. Estimates do not account for changes in population or demographic structure. Since the procedures will be parallel, the mortality estimates from this study are directly comparable to those given in Table 1 from Hayhoe et al. (2004).

2.3.2. Climate Data

In this study, we analyze the onset, occurrence, persistence, and intensity of extreme heat for all of California as well as for five urban centers based on historical observations, historical model simulations, and future climate projections. This analysis is based on simulations from three atmosphere-ocean general circulation models (AOGCMs), the UKMO HadCM3 (Pope et al. 2000), NOAA/GFDL CM2.1 (Delworth et al., 2005), and the DOE/NCAR PCM (Washington et al. 2000), with simulations forced by the *IPCC Special Report on Emission Scenarios* (SRES, Nakićenović et al. 2000) higher (A1fi), mid-high (A2), and lower (B1) emissions scenarios. These scenarios describe internally consistent pathways of future societal development and corresponding greenhouse gas emissions. The SRES scenarios are not assigned probabilities, but rather can be viewed as plausible futures, with the actual path dependent on technological development as well as the collective choices and political decisions society will make during this century. At the higher end (A1fi), rapid expansion of technologies, extensive economic globalization, and a fossil-intensive energy path cause CO_2 emissions to climb throughout the century, reaching almost 30 gigatons of carbon per year (GtC/yr) or six times 1990 levels by 2100 (Houghton et al. 2001). The A2 scenario describes a very heterogeneous world where economic development is regionally oriented and economic growth and technological change are relatively slow. Its emissions also reach ~30 Gt/yr by 2100, but since it follows a very different pathway than A1fi, global temperature projections are approximately 25% lower. Emissions under the B1 scenario are the lowest of the SRES family, based on a world that transitions relatively rapidly to service and information economies. CO_2 emissions in the B1 scenario peak at just below 10 Gt/yr (around two times 1990 levels) at mid-century and decline slowly to below current-day levels by the end of the century. These scenarios represent the range of IPCC non-intervention emissions futures with atmospheric CO_2 concentrations reaching approximately 550 ppm (B1), 830 ppm (A2) and 970 ppm (A1fi) by 2100.

AOGCM projections of changes in mean daily temperature are used directly for an analysis of California trends statewide, and are statistically downscaled with matching historical temperature distributions for five urban centers (Los Angeles, Sacramento, Fresno, San Francisco, and San Bernardino) using monthly regression relations. This station-level downscaling employs a deterministic method in which grid-cell values of temperatures and precipitation from the reference period are rescaled by simple monthly regression relations, thus ensuring that the overall probability distributions of the simulated daily values closely approximate the observed probability distributions at selected long-term weather stations (Dettinger et al. 2004). The same regression relations are then applied to future simulations, such that rescaled values share the weather statistics observed at the selected stations. At the daily scales addressed by this method, the need to extrapolate beyond the range of the historically observed parts of the probability distributions is rare, even in the future simulations (typically, less than one percent of the future days), because most of the climate changes involve more frequent warm days than actual warmer-than-ever-observed days.

2.3.3. Projected Changes in Mean and Extreme Temperatures

Across California, summer (May–September) daily maximum temperatures are projected to increase by 1.2°–4.2°C by 2035–2065 relative to 1971–2000, with slightly higher increases for the higher emissions scenarios (A1fi, A2) and more sensitive models (HadCM3, GFDL2.1). By end-of-century (2070–2099), the difference between emission scenarios and model sensitivity becomes more pronounced, with increases of 3.8°–7.1°C projected under the higher A1fi scenario, 2.6°–6.2°C under the mid-high A2 scenario, and 1.8°–4.2°C under the lower B1 scenario (Table 2; see also Figure 1).

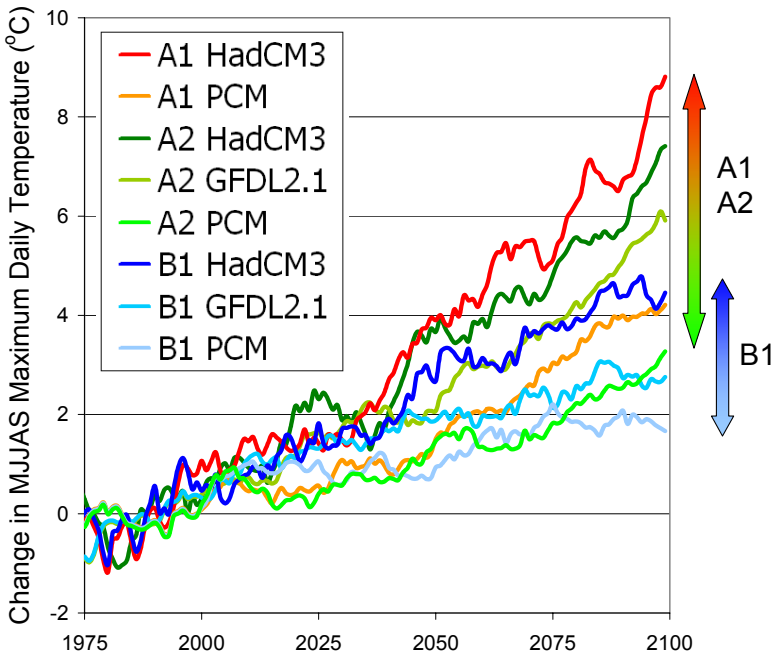

Figure 1. Projected increase in summer (May-Sept) daily maximum temperatures relative to 1971-2000 mean for the HadCM3, GFDL2.1 and PCM models as simulated for the A1fi (higher), A2 (mid-high) and B1 (lower) scenarios. 10-year running mean is shown.

Projected changes in the daily temperature range—the difference between daytime maximum temperatures and nighttime minimum temperatures – are more difficult to discern, with model sensitivity playing a greater role than emission scenario in determining the magnitude of the change. By 2070–2099, however, seven out of eight model/scenario combinations show increases in the daily temperature range. The largest increases are for the more sensitive HadCM3 model, with slightly lower increases for GFDL2.1 and little change for PCM (Table 2; also Figure 2). Overall, these results suggest that daytime temperatures will rise more quickly than nighttime temperatures, further increasing the risk of extreme heat.

Table 2. Projected increase in summer (May-Sept) daily maximum temperatures and daily temperature range for 2035-2064 and 2070-2099 relative to 1971-2000 mean for the HadCM3, GFDL2.1 and PCM models as simulated for the A1fi (higher), A2 (mid-high) and B1 (lower) scenarios.

	A1fi		A2			B1		
	HAD	PCM	HAD	GFDL	PCM	HAD	GFDL	PCM
Maximum Daily Temperature								
2035-2064	4.2	1.7	3.6	2.6	1.3	2.8	2.1	1.2
2070-2099	7.1	3.8	6.2	5.2	2.6	4.2	2.8	1.8
Daily Temperature Range								
2035-2064	0.62	-0.10	0.67	0.33	-0.16	0.71	0.09	-0.03
2070-2099	0.15	0.07	0.57	0.43	-0.11	0.79	0.29	0.13

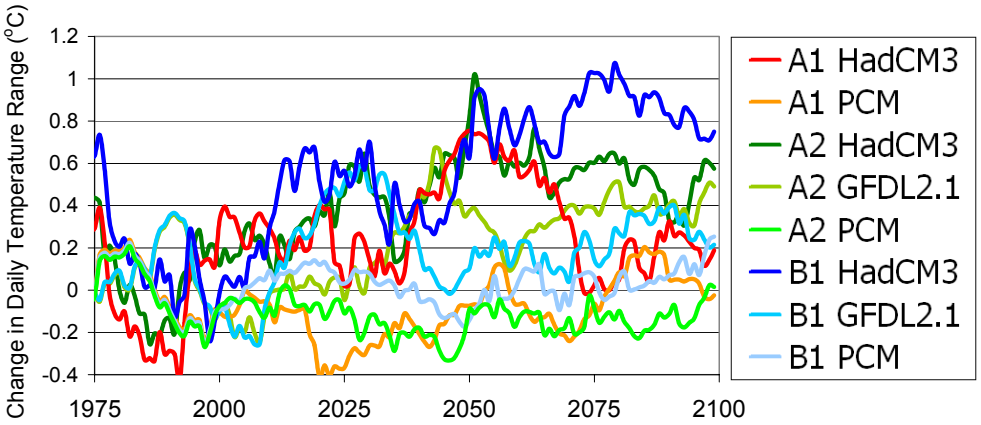

Figure 2. Projected change in summer (May-Sept) daily temperature range relative to 1971-2000 for the HadCM3, GFDL2.1 and PCM models as simulated for the A1fi (higher), A2 (mid-high) and B1 (lower) scenarios. 15-year running mean is shown.

Additional analyses of climate change projections for the coming century indicate that extreme heat conditions are also likely to increase. Extreme heat intensity and duration are calculated here as the days above the climatological (1961–1990) 90th percentile (T90) for each location. The mean-daily T90 is an important metric used in California energy capacity analyses and is often described as the 1-in-10 JJAS (June, July, August, September) high temperatures. Statewide, the number of days per year over the current-day T90 threshold (which currently averages ~6 weeks) is projected to increase by approximately an additional 4–6 weeks under B1, and up to 9–13 weeks per year under A2 or A1fi.

Further analysis of statewide climate change projections for the coming century also indicates that all models and scenarios show a consistent trend in JJAS T90 events towards more intense, longer-lasting events that occur earlier in the season relative to the historical reference period (1961–1990). Figure 3 shows a JJAS time series of the average number of T90 exceedance events, duration (days), and intensity (°C-days, denoted by the color of the bar), for GFDL, PCM, and HadCM3–based temperature projections for the A1fi, A2, and B1 emission scenarios. This figure presents two important results. First, the average duration of T90 events (meaning more prolonged heat with less of a break in between) is projected to increase from its current-day range of ~10–30 days up to 25–40 days—in other words, from a few weeks to over a month, with the potential for reduced variability (i.e., less of a range and more consistently long events). This increase is seen across all models and scenarios, with the increase being slightly larger (30-40 days) under the A1fi scenario relative to A2 or B1. The 1960–2000 average intensity, which ranges between 10–50°C-days (denoted by green), increases to 50–150°C-days by 2050, and by 2100, lies between 130–20°C-days for all but the less sensitive PCM model (Figure 3). Increase in intensity is affected by the sensitivity of the model, with the more sensitive GFDL and HadCM3 models showing the larger change (most events > 170°C-days by 2080) and PCM showing a lesser change. For any given model, however, the higher-emission-scenario simulations tend to show more intense and longer events than for the lower-emission-scenario simulations from the same model.

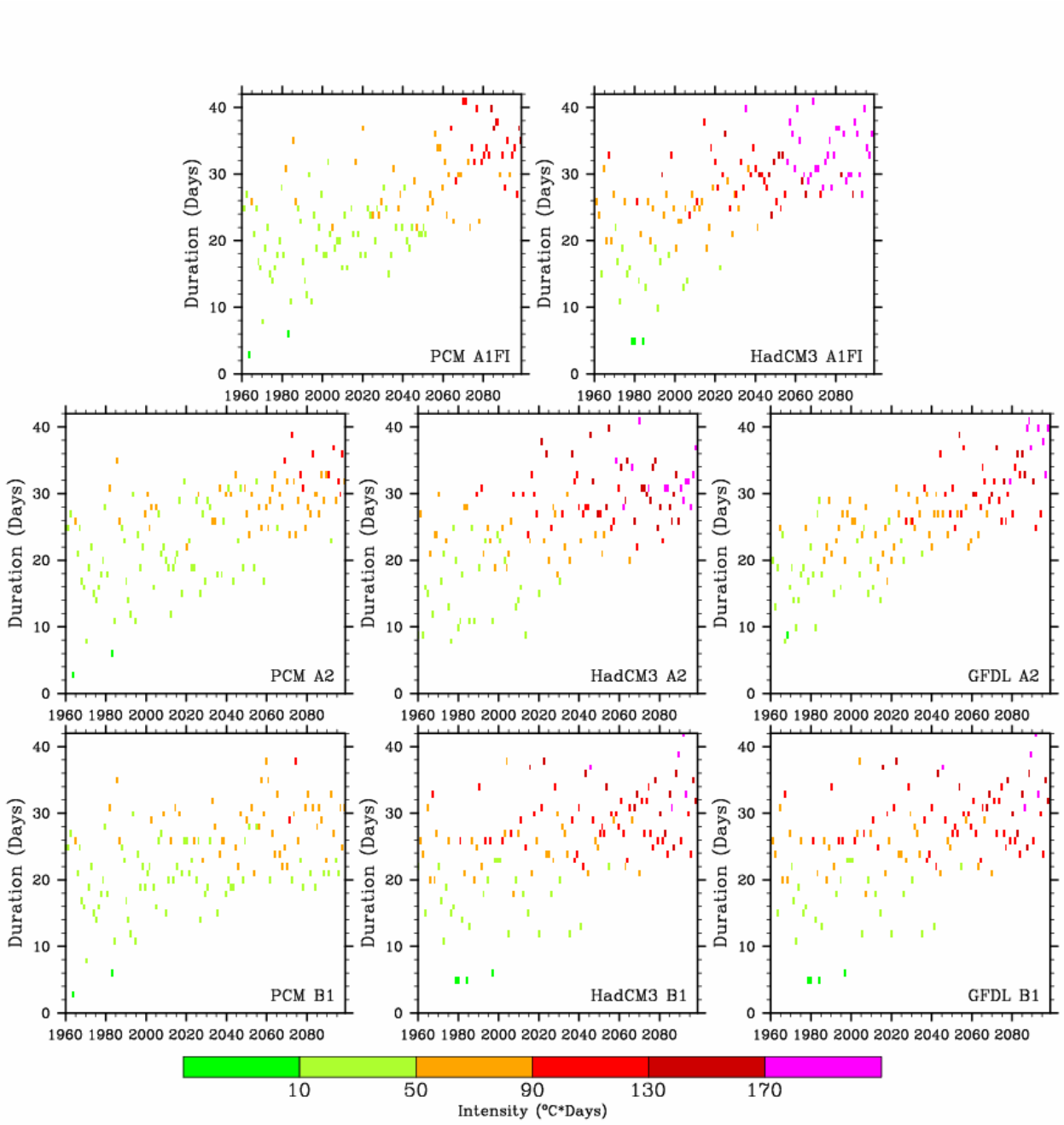

Figure 3. Projected frequency, duration and intensity of T90 events for HadCM3, PCM, and GFDL for A1fi, A2, and B1 for the JJAS season. Duration is shown on the y-axis, number of events is indicated by the frequency of boxes over time, and intensity is denoted by the colour of the box.

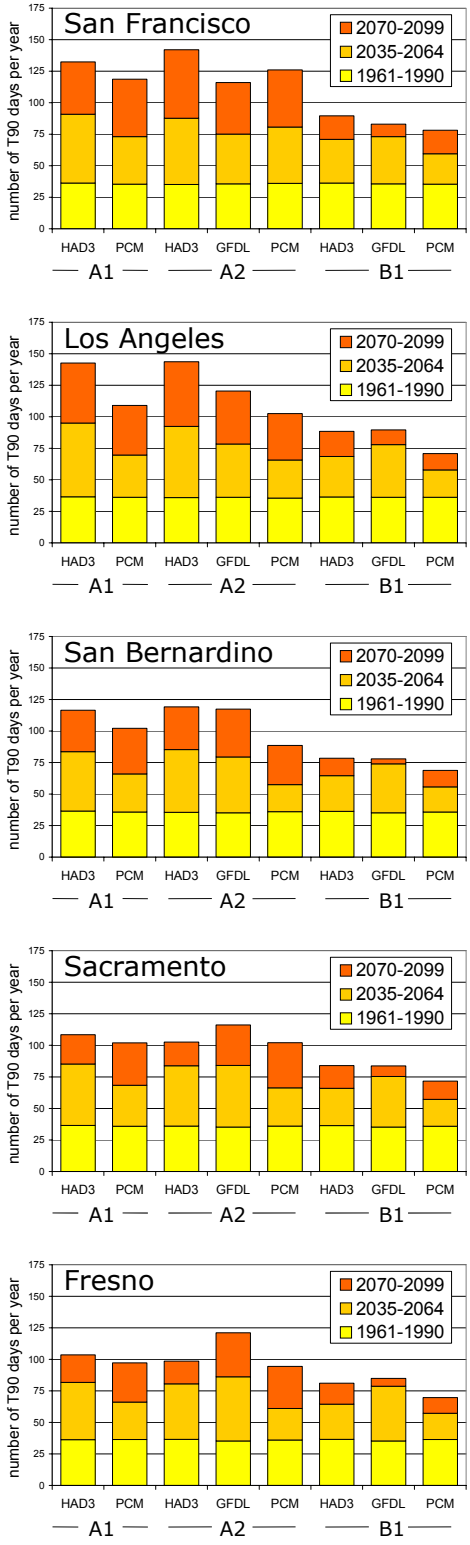

Figure 4. Projected change in number of T90 days for 5 urban centers in California as simulated by the HadCM3, GFDL2.1 and PCM models for the A1fi (higher), A@ (mid-high) and B1 (lower) emission scenarios. Yellow denotes the number of 90th percentile exceedance days during historical reference period (~36 days), orange the number of days by mid-century, and red the number of days by end-of-century.

Temperature projections downscaled to the five urban locations (Figure 4) also indicate large increases in the number of T90 days relative to the present day. Although projections suggest there is little difference between the scenarios prior to 2035, all of the cities show significant increases in T90 days by end-of-century, with proportionally larger (2 to 5 times) increases under the higher emissions scenarios (A1fi and A2) relative to the lower B1. Increases tend to be greater for coastal cities that have current-day T90 thresholds that are relatively low due to the moderating effects of the ocean (25°C for San Francisco, 31°C for Los Angeles), and smaller for inland cities that already experience relatively high T90 thresholds (35°C for Sacramento, 37°C for San Bernardino and Fresno). As indicated in Figure 4, however, T90 projections for San Bernardino, located inland from Los Angeles, are more of a hybrid of the coastal and inland responses, with increases being lower than those seen for coastal cities but slightly higher than inland ones.

Specifically, by 2070–2099 the number of T90 days in Los Angeles, currently at ~36 days per year, is projected to range from 110-145 under A1fi and A2, and 70-90 under the lower B1 scenario. San Francisco shows similar increases of 115–140 under A1fi/A2 and 80-90 days under B1. Inland, Sacramento is projected to exceed the T90 threshold 70–85 days under B1, and 100–115 days under A1fi/A2 by end-of-century. Fresno is similar, with 70-85 days under B1 and 95–120 days under A1fi/A2. Finally, San Bernardino has projected increases of up to 100–120 days under A1fi/A2 and 70–80 days under B1.

2.3.4. Projected Impacts on Heat-Related Human Mortality

Meteorologically "oppressive" conditions are here determined by identifying maximum apparent temperature thresholds that have been associated historically with rising heat-related mortality. Apparent temperature is a combination of the impact of temperature, relative humidity, and wind speed on the human body, and can be considered an adequate surrogate to evaluate heat transfer effects on humans (Watts and Kalkstein 2004).

Mortality data for the entire U.S. are available in digital format since 1975, and include date and cause of death, and the county in which the deceased had passed away. These data are derived from files at the National Center for Health Statistics (NCHS 2000), and are standardized to remove as much variation on mortality as possible that is related to non-meteorological causes, such as trends in population during the period of evaluation. Total deaths per day are evaluated in this analysis, as this has been shown to be superior than subdividing deaths into individual causes (Ebi et al. 2004).

Daily human mortality can be compared daily temperature or apparent temperature values, and a threshold temperatures can be determined: the value for both Los Angeles and Sacramento is 34°C (93°F) maximum apparent temperature; for San Francisco, 18°C (64°F) minimum temperature; for Fresno, 36°C (97°F) maximum apparent temperature; and for San Bernardino/Riverside, 39°C (102°F) maximum temperature. The daily threshold is determined by the lowest value, which, when reached or exceeded, yields a mean mortality value that is statistically significantly higher than the long-term mean ($p = 0.05$). For example, we found mean mortality in Los Angeles and Sacramento on all days of apparent temperature 33°C (91°F) or higher to be not statistically significantly above the long-term mean, whereas those above 34°C (93°F) and higher were above that mean.

The statistical relationships between heat and mortality were developed through location-specific algorithms for Los Angeles, San Francisco, San Bernardino/Riverside, Sacramento, and Fresno for all days with maximum apparent temperatures at or above the city-specific threshold. These algorithms include environmental factors responsible for explaining the variability in mortality during oppressive weather. Both meteorological (maximum and minimum air temperature, maximum and minimum apparent temperature and dew point, cloud cover, etc.) and non-meteorological (consecutive days of oppressive weather, time of season when oppressive weather occurs) factors are potential independent variables within this algorithm. The final algorithm for Los Angeles ($p<0.001$), for example, is:

$Mort_p = -8.481 + 0.326\ AT + 1.891\ CD - 0.012\ TS$

where estimated daily mortality ($Mort_p$) is given as a function of maximum apparent daily temperature (AT), the day's position in a sequence of consecutive days with maximum apparent temperatures equal to or exceeding 34°C or 93°F (CD), and days after May 1 (TS).

For Sacramento, the algorithm is ($p<0.01$):

$Mort_p = -8.817 + 0.265\ T_x - 0.013\ TS$

where T_x is daily maximum air temperature. Another variable used in the city-specific algorithms is DIS ("day in sequence"), which refers to the number of consecutive days on which the threshold temperature value has been met or exceeded.

The Sacramento algorithm shows a somewhat flatter slope than that for Los Angeles, indicating a less dramatic relationship between heat and mortality in this generally hotter city in summer. Current-day Sacramento heat-related mortality is six percent that of Los Angeles in terms of actual numbers. With a population about 15 percent that of Los Angeles, this translates into an equivalent mortality of 40 percent that of Los Angeles. Algorithms for each city are summarized in Table 3.

City	Unacclimatized Algorithm
San Francisco[1]	Mortp = -4.05 + 0.173 AT
Los Angeles	$Mort_p = -8.481 + 0.326\ AT + 1.891\ CD - 0.012\ TS$
San Bernardino	$Mort_p = -0.352 + 0.03\ T_x + 0.221\ DIS - 0.008\ TS$
Sacramento[2]	$Mort_p = -8.817 + 0.265\ T_x - 0.013\ TS$
Fresno	$Mort_p = -4.807 + 0.137\ AT.$

Table 3. Heat mortality – temperature algorithms for each city. AT = apparent temperature, CD = position in consecutive sequence of hot days, TS = day of the season, Tx = afternoon temperature and DIS = day in sequence.

[1] Note that the algorithms for San Francisco and Sacramento been updated from those used in Hayhoe et al. (2004). Previous algorithms were: Mortp(SF) =-2.962 + 0.18 Morning AT, and Mortp(Sc)=-8.02 + 0.265 Tx - 0.013 DIS

Acclimatization is the process by which people tend to become accustomed to heat over the course of a summer season or the duration of a heat wave. When projecting future heat-related mortality, acclimatization must be included to account for the plausible degree to which people are able to accustom themselves to increasingly hot summers and heat waves.

The impact of acclimatization was determined by utilizing a procedure we deem superior to the "analog city" approach used in previous studies (Kalkstein and Greene, 1997). The new acclimatization procedure assumes that people will most likely respond to heat under climate change conditions in a given city as they do today during the very hottest summers. Thus, instead of choosing analog cities, which typically possess different demographics and urban structure than the target city, we have selected "analog summers" within the same city. These analog summers best replicate the projected summers seen under the climate change scenarios, and are basically the hottest summers for each locale. For each of the target cities, the hottest summers were determined based on mean summer apparent temperature values, and a new acclimatization algorithm was developed for days during these hottest summers that equaled or exceeded the apparent temperature threshold (e.g., for Los Angeles, 34°C or 93°F). The acclimatization algorithm for Los Angeles thus becomes:

$Mort_p = -4.774 + 0.178\ AT + 1.928\ CD - 0.013\ TS$

For Sacramento, the acclimatization algorithm is:

$Mort_p = -5.323 + 0.160\ T_x - 0.0078\ TS$

For Fresno, the acclimatization algorithm is:

$Mort_p = -1.16 + 0.033\ AT$

For San Bernardino, no acclimatization to hot summers occurred; therefore the algorithm is the same as the unacclimatized one. For San Francisco, on the other hand, there was no heat-mortality relationship in the hottest summers within the historical record, suggesting the acclimatized value would be zero.

		1971-2000	2035-2064		2070-2099	
		BASE	UNACC	ACC	UNACC	ACC
San Francisco (pop. 3.62 million)						
HAD	A1	1	6	0	35	0
PCM	A1	0	2	0	12	0
HAD	A2	0	1	0	15	0
PCM	A2	0	0	0	0	0
HAD	B1	1	3	0	6	0
PCM	B1	0	1	0	4	0
Los Angeles (pop. 9.93 million)						
HAD	A1	91	412	322	868	696
PCM	A1	103	283	220	609	487
HAD	A2	90	396	310	901	725
PCM	A2	179	792	657	930	774
HAD	B1	95	231	176	385	301
PCM	B1	104	222	171	334	262
San Bernardino (pop. 2.21 million)						
HAD	A1	11	45	45	85	85
PCM	A1	12	30	30	69	69
HAD	A2	11	47	47	101	101
PCM	A2	22	109	109	121	121
HAD	B1	10	27	27	43	43
PCM	B1	12	27	27	39	39
Sacramento (pop. 1.325 million)						
HAD	A1	15	49	29	104	63
PCM	A1	10	26	16	72	43
HAD	A2	11	46	28	74	45
PCM	A2	20	92	55	107	65
HAD	B1	11	36	22	52	31
PCM	B1	10	20	12	34	21
Fresno (pop. 0.61 million)						
HAD	A1	32	77	19	130	31
PCM	A1	28	56	14	104	25
HAD	A2	29	72	17	105	25
PCM	A2	27	92	22	102	25
HAD	B1	28	59	14	79	19
PCM	B1	28	46	11	64	15

Table 4. Projected changes in heat-related mortality as simulated for the base period (1971-2000), with average population for each of the 5 urban centers during that period, and for mid-century (2035-2065) and end-of-century (2070-2099) with (ACC) and without (UNACC) acclimatization.

The results for unacclimatized and acclimatized mortality rates for all five cities and three climate scenarios are summarized in Table 4. As one would expect, these estimates for 2035-2064 and 2070-2099 are slightly lower than those given in Table 1 for the 2050s and 2090s. The only major difference between the two sets of projections is for San Francisco, where revision of the mortality algorithm and acclimatization potential for this study yielded significantly lower estimates of unacclimatized mortality and no net acclimatized mortality by end-of-century under all model/scenario combinations.

In general, inter-scenario differences already begin to emerge by mid-century. For Los Angeles, for example, projected increases for 2035-2064 range from 1.6 to 1.8 times the base values under B1, even including acclimatization, while increases of 2 to 3.6 times base values are seen under A1fi and A2. By end-of-century, under B1 increases of 2.5 to 3 times are shown, while under A1fi/A2 increases are much greater, 4 to 8 times base values. In general, projected increases in heat-related mortality under the A1fi/A2 scenarios tend to be almost twice that projected under B1. Overall, results indicate a high sensitivity to heat in Los Angeles, which possesses excessive mortality totals well above the other cities. Of course, Los Angeles represents the

largest metropolitan area of the five cities evaluated, so the higher totals are not an immediate surprise. During a typical present summer in the 1990s, approximately 160 excess deaths attributed to heat occur in Los Angeles (Hayhoe, Kalkstein, Sheridan, et al., 2004; see also Table 1). All the modeled projections greatly exceed this number, and for some of the climate models for the late 21st century, the exceedances are several times the present heat-related mortality value. With the exception of San Francisco, the other cities show marked increases over present-day mean annual heat/mortality totals. For example, in Sacramento, there were about 15 excess deaths attributed to heat during an average summer in the 1990s; this number could rise nearly sevenfold by century's end.

As expected, in general, the acclimatization algorithm for the hottest summers shows a decreased sensitivity to heat because of intra-seasonal acclimatization (this is apparent by noting the lower coefficient for the AT variable in the algorithms given earlier in the text and in Table 3). Using the acclimatization algorithm, revised mortality totals are derived for Los Angeles that are 17 to 22 percent lower than those yielded from the original unacclimatized algorithm. The reductions are even greater for the hotter inland cities, with Sacramento showing a 40 percent reduction and Fresno a 75 percent reduction in mortality estimates when acclimatization is taken into account (Table 3).

Fresno's outcome is similar to many very hot semi-arid cities such as Phoenix, Arizona, where the population and general urban structure are already well adapted to frequent and extreme heat (Kalkstein, 2003). In fact, Fresno's acclimatized excessive mortality totals are not much higher than today's numbers. Considering the fact that Fresno is a hot Central Valley city, this is not surprising. The residents can adapt very well during excessively hot conditions, and clearly the health response is not dramatic during the hottest summers. Thus, it is probable that, unless temperatures actually exceed a human threshold of tolerance, residents in the Fresno area will not respond in extreme fashion if the climate warms as the models suggest.

For San Francisco, the acclimatized heat-related mortality values are zero, indicating perfect adaptation to warmer summers due to the relatively cooler climate. At the opposite end, no capacity for adaptation is seen in San Bernardino. The results here actually indicate increased sensitivity during the hottest summers, is counter-intuitive to what might be expected in hotter urban areas and the results found for Fresno. We are currently investigating alternative explanations by taking greater account of socio-economic factors (such as the availability of air conditioning, age structure of the population, and the housing stock) that might explain these non-intuitive results. If, for example, the San Bernardino/Riverside area has a lesser proportion of air-conditioned residents than Fresno, increased heat could create an indoor environment that is almost intolerable and could lead to greater numbers of deaths. It is clear that a thorough investigation of these social issues is necessary to understand the increased sensitivity of San Bernardino/Riverside residents to heat during the hottest summers.

In Table 5, mortality projections are standardized to values per 100,000 by 1971-2000 average population for each city. Under these circumstances, Fresno displays the largest relative mortality for present-day, followed by Sacramento, Los Angeles, San Bernardino, and last, San Francisco. This ranking is maintained under future projections with no allowance for acclimatization.

		1971-2000 BASE	2035-2064 UNACC	2035-2064 ACC	2070-2099 UNACC	2070-2099 ACC
San Francisco (per 100,000)						
HAD	A1	1	17	0	96	0
PCM	A1	1	5	0	32	0
HAD	A2	0	1	0	41	0
PCM	A2	0	0	0	0	0
HAD	B1	2	8	0	17	0
PCM	B1	0	3	0	11	0
Los Angeles (per 100,000)						
HAD	A1	92	415	324	874	701
PCM	A1	104	285	221	613	490
HAD	A2	91	398	312	907	730
PCM	A2	180	798	662	937	779
HAD	B1	96	233	177	387	303
PCM	B1	105	224	172	336	264
San Bernardino (per 100,000)						
HAD	A1	48	205	205	384	384
PCM	A1	56	134	134	314	314
HAD	A2	48	212	212	457	457
PCM	A2	98	493	493	548	548
HAD	B1	47	124	124	193	193
PCM	B1	54	122	122	176	176
Sacramento (per 100,000)						
HAD	A1	116	367	221	786	475
PCM	A1	74	196	118	540	327
HAD	A2	85	343	208	559	337
PCM	A2	147	694	415	808	491
HAD	B1	85	269	163	390	235
PCM	B1	75	151	91	257	158
Fresno (per 100,000)						
HAD	A1	530	1264	305	2131	513
PCM	A1	461	920	221	1710	411
HAD	A2	467	1174	282	1720	415
PCM	A2	449	1508	361	1672	410
HAD	B1	451	961	231	1290	311
PCM	B1	459	754	180	1049	246

However, when acclimatization is accounted for, Los Angeles again seems to stand out as particularly sensitive, even when the population disparities are taken into account. Sacramento, Fresno, and San Bernardino are warmer cities, and thus, urban structures and general acclimatization to heat is more complete in these locales than for coastal and more moderate Los Angeles. San Francisco shows little change between historical summer excess mortality totals and the future simulated values. Clearly, summers there are cool enough now, and are projected to remain so in the future, to inhibit increases in mortality as are projected for other cities.

Table 5. Projected changes in heat-related mortality (as given in Table 4), normalized by 1971-2000 population to values per 100,000.

2.3.5. Conclusions

From this analysis, it is clear that extreme heat represents a growing threat to California—a threat shared by many other regions of the world. Increases in summer temperatures combine with longer heat wave seasons, greater temperature extremes, and more frequent, longer, and more intense events to suggest that climate change in California could pose a significant risk to human health.

By mid-century (2035-2064), temperatures currently seen on only ten percent (or ~36 days) of the year will be exceeded on average 1½ to 2½ times more frequently each year. By end-of-century, extreme temperatures will be exceeded 2 to 2½ times more frequently under B1 and

2 ½ to 3 ½ times under A1fi/A2 for inland cities. The value rises to 3 to 4 times for coastal cities (San Francisco, Los Angeles) under A1fi/A2.

The frequency, length, and intensity of individual heat waves as well as the duration of the entire heat wave season are also projected to increase for all cities considered here. Inter-scenario differences are evident by mid-century, with significantly greater increases by century's end under the higher A1fi/A2 scenarios and for the more sensitive models (GFDL, HadCM3). Results indicate large increases in the projected heat intensity, as compared to historical (i.e., 40-80^{o}C-days for 1961-1990, 80-130 ^{o}C-days by 2050, and 180-250 ^{o}C-days by 2100).

Significant increases in heat-related mortality are projected, with A1fi/A2 projections being almost double those for B1 by end-of-century. Unacclimatized mid-century projections show increases of 1.5 to 3 times 1971-2000 values under B1 and 2 to 4.5 times under A1fi/A2, while end-of-century increases range from 2 to 4 times the historical values for each city for B1 and 3.5 to 9.5 times for A1fi/A2. Greatest overall increases are projected for Los Angeles, the largest city in terms of population. This is true for both absolute numbers as well as for normalized projections that include acclimatization. Overall, acclimatization is most successful at reducing projected mortality rates for inland cities that already experience extended periods of extreme heat, reducing mortality rates projected for Sacramento by 40% and for Fresno by 75%.

It is important to note that demographic changes, societal decisions affecting adaptation, and changes in the health care sector will determine actual mortality rates. Model uncertainties notwithstanding, extreme heat and associated human health risks under the lower-emissions scenario are significantly less than under higher-emissions scenarios (Table 4). Significant efforts will have to be undertaken to provide effective early warning systems, public education, air conditioning, "cooling centers," and other adaptations (especially for the elderly, children, poor, and those already ill) to avoid major increases in the number of heat-related deaths in California. The urgency for such measures only grows in light of expected population increases, urbanization, and demographic shifts. Of note, heat watch-warning systems presently in operation in some major U.S. cities have already been shown to save a number of lives when coupled with effective intervention plans (Ebi et al., 2004). Thus, such systems should prove to be an effective adaptive response tool if the climate warms as the models suggest.

These projected increases in extreme heat and heat-related mortality quantify the difference between a lower and a higher emissions scenario and potential climate change impacts. It is also important to note that increases in summer mean temperatures and the frequency, intensity and duration of extreme heat events have significant implications for human health and energy demand in the heavily air-conditioned southern California, a region that currently experiences energy shortages. Intensity of heat events is a concern not only for their direct relationship to heat-related mortality, but also through indirect effects of energy shortages in the face of sudden increases in demand, which could enhance overall mortality beyond the estimates provided here. The feedbacks between temperature increases, the demand for energy during extreme heat events, air conditioning use, and adaptation and acclimatization to extreme heat is part of an ongoing more comprehensive study based on the results presented here.

2.4. Adaptations

As mentioned above, the number of deaths attributed to heat and cold over the past 30 years has declined (Davis et al., 2003a,b; CDC, 2005a,b; Donaldson et al., 2003). Several investigators believe that this reduction is related to increasing penetration of air conditioning into the residential, commercial and vehicular sectors, in addition to community heat emergency programs. Several studies (Kaiser et al., 2001; Naughton et al., 2002; Davis et al., 2003a,b; CDC, 2005b; Donaldson et al., 2003) have reported that presence of a working air conditioner, particularly a central air conditioning system, was the strongest protective factor against heat-related mortality. Fans, on the other hand, provided no protective benefit (Naughton et al., 2002; Kaiser et al., 2001; Bernard and McGheein, 2004). Kilbourne (2002) has suggested that municipal housing codes be modified to require functional air conditioners in rental housing, in addition to existing requirements for heat.

The U.S. Dept. of Commerce expects that air conditioning will be universal in the U.S. by 2050 (McGheein and Mirabelli, 2001), which will increase demand for electricity for residential cooling. Miller et al. (2005) estimated that summer time peak demand for electricity in California could increase by at least 10%, although more research is required.

Kalkstein and colleagues have established numerous real-time operational heat-watch-warning systems in major cities throughout the United States, although but none in California. Kalkstein et al. (1996) designed and implemented the first hot weather warning system in the United States for the city of Philadelphia in 1995. Recently, Ebi et al. (2004) evaluated the Philadelphia operational system, and found that the system developed by Kalkstein et al. (1996) was effective both in terms of lives saved, and in terms of economic cost. Finally, Sheridan and Kalkstein (2004) have described the methodology for development of synoptic climatology-based hot weather warning systems. Since 2000 successful hot weather warning systems based on this model have been established in a number of American cities, as well as in several cities in Europe and Asia. This methodology is considered the state-of-the-art approach for development of hot weather warning systems, and should be considered as a model for any such plans developed specifically for California cities.

In addition, other U.S. cities, for example Chicago (Naughton et al., 2002) and Milwaukee (Weisskopf et al., 2002), as well as Canada (Smoyer-Tomic and Rainham, 2001), have developed effective heat emergency plans that could also serve as models for California. The effectiveness of heat emergency programs was validated by Naughton et al. (2002) and Weisskopf et al. (2002) in studies in Chicago and Milwaukee, respectively, which compared mortality during heat waves in 1995 and 1999. In both cities, heat-related mortality was considerably lower during the 1999 heat wave, during which the action plans developed in response to the 1995 heat wave were activated.

However, Bernard and McGeehin (2004) reviewed heat emergency plans from 18 cities, and found that many plans were inadequate, and that many other at-risk cities had no heat emergency action plans. These findings point to the urgency of developing heat emergency action plans for California before the need arises, and to inclusion in these plans of objective criteria for assessing the effectiveness of the plans.

Some communities also extend hours at public pools, provide for visitation of the elderly and isolated, and provide transport to community cooling centers as needed. Public service announcements, through TV, radio and print media that announce expected heat events and include advice and information about effective mitigating actions and available coping assistance have been effective in cities in the eastern United States. In our study, we also discuss adaptation strategies and provide a quantitative analysis of the potential for acclimatization under future increases in summer heat.

3.0 Global Climate Change and Air Pollution in California

3.1. "Background" Ozone and Particle Pollution in California: Present and Future

Not all pollutants in California originate solely from local, controllable sources such as industrial emissions or automobile tailpipes. Pollutant concentrations not due to regulated emissions are commonly termed "background." Background ozone and particulate matter (PM) in California come from a mix of sources that range from local and global natural processes to intercontinental movement of anthropogenic pollution. Although background pollutant concentrations in California today are of secondary concern in air quality programs, projections of future pollutant loads due to global change suggest that some air quality standards could be exceeded by background alone if present global emission growth patterns do not change.

Climate effects on background air pollutant concentrations range from simple, direct relationships such as rain suppressing soil dust, to complex processes such as pollutant distribution by global wind patterns. In addition, pollutants can alter climate at local, regional, and global scales (Ramanathan et al., 2001). Background pollutant concentrations complicate air quality planning by limiting the effectiveness of control programs applied to local (California) sources.

This section briefly summarizes current knowledge of background air pollution in California and discusses some possible effects of climate change.

3.2. Ozone

3.2.1. "Natural" Ozone

Ozone in the atmosphere is formed by sunlight acting on gases. In the stratosphere (10-90 km above the surface) ozone in formed when oxygen atoms ionized by solar ultraviolet (UV) light combine with other oxygen molecules; about 90 percent of Earth's ozone is in the stratosphere. In the troposphere (surface to 10km) direct ozone formation by sunlight is weak, and most ozone comes from reactions of UV with "ozone precursors"—volatile organic compounds (VOCs), and nitrogen oxides (NOx). Because ozone is chemically reactive and is quickly destroyed, ozone concentrations represent a balance between formation and loss processes. Under "natural" conditions, VOCs from biologic sources are much more abundant than NOx, thus natural ozone formation at Earth's surface is termed "NOx limited" (Lelieveld and Dentener, 2000).

3.2.1.1. Stratospheric ozone

Under stable meteorological conditions, the troposphere and stratosphere do not mix. Strong storms occasionally cause stratospheric intrusions, or "tropopause folding events" (TFEs), that bring concentrations of 50 - 75 ppbv down to 5-6 km and 50–60 ppbv at mountain sites above 3km (STACCATTO, 2003). Over California these events occur in winter and spring accompanying strong storms. Effects near sea level are usually small and infrequent (Lelieveld and Dentener, 2000); only one sea level event has been observed in California since widespread ozone monitoring began in the 1960s. Modeling for typical

summer days in California (Fiore et al., 2002a) indicates no more than 2 ppbv comes from the stratosphere.

3.2.1.2. Tropospheric ozone

"Natural" ozone at ground level is a combination down-mixing from the stratosphere and photochemical reactions of natural precursors from natural sources—VOCs from vegetation, NOx from soil and lightning, and both from large biomass fires. Sparse 19th century ozone measurements from Europe and America show a strong seasonal trend, peaking in spring, with daily maxima of 30–50 ppbv (Bojkov, 1986; Lisac and Grubisic, 1991). Global models of "preindustrial" ozone (Lelieveld and Dentener, 2000; Hauglustaine and Brasseur, 2001) are in rough agreement, and show wide global variation by region and season.

Model estimates of average "natural background" ozone in California are 15–35 ppbv in coastal areas, with a maximum monthly mean near 40 ppbv at low altitude inland sites. At altitudes above 2 km stratospheric intrusions can occasionally push peak "natural background" concentrations to 45–50 ppbv.

3.2.1.3. "Natural" ozone climate sensitivity

Natural ozone may be altered by climate change either through changes in atmospheric circulation or changes in precursor emission rates.

Changes in the frequency and/or intensity of storms could alter stratospheric contributions by shifting the frequency and/or intensity of TFEs. The effect of this would likely be confined to high mountain areas.

Within the troposphere, changes in storm tracks or storm activity could alter the amount, timing, and location of ozone in the upper troposphere (> 5 km) because there lightning-generated NOx causes 10 – 40 % of ozone (Lelieveld and Dentener, 2000). Although changes in lightning distributions under future climates are highly uncertain, the present effect of lightning on surface ozone in California is small, so the change should be minor.

In the low altitude coastal and inland valley areas of California, the largest climate effect on natural ozone will probably be due to changes in natural precursor emissions, especially changes in vegetation patterns, and, secondarily, temperature changes. For some individual plant species, biogenic VOC emissions will rise with temperature, but the large variation across plant types, coupled with uncertain changes in water supply and vegetation patterns make reliable projections difficult. One model study estimated biogenic VOC emissions would increase by three-fold for some California vegetation types (Constable et al., 1999), but offsetting changes in vegetation patterns would yield only a doubling of net VOC emissions. Soil biota NOx emissions may rise with temperature, but they are strongly modulated by amount and timing of rainfall, which is also very uncertain. Since the system is NOx limited, truly "natural" ozone cannot rise in proportion to changes in biogenic VOCs, but may respond to coeval NOx emission increases. Downwind of major urban areas, ozone generated by reaction of natural VOCs with anthropogenic NOx could be exacerbated by increased biogenic VOCs.

3.2.2. Transported Anthropogenic Ozone

3.2.2.1. Present conditions

At present, large contributions to ozone due to emissions outside the State are limited to short range, short term effects such as ozone transport from border cities like Tijuana, Mexico. However, global increases in industrial activity and motor vehicle use pose a significant risk of rising global (at least northern hemisphere) ozone levels.

Recent research has shown that urban plumes lofted high into the atmosphere can be entrained in global circulation and effectively transport ozone thousands of kilometers (, Logan and Murti, 1999; Fiore et al., 2002a; Jaffe et al., 2003 a,b). Individual pollution plumes from urban / industrial areas have been traced from the eastern United States to Europe (Trickl et al., 2003), from Europe to Asia (Pochanart et al., 2003), Asia to the north Pacific Ocean (Thouret, et al., 2001), Asia to North America (Jaffe, McKendry, Anderson, and Price, 2003), and from all the industrialized regions of the Northern Hemisphere to the Arctic (Browell et al., 2003). Globally, injection of anthropogenic ozone precursors (especially NOx) into the free troposphere has been estimated to enhance tropospheric ozone by 12 percent (Lawrence, et al., 2003).

Ozone due to urban and industrial emissions in east Asian megacities (Beijing, Tokyo, Hong Kong, Taipei, Shanghai, etc.) has been observed to reach western North America in springtime (Jaffe et al., 1999; Jaffe et al., 2003b; Jaffe, McKendry, Anderson, and Price, 2003). Modeling shows mean Asian ozone impact in western North America would increase from around 1 ppbv in 1985 to as much as 7 ppbv in 2010 if Asian NOx emissions continue to grow at late 20th century rates (4-5 percent /year) (Jacob, Logan and Murti, 1999). Statistical analyses of ozone records from rural northern California to Washington show a broad regional increase in "background" ozone with a statistically significant increase in springtime ozone (about 4 ppbv/decade) for air masses coming off the Pacific (Jaffe et al., 2003b). This is consistent with the vertical gradient pattern of Asian PM impacts (VanCuren and Cahill, 2002), ozonesonde observations (Newchurch, et al., 2003), and increased transport exposure above the marine boundary layer shown in transport modeling (Jaegle et al., 2003).

3.2.2.2. Future conditions

There is a significant potential for large increases in hemispheric - scale ozone concentrations due to rapid emissions growth as populous nations like India and China develop more industrialized, energy-intensive economies. For example, air pollution emissions in China are projected to quintuple by 2020 if current emission patterns and growth rates continue (Zhang, 2005).

Metropolitan and regional scale ozone control focuses on rapid ozone formation processes, but at global scales, less reactive carbon species such as CO and CH_4 are significant ozone precursors (Lelieveld and Dentener, 2000; Prather, 1996). Model studies project modest near-surface ozone increases in the range of 5–7 ppbv over much of the northern hemisphere by 2030 (Fiore et al., 2002b; Prather et al., 2003); continued emission growth projected to 2100 could cause, depending on emission assumptions, increases of 4–10 ppbv (low emission case) to more than 20 ppbv (high emission case) (Prather et al., 2003). If the latter were to occur,

much of California would violate the State 8-hr ozone air quality standard even with near-zero local emissions.

Increased hemispheric ozone would not only cause a rise in ozone concentrations, but would likely prolong the ozone season in California. Model estimates for 2030 for the IPCC A1 emission scenario indicate a large increase in the number of hours over 70 ppbv in the U.S in spring (March – June), when present ozone is moderate, while changes in late summer and fall are projected to be much smaller (Fiore et al., 2003b).

Analysis of the causes of these ozone increases under future climate conditions show that it is not simply a matter of increased emissions, but also increased oxidizing capacity in the atmosphere, due, in part, to increased hydroxyl radical concentrations resulting from increased evaporation and the greater water capacity of a warmer atmosphere, and increased stratospheric intrusions due to stronger global circulation (Dentener et al., 2004).

The non-linear response of global ozone to emissions also leads to novel approaches to ozone control. Model studies have shown that methane (CH_4) reductions, which are not important at metropolitan scales, may force global ozone downward while also reducing total green house gas warming potential as well (West and Fiore, 2005). Methane controls would be particularly attractive economically, because the recovered fuel value of methane would give some controls (up to 10 percent of emissions) negative costs (West and Fiore, 2005).

Similarly, analysis of tropospheric ozone formation processes indicates that carbon monoxide (CO) reduction can also reduce tropospheric ozone formation, (Lelieveld and Dentener, 2000). Although the largest source of global CO is biomass fires, CO reductions due to emission controls on presently uncontrolled fossil fuel–fired sources are "leveraged," since they provide both local public health gains and global benefits.

3.3. "Background" Particulate Matter (PM) in California

3.3.1. "Natural" PM

Natural components of airborne particles include sea salt and marine sulfate, smoke from wildfires, wind-blown dust, and volcanic dust and sulfate. Since the chemistry of these particles overlaps with anthropogenic particles, "natural background" PM cannot be easily determined.

3.3.1.1. PM at remote sites

Mean measured PM_{10} and PM2.5 from a range of remote sites are shown in Table 6. Since anthropogenic PM can also reach these sites, these values should be taken as upper bounds on mean natural PM concentrations.

Table 6. Mean PM10 and PM2.5 concentrations at remote sites in California (USEPA/NPS IMPROVE monitoring data)

Site	PM10	PM2.5	Environment
Lassen Volcanic N.P.	6.5	3.2	High Mountain
Redwood N.P.	10	4.7	Coastal Mountains
Point Reyes N.S.	17	7.1	North Coast Seashore
Death Valley N.P.	4.7	1.5	Desert

Unfortunately, many California environments, such as the floor of the Central Valley or the Southern California coastal plain, have no remote, undisturbed sites from which to even set bounds for "natural" PM levels. The data in Table 6 show that there is no correlation between precipitation and observed PM levels, suggesting that undisturbed natural vegetation tends to hold soil except in the driest of sites (*e.g.* dry lake beds). It follows that natural PM concentrations in the rest of California probably would fall in the range of the values in the table.

Natural PM concentrations are highly variable. Since sea-spray dominates at Point Reyes PM there is dependent on the strength of the sea breeze; Mt. Lassen PM is generally low, but there are occasional severe impacts from wildfires; despite generally low PM, extreme winds may cause dust storms in Death Valley. Even without directly altering the land, human activities can also alter "natural" emissions: fire suppression can reduce the frequency of smoke exposure; water diversions can dry up lakes or streams leaving exposed sediment vulnerable to wind erosion; grazing can reduce vegetation cover and break up soil, making dust easier to loft.

3.3.1.2. Global natural PM sources

Several natural PM sources are known to have impacts on continental to global scales. Major volcanic eruptions can impact the whole planet, but are infrequent; biogenic emissions and wildfire smoke vary seasonally; dust from the driest deserts is raised almost daily by even modest winds, and salt and biogenic aerosol from the oceans is emitted nearly continuously.

Coastal California sites experience strong exposure to oceanic aerosols embedded in the Marine Boundary Layer (MBL). These consist primarily of sea salt (generally >2.5 μm) and biogenic sulfate (generally <2.5 μm) (O'Dowd et al, 1997; Lewis and Schwartz, 2004). At Trinidad Head in Humboldt County, typical near-beach concentrations of ammonium sulfate are 1-5 (mode about 2) $\mu g/m^3$ (PM2.5) while sea salt is 0.5-4 (mode about 1.5) $\mu g/m^3$ (PM_{10}) (ITCT2K2). At Point Reyes in Marin County, higher winds increase sea spray and consequently salt increases to about 0.5-7.5 (mode about 2) $\mu g/m^3$ (PM_{10}) (IMPROVE). Marine influence falls off rapidly with altitude or distance from the shore, dropping by about 90% at the crest of the Coast Ranges or at interior coastal sites, and it is negligible at far inland desert and mountain sites (IMPROVE).

Away from the coast and above the MBL the dominant global PM sources affecting North America are soil dust, biomass smoke from wildfires, and highly variable amounts of volcanic ash and sulfate. Long term records of dust retrieved from the Greenland Ice Cap show that Asian deserts are the dominant dust source for mid- and high latitudes of the

Northern Hemisphere (Biscaye et al., 1997; Bory et al., 2003), while dust from North Africa dominates in the subtropical regions (Prospero et al., 2002; Prospero and Lamb, 2003).

Asian dust loading in air over California ranges from near zero in midwinter to about 1-5 (mode about 2) $\mu g/m^3$ PM_{10} in summer (VanCuren and Cahill, 2002; VanCuren, 2003), with very rare extreme dust storms exceeding 40 $\mu g/m^3$ PM_{10} (Husar *et al*., 2001). Biomass smoke from fires in Asia (SE Asia in spring, Siberia in summer) observed over California ranges from near zero in midwinter to 3 or more (mode about 1) $\mu g/m^3$ PM_{10} in summer (VanCuren, 2003). Dust from North Africa can reach southern California through the Caribbean and Gulf of Mexico, but this appears to be too infrequent to meaningfully contribute to California PM.

3.3.1.3. North American natural PM sources

Dust generated from undisturbed soils in most of California and the West is modest compared to the African and Asian sources, and wildfire smoke is generally low due to fire suppression. There is limited data on natural PM in California, but an indication comes from analyses for Crater Lake, Oregon and Mt. Lassen, California, which report typical summer local dust to be about 2 $\mu g/m^3$ PM_{10} and mean regional smoke (*i.e.* not due to large fires near the monitoring sites) to be about 0.5 $\mu g/m^3$ $PM_{2.5}$ (VanCuren, 2003). Wildfire impacts estimated for the West as a whole (including large fires) show typical summer concentrations range from 1-6 $\mu g/m^3$ $PM_{2.5}$, with very large spatial and interannual variation (VanCuren and Lamb, 1996).

3.3.1.4. Global anthropogenic PM sources

Recent research has roughly characterized the impacts of global PM emissions on California. The stable MBL along the California coast generally keeps global pollutants embedded in the troposphere from reaching the surface, so global pollution impacts in coastal areas are effectively suppressed. Conversely, mountain sites above about 1km altitude are fully exposed to global circulation and generally isolated from the MBL. Winter rains suppress PM concentrations, but during spring, summer, and fall, global anthropogenic (i.e., combustion-related) PM concentrations over California are in the range of 1-5 (mode 3) $\mu g/m^3$ PM2.5. The composition of this material is approximately 30% mineral, 40% organic matter, 4% elemental carbon, 10% sulfate, and less than 5% nitrate (VanCuren, 2003).

3.3.2. Climate sensitivity of global and local "background" PM

Climate change may alter background PM concentrations, primarily through changes in local emissions of soil dust and rates of VOC oxidation to particles. Since local sources are weak compared to either the coastal oceanic effect or the upland global impact, natural background PM is not expected to change significantly over most of the State. However, anthropogenic "background" may change dramatically due to global economic development. Air pollution emissions in China are projected to quintuple by 2020 (Zhang, 2005) if current emission patterns and growth rates continue. Actual emissions may be less due if aggressive new control programs are implemented.

4.0 Emissions and Climate Change

Climate change is one of the greatest environmental challenges of our time, with the potential to alter all aspects of human life. A significant factor in climate change is the emissions that are released into the atmosphere by human activity. It has long been recognized that climate conditions directly affect many aspects of ozone and particulate matter (PM) formation—beyond straightforward meteorological factors such as the atmospheric mixing height (Semazzi, 2003). For example, higher temperatures lead to increased emissions of volatile organic compounds (VOCs) from fuels, solvents and coatings, increased rates of chemical reactions driving smog formation, greater demands for cooling energy and hence increased oxides of nitrogen (NO_X) emissions, as well as enhanced biogenic VOC emissions from vegetation.

Many plant species found in California's landscapes emit biogenic volatile organic compounds (BVOCs), such as isoprene, monoterpenes, and other compounds into the atmosphere. California's BVOC emissions are approximately 750,000 tons per year (CARB 2005). When mixed together with man-made emissions, these compounds participate in the formation of air pollution. Biogenic VOC emissions are sensitive to environmental factors, such as temperature and sunlight levels. Climate change may increase BVOC emissions, by increasing temperatures and by altering the plant species composition of landscapes. In one published study (Constable, et al. 1999), researchers used computer models to predict future changes in U.S. biogenic VOC emissions resulting from climate change. Global model simulation output represented the magnitude of climate warming predicted for the years 2070-2099 for a doubled CO_2 atmosphere. They estimated that biogenic VOC emissions would increase nationally by an average factor of 2. Regions of the western United States (including California) were predicted to increase BVOC emissions by almost a factor of 3 for some vegetation types.

Higher outdoor temperatures will reduce the demand for heating services during winter, and increase the demand for cooling services during summer. To the extent that these services are provided by fossil fuel combustion, emissions of associated pollutants, such as CO, NO_X, and VOCs will change. A preliminary estimate by staff from California Energy Commission (Energy Commission) used hourly NO_X emissions data available from the U.S. EPA Acid Rain Program, and maximum daily temperature data from Los Angeles, Fresno, San Jose, and Sacramento. Only weekday, non-holiday-days were included in the analysis. The following graph, Figure 5, shows the combined mass NO_X emissions from large power plants in California as a function of maximum temperature for July, August, September 2004, from Sacramento, San Jose, Fresno, and Los Angeles.

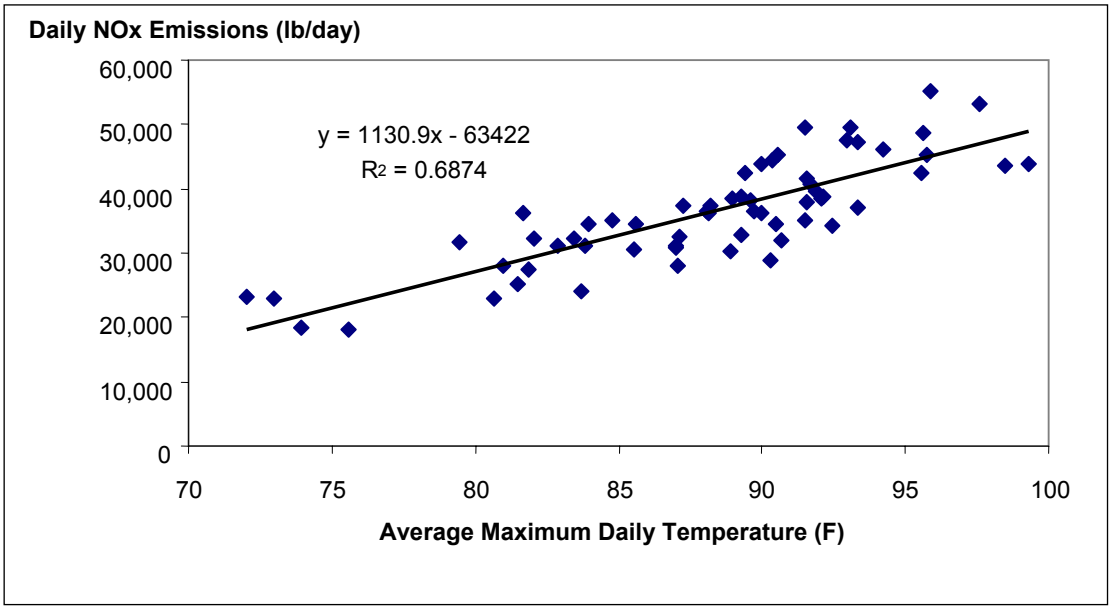

Figure 5. Selected power plants NO_X emissions versus daily maximum temperature during summer (July-September) at Sacramento, San Jose, Fresno and Los Angeles.

Using the California Energy Commission's trend line for NO_X, a preliminary estimate by ARB staff indicates about a three percent linear increase in NO_X from power plants per degree F increase in the average daily maximum temperature. This was determined by taking the percent increase of NOx from the average of the temperatures in the Energy Commission data (88°F) to the next highest degree (89°F). This produced a three percent increase in NOx (applied as a linear trend, not an exponential one). However, the overall net effect on future emissions, after taking into account future emissions controls changes in power plant and air conditioning technologies, and population changes, is unclear.

Mobile source technologies in the distant future are likely to be very different than current ones and, thus, it is not possible to make quantitative predictions of California's mobile source emissions inventory for 2050 and 2100. However, investigating the response of the current mobile source inventory to possible future temperatures can provide insights for the near future and suggest responses. In general, higher summer temperatures will increase emissions from mobile source. In particular, high temperatures cause increased VOC evaporative emissions when people fuel and operate motor vehicles. To perform this sensitivity study, the staff at the ARB used the baseline 2050 and 2100 3-hour temperature data from climate model (GFDL CM2.1) simulations for two greenhouse gases (GHGs) emission scenarios (A2 - higher emissions, and B1 - lower emissions), to create a future diurnal temperature profiles. Applying these temperature curves in the EMFAC model permits estimating the change in current emissions due to the future increase in temperature.

GHG emissions scenarios A2 (relatively high emissions) and B1 (low emissions) were based upon decisions made by IPCC4, and availability of relatively crucial output from model

climate simulations. The B1 scenario has CO_2 emissions peaking just below 10 gigatonnes per year (Gt/yr) in mid-century before dropping below current-day levels by 2100. This corresponds to a doubling of CO_2 concentration relative to its pre-industrial level by the end of the century. For the A2 scenario, CO_2 emissions continue to climb throughout the century, reaching almost 30 Gt/yr, so that by the end of the century CO_2 concentration reaches more than triple its pre-industrial level.

EMFAC 2002 v.2.2 (Apr2003), the program used to develop California's on-road mobile source inventory, uses a diurnal temperature profile in the emission calculation. To investigate the impact of changes in climate on this sector of the inventory the default temperature profile was replaced by new profiles which reflect changes in temperatures based on GCM results for 2050 and 2100 for the A2 and B1 scenarios. The change in temperature (ΔT) between historical temperature calculated by the climate model and future years was applied to the default temperature profile in EMFAC. Three-hour temperature data from climate model (GFDL CM2.1) for two grid cells—one over northern California and one over southern California were used. The modeled historical temperature data used were from January 1, 1991 through December 31, 2000. The future temperatures are for two periods: January 1, 2046, through December 31, 2050 and January 1, 2095 through December 31, 2100 for A2 and B1 GHG scenarios. The statewide hourly average temperature (mean values of two grid points) was calculated for 10 year historical records and for 5-year block around 2050 and 2100 time periods. Then hourly temperature difference between mean historical records and mean temperature profiles from each GHG scenarios for 2050 and 2100 period were added to the 2005 baseline EMFAC hourly temperature to create eight new temperature profiles.

Three-hour temperature data from climate model (GFDL CM2.1) for two grid cells—one over northern California and one over southern California were used to estimate the effect of temperature on motor vehicle emissions. The modeled historical temperature data used were from January 1, 1991 through December 31, 2000. The climate change simulation data are for two periods: January 1, 2046, through December 31, 2050 and January 1, 2095 through December 31, 2100 for A2 and B1 GHG scenarios. The statewide hourly average temperature (mean values of two grid points) was calculated for 10 year historical records and for 5-year block around 2050 and 2100 time periods. Then hourly temperature difference between mean historical records and mean temperature profiles from each GHG scenarios for 2050 and 2100 period were added to the 2005 baseline EMFAC hourly temperature to create eight new temperature profiles.

Eight new temperature profiles were used, including both high and medium climate change scenarios for July 2050, August 2050, July 2100, and August 2100. The runs were performed for the current calendar year, 2005, using the statewide simple average option in EMFAC. Results were compared to baseline July 2005 and August 2005 emissions calculated with default EMFAC temperature profiles. Table 7 summarizes the EMFAC model output data for July and August for each of A2 and B1 GHG scenarios, and indicates percent differences from the baseline case for total reactive organic gases (ROG), evaporative ROG, oxides of nitrogen (NO_X), carbon monoxide (CO), methane (CH_4), and carbon dioxide (CO_2).

Table 7. Impact of diurnal temperature change on statewide on-road motor vehicle emission

Scenario	Date	Total ROG	Evaporative-ROG	NO_X	CO	CH_4	CO_2
EMFAC2005 Baseline	July	692*	300*	1,298*	6,843*	57*	505*
	August	695*	302*	1,285*	6,886*	58*	507*
A2-2050	July	5%	11%	-4%	3%	1%	3%
A2-2050	August	4%	9%	-4%	4%	1%	3%
B1-2050	July	4%	9%	-3%	3%	1%	2%
B1-2050	August	5%	10%	-4%	3%	1%	3%
A2-2100	July	13%	27%	-9%	11%	4%	8%
A2-2100	August	16%	31%	-11%	14%	5%	9%
B1-2100	July	6%	13%	-4%	4%	1%	4%
B1-2100	August	6%	13%	-5%	5%	2%	4%

* - Indicates baseline EMFAC emission in tons per day (tpd).

Increases were predicted for total and evaporative ROG, CO, CH_4, and CO_2, ranging from 1 to 31%. However NO_X decreased between 3% and 11%. EMFAC does not provide a temperature correction for particulate matter so no change in PM was predicted by EMFAC.

It is important to realize that these runs reflect the effect of temperature on the statewide average 2005 on-road mobile source emissions inventory. It does not reflect increases in population, or changes in vehicle technology and vehicle activity or the different temperature profiles which would be expected in different areas of the state. Thus, these changes in emissions do not represent what is expected in 2050 and 2100, but rather are a representation of on-road emissions assuming the forecasted 2050 and 2100 temperature profiles in 2005. Given that the statewide approach of the EMFAC model adds up all regional emissions in California, percentage differences in emissions estimates due to temperature do not necessarily represent percentage differences that might occur for specific air basins, air districts or counties.

Societal responses to variations in one or more of relevant climate parameters can influence energy usage and other behaviors (e.g., transportation) that in turn affect primary pollutant emissions. In addition, alteration of behavior in reaction to changes in the climate may also directly impact time-activity patterns that ultimately affect pollution emissions. Population growth, urbanization, and technological innovation are among a number of societal factors that directly affect emission rate and air quality. Accordingly, these connections must be identified and analyzed to achieve accurate forecasts, and to evaluate the relative contributions of various factors to the ultimate outcomes.

5.0 Impact of Climate Change on Meteorology and Regional Air Quality in California

5.1. Background

California's unique combination of large urban populations situated in confined air basins that are subject to severe air pollution events causes significant public health concerns. Ozone and airborne particulate matter are two of the main ingredients of the photochemical "smog" that can form when atmospheric mixing is low, causing pollutants to be trapped near the earth's surface. The adverse health effects of ozone and airborne particulate matter are widely acknowledged, and reducing the concentrations of these pollutants is an important objective for the State of California.

Meteorology plays a significant role in the determination of air pollution concentrations in California. Measurements show that large scale meteorological patterns such as El Niño events can significantly change the frequency and severity of air pollution episodes. El Niño events change meteorological patterns for 1 year, and they typically occur every 5-7 years. In contrast, climate change refers to a sustained shift in meteorological patterns that gradually occurs over a longer time period. It is expected that climate change will significantly affect meteorological patterns in California over the next decade and longer. The implications of climate change on air quality problems in California are largely unknown.

Previous studies have examined the effect of climate on regional air quality in the central and eastern portions of the United States (Hogrefe et al., 2004; Mickley et al., 2004). These studies used output from Global Climate Models (GCMs) to study the frequency of large scale weather patterns that promote the formation of air pollution events. The GCM output can also be dynamically downscaled using regional meteorological models to simulate air pollution formation with regional air quality models. The results of these previous studies predict that the frequency of summer ozone air pollution events will increase in the future due to altered climate and increased background concentrations of ozone.

A directed study of the eastern U.S. (Hogrefe et al., 2004) found that, around 2050, climate change would be the most important factor leading to increases in the upper quartile of 8-hour average surface ozone concentrations, whereas projected changes in anthropogenic emissions would cause increases only half as large. Moreover, estimated changes in surface conditions (e.g., vegetation cover) would have the least effect on the upper quartile of 8-hr ozone abundances. Similar conclusions were reached by Langner et al. (2005) regarding future surface ozone concentrations in Europe. This research strongly suggests changing climate will be the primary driver of variations in surface ozone by 2050. Nevertheless, substantial contributions associated with changes in emissions (and surface conditions) should also be taken into account.

The analysis of climate change on regional particulate matter concentrations is less certain because the atmospheric processes which lead to the formation of particulate matter are more complex and computationally challenging than ozone models. Sensitivity studies have been carried out to examine how regional particulate air pollution responds to direct changes in temperature, relative humidity, and mixing depth during a typical air pollution episode that occurred in California's South Coast Air Basin (SoCAB) (Aw and Kleeman, 2003). The results of this analysis suggested that increased temperature increases ozone concentration

and the production of semi-volatile secondary products, but reduces the partitioning of those semi-volatile products to the particle phase. These studies suggest there is an urgent need to project air quality and exposure levels for future climate change scenarios by performing a more comprehensive analysis of the effect of climate change on air quality in California.

5.2. Quantitative Analysis Method

The goal of this project is to identify linkages between climate and air quality for major airsheds in California. Two methods were used to accomplish this goal: perturbations of regional air quality models and statistical downscaling of GCM results.

A detailed perturbation analysis was carried out to study the effect of meteorology on ozone and $PM_{2.5}$ concentrations during present-day air pollution events. Two air pollution episodes in the South Coast Air Basin (SoCAB) (September 7-9, 1993; September 23-25, 1996) and one air pollution episode in the San Joaquin Valley (SJV) (January 4-6, 1996) were used to span the wide range of meteorological conditions and pollutant concentrations experienced in California. The SoCAB and the SJV are the two most heavily polluted air basins in California. The air pollution episodes described above are distinctly different in character but each episode has ozone and/or $PM_{2.5}$ concentrations that greatly exceed the standards designed to protect human health.

The extensive meteorological, emissions, and air quality information needed to support detailed modeling of each episode has been assembled previously. Each base-case episode has been extensively validated against measured concentrations in previous studies providing a solid foundation for the perturbation analysis. Temperature, humidity, mixing depth, and wind speed were systematically perturbed and the corresponding change in the regional distribution of 1-hr average ozone concentrations and 24-hr average $PM_{2.5}$ concentrations was calculated.

Temperature perturbations considered in this study were +2K and +5K. These values span the range of IPCC projections for global mean surface temperature rise over the next 100 years. The actual temperature rise in California is not uniform and it may differ from these values. Never-the-less, +2K and +5K perturbations provide a useful starting point to investigate sensitivity. Humidity perturbations were combined with temperature perturbations to avoid artificially specifying an atmosphere with RH>100%. Each temperature perturbation was evaluated once with constant absolute humidity and once with constant relative humidity. Perturbations in wind speed and mixing depth were arbitrarily chosen to be +20% and +50%, respectively. These values resulted in an observable effect, enabling some evaluation of the sensitivity of pollutant concentrations to these variables.

The internally-mixed version of the UCD-CIT air quality model was used to predict the response of pollutant concentrations to changes in meteorological parameters. Previous studies (Kleeman and Cass, 2001; Mysliwiec at al, 2002; Held et al, 2004) have described the formulation of the UCD/CIT source-oriented air quality model. All of the results from model simulations presented in this research project were produced specifically for the current report. Further updates were also made to the secondary organic aerosol (SOA) formation mechanism that was used for SoCAB simulations in this report as part of a collaboration

with an ongoing U.S. EPA project. The SOA formation mechanism was not updated for simulation of the winter SJV episode because the low photochemical activity during this episode is expected to produce minimal amounts of SOA.

A large body of previous work, and the sensitivity studies above, indicate that the frequency of atmospheric stagnation events, and possibly the occurrence of warm synoptic events, plays a significant role in determining the number of days with unhealthy air quality each year in California. High pressure systems situated just off the coast of California produced warm temperatures aloft that encouraged elevated temperature inversions and weak winds. Climate change will affect the frequency and severity of atmospheric stagnation events in California. A method is needed to asses how this will influence air quality problems.

A statistical downscaling technique was developed to relate high air pollution concentrations to large-scale meteorological variables predicted by global General Circulation Models (GCMs). The variables investigated for the statistical downscaling method were the ones identified to be important in the perturbation analysis described above. Simple linear correlations were calculated between air pollution concentrations and various meteorological parameters. Statistically significant relationships were then used to predict future air quality in the SJV and SoCAB.

5.3. Results and Discussion

Figure 6 summarizes the range of changes in predicted ozone and $PM_{2.5}$ concentrations resulting from the perturbations studied in the current project. The bars shown in Figure 6 illustrate the largest change in pollutant concentrations predicted anywhere in the domain, while the circles illustrate the change in the maximum concentrations. When the circles are located close to the extreme values of the bars, it shows that the greatest change in concentration occurs at the location of maximum concentration.

Figure 6 illustrates that increasing wind speed results in the greatest decrease in ozone and $PM_{2.5}$ concentrations in the SoCAB during both the September 7-9, 1993 episode and the September 23-25, 1996 episode. These reductions occur at the location of maximum base-case concentrations except for the case of ozone in the SoCAB on September 25, 1996 when maximum ozone concentrations are not significantly affected by wind speed. Figure 6 also shows that increasing temperature at constant absolute humidity generally increases peak ozone concentrations and decreases peak $PM_{2.5}$ concentrations in all the episodes studied. Part of this temperature effect on $PM_{2.5}$ concentrations may be caused by reduced particle water content, since relative humidity decreases as temperature increases and absolute humidity remains constant. Increasing temperature at constant relative humidity increases predicted ozone concentrations even further due to the enhanced production of hydroxyl radical. The increased absolute humidity also mitigates the reduction in $PM_{2.5}$ concentrations, and even increases $PM_{2.5}$ concentrations in the SJV in regions with large excesses of gas-phase ammonia.

Figure 6 generally shows that increasing mixing depths usually increases surface ozone concentrations because the extra volume allows for increased dilution of fresh NO_X emissions, reducing the titration of surface ozone concentrations. This effect may not be significant at the location of maximum ozone concentration. The increased mixing depth

usually also reduces primary $PM_{2.5}$ concentrations through increased dilution. This trend generally holds true in the SoCAB, but isolated regions in the SJV may experience slight increases in $PM_{2.5}$ concentrations in response to increased mixing depth.

The trends illustrated in Figure 6 provide a mechanistic understanding of the likely impacts of climate change on air quality in California and suggest some preliminary conclusions. Temperatures will almost certainly rise in future air pollution episodes, leading to increased ozone concentrations. Particulate nitrate concentrations are likely to decrease slightly in the SoCAB as temperatures rise, but they may stay constant or even increase slightly in the SJV depending on the corresponding change to humidity. A regional meteorological model will be used to dynamically downscale representative stagnation episodes in the future during the second phase of this project to support a more detailed analysis of how future meteorology will change pollutant concentrations.

Simple linear correlations were investigated between daily maximum 1-hr average ozone concentrations and the following meteorological variables: temperature at 850 millibars (T850), temperature at 925 millibars (T925), temperature at 1000 millibars (T1000), wind speed at 850 millibars (wsp850), wind speed at 925 millibars (wsp925), and wind speed at 1000 millibars (wsp1000). The most significant variable associated

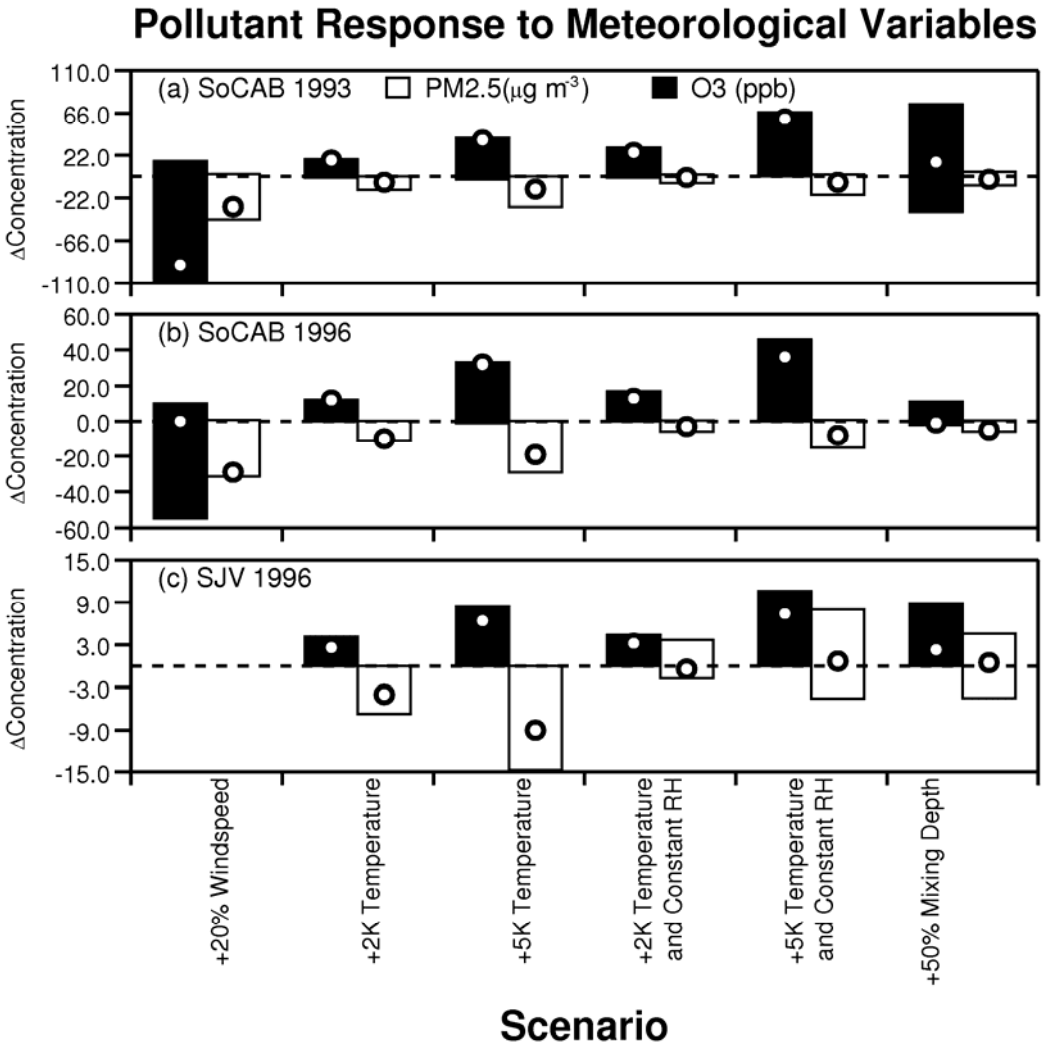

Figure 6. Summary of pollutant response to meteorological perturbations during pollution episodes that occurred in (a) Southern California September 9, 1993, (b) Southern California September 25, 1996, and (c) the San Joaquin Valley January 6, 1996. The bars represent the range of concentration change at any location in the modeling domain in response to the indicated perturbation. The circles represent the concentration change at the location of the maximum concentration for each pollutant.

with daily maximum 1-hr average ozone concentrations measured at locations in both the SJV and the SoCAB was found to be temperature at 850 millibars (T850) on the same day.

Figure 7 shows the predicted number of days each year that would have 1-hr average ozone concentrations greater than 90 ppb at Riverside if the emissions and upwind boundary conditions for the SoCAB remained unchanged between the years 2000–2100. The exceedance days shown in Figure 7 are not intended to predict actual conditions in the future, since the climate model temperature are only a small subset of possible future climate in the California region, and future emissions and upwind boundary conditions will change in response to population growth, control programs, and new technology. Rather, the trends illustrated in Figure 7 illustrate the degree to which future meteorology will encourage a greater frequency of high ozone events relative to present day conditions. All of the trends illustrated in Figure 7 are positive, indicating that climate warming will tend to produce an increased frequency of high ozone days in the SoCAB in the future. The A2 emissions scenario (higher GHG emissions case) has a greater upward trend after the year 2050 than the B1 emissions scenario (lower GHG emissions case).

Figure 8 shows the predicted number of days each year that would have 1-hr average ozone concentrations greater than 90 ppb at Visalia if the emissions and upwind boundary conditions for the SJV remained unchanged between the years 2000–2100. Once again, this figure is designed to show the tendency for future meteorology to encourage ozone formation relative to present conditions (not predict future ozone concentrations). The GFDL simulations combined with the statistical downscaling technique once again predict a greater tendency for future meteorology to encourage an increased frequency of high ozone days, with more exceedances associated with the A2 emissions scenario.

Downscaling techniques were also investigated for airborne particulate matter, but no robust association could be found. Work is continuing to develop a statistical downscaling technique for $PM_{2.5}$. One possible outcome of this analysis is that increased temperatures could lower $PM_{2.5}$ concentrations during the early fall period that has historically experienced the highest $PM_{2.5}$ concentrations in the SoCAB, but $PM_{2.5}$ concentrations later in the year could increase as temperatures rise during the winter months. However, the relative contributions of these changes are still not clear, because it is necessary to determine whether vertical temperature gradients, including inversions will increase or decrease and how wind speeds and directions will be affected as California's regional climate changes. Dynamically downscaled regional atmospheric simulations may be necessary to augment and clarify the larger scale indications from the GCMs. Thus, climate change may not lower the peak $PM_{2.5}$ concentration experienced during the year, and climate change may alter the length of the $PM_{2.5}$ season in unforeseen ways. These questions will be investigated in the second phase of the project.

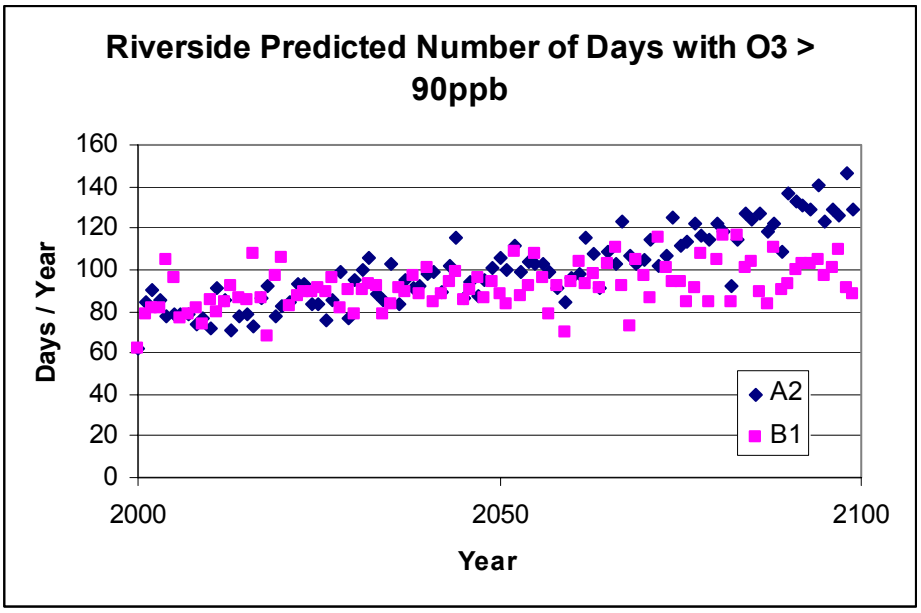

Figure 7. GFDL predictions for monthly mean 850 millibar temperatures in the SoCAB converted to estimates of the number of days each year with ozone greater than 90 ppb at Riverside. Global emissions scenario A2 has higher global CO2 emissions than scenario B1.

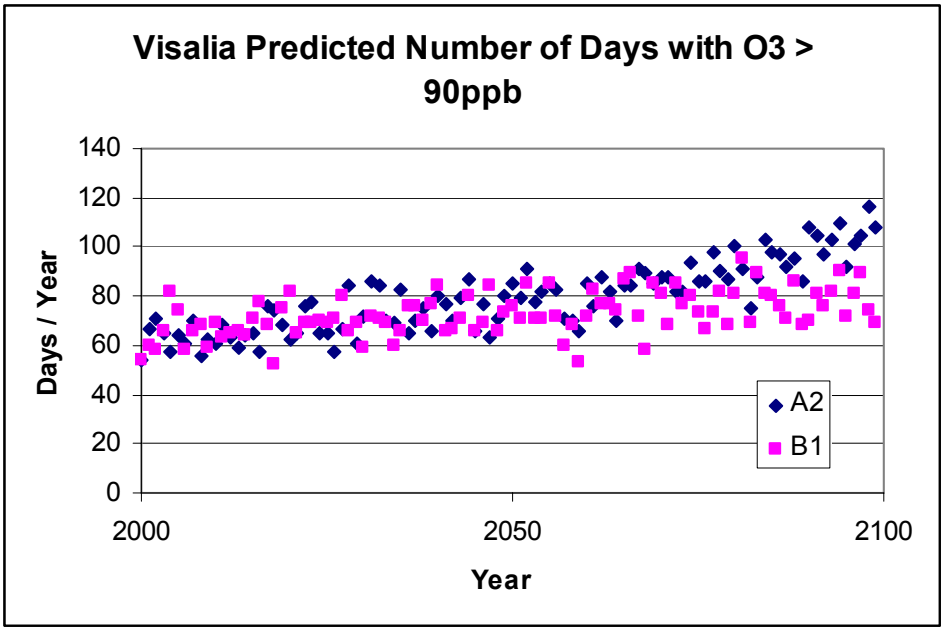

Figure 8. GFDL predictions for monthly mean 850 millibar temperatures in the SJV converted to estimates of the number of days each year with ozone greater than 90 ppb at Visalia (Note: Trends are based on historical data with no change in emissions).

GCM predictions from the GFDL model suggest that climate change will increase the frequency of warm synoptic events that encourage ozone formation in both the SJV and the SoCAB. Global emissions scenarios that have higher carbon emissions appear to encourage this trend. Future emissions reduction and the adoption of new technology will need to offset this tendency for the formation of ozone pollution episodes in order to protect the public health of California residents.

5.4. Summary

Two air pollution episodes in SoCAB (September 7-9, 1993; September 23-25, 1996) and one air pollution episode in the SJV (January 4-6, 1996) were used to investigate the effect of meteorological conditions on air pollution in California. Temperature, humidity, mixing depth, and wind speed were systematically perturbed and the corresponding change in the regional distribution of 1-hr average ozone concentrations and 24-hr average $PM_{2.5}$ concentrations was calculated. The following systematic behavior was observed across all the episodes.

Increased wind speed reduces ozone and $PM_{2.5}$ concentrations by enhancing dilution of primary emissions. Increased mixing depth reduces $PM_{2.5}$ concentrations by enhancing dilution of primary emissions. Surface NO_X concentrations are also reduced by enhanced dilution leading to an increase in surface ozone concentrations because less NO_X is available to titrate the ozone that is produced aloft and mixed to the surface.

Increasing temperature with constant absolute humidity increases ozone concentrations due to increased rate of photochemical reactions but reduces $PM_{2.5}$ concentrations due to increased volatilization of ammonium nitrate and reduced particle water content.

Increasing temperature with constant relative humidity increases ozone concentrations further because water vapor provides a source of hydroxyl radical to the system. The additional water vapor also maintains the particle water content, reducing the volatilization of ammonium nitrate at warmer temperatures. $PM_{2.5}$ concentrations in the SoCAB decrease in response to higher temperature with constant relative humidity. The magnitude of this decrease is smaller than the case with less water vapor. Higher temperatures at constant relative humidity actually increase predicted $PM_{2.5}$ concentrations in some regions of the SJV that have cool base-case temperatures and a large excess of gas-phase ammonia.

A statistical downscaling technique was also developed to relate the frequency of meteorological conditions that encourage high ozone formation to large-scale meteorological variables predicted by GCMs. Based on statistical linkages of ozone and 850 millibar temperatures, the warming predicted by climate model GFDL simulations for 2050 and 2100 results in an increased frequency of meteorological conditions that encourage the formation of ozone in California. The incidence of days with favorable conditions for ozone formation grows as warming increases through the 21st Century. By the end of the 21st Century, assuming the same mechanisms and emissions base conditions prevail as today, the frequency of days with favorable conditions for ozone formation increases by 25%-80%, depending on the amount of warming.

The trends identified above suggest some preliminary conclusions about the likely effect of future climate change on air quality in California. Future temperatures during stagnation

events are likely to be warmer than current temperatures, leading to the conclusion that climate change will produce meteorological conditions that favor higher ozone concentrations and a greater frequency of ozone episodes. Warmer temperatures will also favor decreased PM2.5 concentrations in the SoCAB, and constant or slightly increased PM2.5 concentrations in the SJV.

All of the conclusions stated above are preliminary, since meteorology is only one factor that determines air pollution in California. Changes to emissions inventories through population expansion, application of emissions control programs, interaction between future temperature and future emissions, changes to background pollutant concentrations, and changes to the frequency and duration of stagnation events must also be considered. Phase II of the current project will address some of these issues using dynamically downscaled meteorology combined with detailed air quality modeling in combination with the development of a future emissions inventory for the SJV (part of a project funded by U.S. EPA). This more detailed analysis will support more definitive conclusions about ozone and PM2.5 response to future climate change.

6.0 Air Pollution-related Health Effects

6.1. Background

It is well known that exposure to sufficient concentrations of various air pollutants, including ozone, particulate matter, nitrogen dioxide, sulfur dioxide, and carbon monoxide, can induce a variety of adverse health effects (CARB, 2000). Both the federal government and the state of California have promulgated ambient air quality standards to prevent adverse health effects from these pollutants. Ambient air quality standards are based on health effects, and by definition, few if any health effects are expected at attainment with ambient air quality standards. Consequently, the magnitude of adverse health impacts related to PM and ozone under future climate scenarios depends on the extent to which ambient air quality standards are or are not attained.

The air pollutants of greatest concern are ozone and particulate matter (PM), and these two pollutants are currently believed to be responsible for the majority of observed adverse effects associated with current ambient concentrations of air pollutants (Bernard et al., 2001; CARB, 2000, 2002, 2005). Recent estimates for some of the public health impacts associated with current concentrations of ozone and PM compared to with attainment of the California ambient air quality standards for ozone and PM (CARB, 2002, 2005) suggest that annually the following number of cases occur in California:

- 7130 premature deaths
- 13,200 hospitalizations
- 6.4 million school absences
- 5.9 minor restricted activity days

Attainment of ambient air quality standards is generally through regulations that control emissions. Over the past 30 years considerable progress has been made toward attainment of these health-based ambient air quality standards, however many areas of California have not yet attained the existing ambient air quality standards for ozone or PM. State Implementation Plans (SIPs) have been developed to bring California into attainment with ambient air quality standards, with attainment currently planned for 2020 (CARB, http://www.arb.ca.gov/planning/sip/sip.htm).

Existing air pollution control programs, however, do not consider the impact of climate change even though it could slow progress toward attainment of the ambient air quality standards and increase control costs by boosting emissions, accelerating chemical processes, and raising inversion temperatures during summertime stagnation episodes. The NRC (2004) recommended that "the air quality management system will need to ensure that pollution reduction strategies remain effective as the climate changes, because some forms of air pollution, such as ground-level ozone, might be exacerbated." Air pollution control agencies should build climate change considerations, which are expected to be significant for at least ozone, into efforts to attain the health-based ambient air quality standards.

6.2. Ozone

Ground-level ozone is a secondary air pollutant that primarily forms through a complex series of photochemical reactions between nitrogen oxides and reactive hydrocarbons. The principal source of these precursors in urban areas is motor vehicles and the fuel supply system that supports them, although vegetation can contribute significant amounts of reactive hydrocarbons. Because ozone formation is highly dependent on solar radiation to drive the photochemical reactions, significant concentrations of ozone typically appear only during May through October, and during daylight hours (USEPA, 1996).

In areas near principal emissions sources the ozone concentration profile shows a characteristic mid-day peak that typically lasts for an hour to two. However, areas downwind of urban areas can have elevated ozone concentrations into the evening hours related to regional transport. In addition, downwind areas tend to experience an ozone concentration profile characterized by a lower peak concentration that remains elevated for a longer time period, typically on the order of six to eight hours (USEPA, 1996; CARB, 2005).

The extensive literature on the responses of human subjects to controlled concentrations of ozone was recently reviewed by the California Air Resources Board (CARB, 2005). Collectively, this literature indicates that one- to three-hour exposures to ozone concentrations as low as 0.12 ppm with moderate to heavy exercise can induce decrements in pulmonary function and increases in respiratory and/or ventilatory symptoms for some subjects. Increased airways reactivity and inflammation have been reported with one to three hour exposures to 0.40 and 0.18 ppm ozone, respectively. Concern about the impacts of longer averaging times led to studies using a protocol that simulates a day of active outdoor work or play. These studies demonstrate that statistically significant group mean decrements in lung function, increases in symptoms of respiratory and/or ventilatory irritation, increased airways reactivity and airways inflammation can be induced with 6.6 to 8-hour exposures to ozone concentrations as low as 0.08 ppm.

Animal toxicological studies have shown that chronic ozone exposure can induce morphological changes throughout the respiratory tract, particularly at the junction of the conducting airways and the gas exchange zone in the deep lung. The morphological changes found in animals following chronic ozone exposures are similar to those characteristic of chronic lung disease (Last et al. 1994; Reiser et al. 1987; Harkema et al. 1993). There is some evidence from primate studies that intermittent challenge with a pattern of ozone exposure designed to simulate seasonal episodes, with extended periods of clean air in between extended periods of ozone exposure can lead to greater injury than daily exposures to similar concentrations (Tyler et al. 1988). A series of studies in juvenile monkeys has demonstrated that cyclic multi-day exposures to relatively high ozone concentrations (0.5 ppm) can impact development of the lung (Evans et al., 2003; Schelegle et al. 2003) . These animal data provide a biologically plausible basis for considering that repeated inflammation associated with exposure to ozone over a lifetime may result in sufficient damage to the respiratory tissue such that individuals may experience some degree of chronic lung injury.

A large number of epidemiologic studies published in the last several years have shown positive associations between short-term changes in ozone levels (i.e., daily) and several health effects including hospitalization (e.g., Burnett et al. 1997; Anderson et al. 1997),

emergency room visits for asthma (e.g., Tolbert et al. 2000), restrictions in activity (Ostro and Rothschild, 1989), respiratory symptoms, particularly in asthmatics (e.g., Gent et al. 2003), and school absenteeism (Gilliland et al. 2001). Many of the findings are observed or studied only in the summer season, when ozone is usually highest. A growing body of data now suggests that ozone concentration represents an independent risk factor for premature death (Dominici, 2003; Bell et al., 2004, 2005; Levy et al., 2005; Gryparis et al., 2004; Ito et al., 2005).

Epidemiology has a key role to play in addressing the health impacts of long-term (i.e., months to years) ozone exposures in humans. The following outcomes have been associated with long-term ozone exposure: respiratory inflammation (Kinney et al.,1996), lung function and respiratory symptoms (Kinney and Lippmann, 2000), reduced growth of lung function in children (Galizia and Kinney 1999; Tager et al. 1998; Kunzli et al. 1997; Gauderman et al. 2000), and asthma prevalence (Abbey et al. 1999; McConnell et al. 2002). There is inconsistent and inconclusive evidence for a relationship between long-term ozone exposure and increased risk of death (Abbey et al. 1999; Pope et al. 2002).

Ozone concentrations are highest outdoors and the proportion of outdoor ozone penetrating indoors is variable (20%-80%). There are few indoor sources of ozone. Greater penetration occurs with open windows and doors and in the absence of air conditioning. Consequently, individuals at greatest risk of experiencing adverse health effects from ozone exposure are those who spend prolonged periods of time outdoors while participating in activities that increase the breathing rate. This group is comprised primarily of children, outdoor workers, and recreational and professional athletes.

6.3. Particulate Matter

There are many sources of particulate matter (PM) and the size and chemical composition of particles from different sources varies considerably. Particles smaller than 10 microns in diameter (PM10) can be inhaled into the deep lung, and there is particular concern about particles 2.5 microns or less in diameter (PM2.5) (USEPA, 2004). Some particles are directly emitted from combustion processes, such as through vehicle combustion of gasoline or diesel fuel, or generation of electrical power through combustion of oil, natural gas or coal. PM is also emitted through a variety of industrial processes. Natural sources of PM include soil and dust. Some particles form through chemical reactions in the atmosphere. Examples of these particles include sulfates, nitrates and organic aerosols (Seinfeld and Pandis, 1998; Finlayson-Pitts and Pitts, 1999).

Because of logistical difficulties in performing human and animal exposure studies, the majority of literature on the public health impacts of particulate matter comes from epidemiologic studies. This literature fairly consistently reports statistically significant associations between changes in PM10 and PM2.5 concentrations and a range of adverse health outcomes, both on a daily and a long-term basis. Associations between daily and long-term average changes in both PM10 and PM2.5 and mortality appear to be independent of the effect of weather factors, seasonality, time, and day of week (Dockery et al.,1993; Pope et al., 1995; Krewski et al., 2000; Burnett and Goldberg, 2003; Fairley, 2003; Ito, 2003). Studies over the past several years consistently report associations between PM10 and PM2.5 and several different measures of hospitalization or urgent care for exacerbation of respiratory

(i.e., chronic obstructive pulmonary disease, asthma) or cardiovascular diseases, for example, congestive heart failure (Atkinson et al., 2003; Zanobetti and Schwartz, 2003; Sheppard, 2003). These effects have been reported primarily among elderly individuals, but effects have been also reported among all age groups, including children under age 18 (Ostro et al., 1999; Moolgavkar et al., 2000).

Data from the past quarter century suggest that long-term (i.e., months to years) PM exposures are associated with increased risk of mortality from cardiopulmonary causes (Dockery et al., 1993; Pope et al., 1995, 2002; Krewski et al., 2000). Associations with PM10 and PM2.5 have also been reported for chronic respiratory symptoms or disease, and possibly with decreased lung function (e.g., Ferris et al., 1973, Hodgkin et al., 1984; Mullahy and Portney, 1990).

6.4. Implications of Meteorological Effects on Air Quality for Health

Public health impacts related to air pollution under future climate scenarios are difficult to predict for several reasons. While rising temperature will increase the rate at which atmospheric chemical reactions proceed, thereby increasing concentrations of ozone and particulate matter (PM), our analysis suggests that relative humidity, wind speed, and mixing height all interact with temperature to affect the resulting pollutant concentrations. The analysis also indicates that changes in the concentrations of ozone and PM are unlikely to be uniform across an air basin, making a health impacts analysis based on a simple incremental approach inappropriate. Ultimately, health impacts of air pollution exposure under climate change scenarios will depend on the extent to which California is able to attain ambient air quality standards.

California is taking steps toward attaining existing ambient air quality standards for ozone and PM. Consequently, the magnitude of health impacts attributable to ozone and PM in the future will be proportional to the degree to which ambient air quality standards are not attained. It is clear that increasing temperature will make attainment of these standards more difficult.

6.5. Adaptations

The need for adaptations to address air pollution-related health effects is fundamentally tied to the extent to which ambient air quality standards are not attained throughout the State. Increasing temperatures will likely increase the difficulty of attaining current ambient air quality standards, and increase the time period required to reach attainment.

It is likely that as temperatures increase people will alter their behavior and activity patterns, resulting in increased time indoors where ozone levels are considerably lower than outdoors. In addition, air conditioning, which is projected to become increasingly common over the next few decades (McGheein and Mirabelli, 2001), removes ozone, and a large fraction of PM (Hanssen et al. (2001) from the air. Consequently, if global warming causes people to increase the amount of time they spend indoors in air conditioned environments where ozone and PM concentrations are lower than outdoors, ozone- and PM-related health effects would be expected to decrease, even if outdoor concentrations increase.

Adaptations should also include development of improved action plans to inform the public of anticipated air quality standard exceedances through various media, plans to reduce emissions during air pollution emergencies, and public education campaigns on the health impacts of ozone and PM exposures as well as effective air pollution avoidance behaviors.

7.0 Infectious Diseases

Meteorological changes can influence human disease through both direct and indirect effects on pathologic microorganisms, vectors, reservoirs and hosts (Colwell and Patz, 1998). Available evidence suggests that the incidence and spread of a number of infectious diseases can be affected by various weather-related factors, and suggests that climate change has the potential to affect their range, incidence and spread (Colwell and Patz, 1998). As noted above, weather refers to meteorological conditions at a specific place and time with a relatively short time frame, up to a year or two. Climate, on the other hand, refers to the same meteorological conditions, but over a longer time frame, for example, decades or centuries.

Most research to date on the impacts of climate change on infectious diseases has focused on short-term changes in weather patterns, primarily in rainfall and ambient temperature, as opposed to long-term changes related to global climate change, largely because of the large influence of relatively short-term weather patterns of the ecology, and range of pathogens.

7.1. Waterborne Diseases:

Waterborne diseases typically occur in sporadic outbreaks (Curriero et al., 2002; Charron et al. 2004; Colwell and Patz, 1997; Louis et al., 2003). Historical data link many outbreaks of waterborne disease to water contamination subsequent to runoff from heavy rainfall, flooding, and/or sewage overflow. For example, Curriero, et al. (2002) found that for the period of 1948 to 1994, 51% of waterborne disease outbreaks in the United States were preceded by rainfall events that were above the 90th percentile in intensity, and 68% were preceded by rainfall events above the 80th percentile. Outbreaks related to surface water contamination showed the strongest association with extreme precipitation during the month of the outbreak, while there was a two month lag for groundwater contamination events.

Polluted runoff is increasingly an issue of concern in coastal waters of California where urban growth and development, and land use decisions impact the quality of runoff water that flows through creeks and rivers to coastal beaches. California's greatest urban runoff problems are in the southern part of the state where expanding urbanization, development and an increasing population generate pollution that is discharged to the watershed, and flows into the Pacific Ocean (Dwight et al., 2002). Temporal and spatial analysis of two years of data on discharge from the Los Angeles, San Gabriel and Santa Ana Rivers into the Pacific Ocean showed that bacteria levels were highest near the river mouths, and that precipitation was significantly associated with an increase in the bacteria load at beaches in the vicinity of the river outflows (Dwight et al., 2002). Louis et al. (2003) reported similar findings for the Chesapeake Bay on the East Coast of the United States.

Groundwater is not immune from effects related to severe precipitation events. It can become contaminated through contamination of surface waters that feed the aquifers, leakage from septic systems or sewers that overflow, and leaking dumps. Contamination can also occur during or after water treatment if treatment is insufficient for the pathogen load, of if the water delivery system is breeched (Rose et al., 2001).

The most common waterborne diseases in the United States are cryptosporidiosis and giardiasis, which are caused by parasites that often infect livestock and wild animals. Oocytes of these parasites are shed in the feces of infected animals, and can be washed into streams, rivers, and lakes, and subsequently to coastal beaches by rainfall events. Infection with these organisms typically causes gastrointestinal illness (Rose et al., 2001; Charron et al., 2004).

Humans become infected with waterborne diseases through direct ingestion, absorption through the skin, water contamination of food, and contamination of seafood due to toxic algal blooms (Rose et al., 2001). People must be directly exposed to an infectious organism to acquire disease, meaning that they must do such things as drink contaminated water, swim in contaminated water, or eat contaminated food (Rose et al., 2001).

An additional concern for this sector is that wells, water and sewage treatment facilities have been designed to operate within an expected range of rainfall, temperature, snow pack and melt, water and sea levels and coastal dynamics (Charron et al., 2004). Consequently, the risk of water contamination increases in proportion to the extent that these systems are overtaxed.

Combined sewer systems are a significant source of drinking and recreational water contamination, and although they are considered antiquated, some communities in California continue to be served by combined systems. These systems carry both storm water and raw sewage to treatment plants. When the system is overtaxed, for example by heavy rainfall, the sewers overflow directly into a surface water body, for example a river or lake. This introduces untreated storm runoff water and sewage, along with any pathogens, pollutants, chemicals and industrial wastes they contain, directly into a water body, contaminating drinking water sources, beaches, fish and shellfish (Charron et al., 2004).

Climate change is expected to alter historical rainfall patterns, and it is likely that the larger number of severe precipitation events predicted will lead to an increased number of instances where water and sewage treatment facilities fail, leading to exposure of the public to contaminated water.

It is unlikely that climate change will affect the mammalian reservoirs for organisms such as chryptosporidia and giardia, although it could impact the viability of oocytes once they are shed by mammalian hosts, depending on oocyte tolerance to changes in heat, humidity and other weather-related factors (Rose et al., 2001). The population of many pathogens increases at higher temperatures, and this is likely to occur in lakes, streams and coastal zones as water temperature increases (Rose et al., 2001). In the coastal zone, toxic algal blooms will likely be more frequent as ambient, and consequently water, temperature rises, increasing the risk of illness originating from aquatic recreation, such as swimming and surfing, and from contamination of seafood (Rose et al., 2001). Food supplies could also become contaminated through use of contaminated irrigation water, and lack of field sanitation (Rose et al., 2001).

The gastrointestinal diseases that usually result from exposure to contaminated water may be underreported, since illnesses with similar symptoms have many non-water-related causes. In addition, most cases of these diseases are self-limiting in a generally healthy

population. It is, however, clear that the potential for public exposure to contaminated water is increased with increasing ambient temperature (Rose et al., 2001).

Although it is well known that periods of heavy rainfall, flooding and sewage overflow are associated with outbreaks of waterborne illness (Curriero et al., 2002), it is not possible to forecast likely incidence of these diseases. Outbreaks of waterborne illness are related to complex interactions between the water contamination potential of discrete rainfall events, the capabilities of water and sewage treatment facilities, the effectiveness of public health programs designed to minimize exposure of the public to contaminated water, and the public's compliance with these programs and recommendations.

The people most at risk of experiencing serious illness with exposure to contaminated water include the very young, the elderly and infirm, and those with compromised immune systems. Those living in poverty may also be at increased risk if they do not have access to adequate supplies of bottled water during contamination events.

7.1.1. Adaptations

The local, State and Federal governments have protocols in place to address health issues arising from water contamination. Adaptations include public information campaigns and public service announcements to alert the public that there is a water-related health threat. Public compliance with beach closures, and widespread availability and use of bottled water during periods of water contamination is key to prevention of waterborne illness. Availability of adequate stocks of antibiotics for treatment of active infection is also necessary.

Recommendations for future action by the State and communities include evaluation of the capacities of water and sewage treatment facilities, and modernization and expansion of these facilities as necessary to meet predicted worst-case precipitation scenarios, along with replacement of the remaining combined sewage systems in the State with modern systems.

7.2. Vector-borne Diseases

Vector-borne diseases are infectious diseases that are transmitted to humans and other animals by blood-feeding insects, such as mosquitoes, ticks and fleas. These diseases are caused by a variety of viruses, bacteria and protozoa that spend part of their life cycle in an insect host, and are spread to humans and animals during insect feeding. Because insects are cold-blooded, their life cycles are affected by changes in climate, and this in turn can also affect the life cycles of these infectious organisms.

Although twelve mosquito-borne diseases are known to occur in California, only Western Equine Encephalitis (WEE), West Nile Virus (WNV), and St. Louis Encephalitis Virus (SLV) are significant causes of human disease. Humans are dead-end hosts for these zoonotic diseases; rather, these diseases are maintained through a cycle that depends of wild birds and mosquitoes, with humans an incidental host. The primary vector in California appears to be the *Culex tarsalis* mosquito, although other mosquito sub-species can also carry these diseases (California Department of Health Services, 2004). Natively acquired cases of anthropogenic vector-borne diseases such as malaria and dengue fever, which require no animal host, are extremely rare in the United States (Gubler et al., 2001).

Table 8 below, based on the California Department of Health Services surveillance report (CDHS, 2004—available at www.dhs.ca.gov/ps/dcdc/pdf/cdtables/CM-DEC%202004.pdf) gives the number of reported cases of several vector-borne diseases for the period 2002 through 2004.

Table 8. Reported Cases of Vector-borne Diseases in California

Disease	2004	2003	2002
Arboviruses*	91	0	0
Lyme Disease	51	84	97

*WEE, SLV, and WN combined

Mosquitoes and these three viruses appear to be temperature sensitive. However, transmission and maturation of the viruses is dependent on many factors in addition to ambient temperature, including the specific organism, the interaction of the various aspects of climate change (temperature, humidity, rainfall) on the ecology, development, behavior and survival of both the organism and its host. Consequently, increasing temperature may or may not increase the rate of transmission of these diseases depending on the outcome of interactions between aspects of climate, the organism itself, and the insect host (Gubler et al., 2001).

Each of these viruses has a different pattern of susceptibility to climate factors, including temperature, humidity, and rainfall. In some cases, a specific weather pattern over several seasons appears to be associated with increased pathogen transmission rates. These three viruses appear to differ in their responses to climate stresses. For example, WEE activity is typically highest during El Niño conditions with wet winters, extensive run-off, cool springs, increased *Cx. Tarsalis* abundance, and virus spillover to other mosquito subspecies, particularly *Ochlerotatus*. SLE activity appears to be greatest during conditions of drought and hot summer temperatures, such as associated with La Niña conditions (Barker et al., 2003). Little is known about the ecology of WN virus in California, and currently the SLE pattern is assumed (California Department of Health Services, 2004).

The most common tick-borne disease in the United States is Lyme Disease, caused by the bacteria *Borrelia burgdorferi,* and transmitted in the West by the *Ixodes pacificus* tick. Transmission of the disease is most frequent during early summer, during the questing period of the nymphal stage of tick development. The primary hosts for this disease are deer and mice, and risk of infection is increased in proportion to the populations of each (Gubler et al., 2001). Lindgren et al. (2000) reported a northern shift in the distribution of ticks related to fewer very cold days during the winter season in Sweden. Although not the same tick species as that seen in California, the results of the analysis support the notion that a vector's geographical range can alter with changing ambient temperature.

Climate affects the life cycle of ticks both directly and indirectly. Temperature must be high enough for completion of the tick's life cycle, and humidity must be high enough such that the eggs do not dry out. Temperatures above, and humidities below the optimal reduce tick survival rate, and consequently disease transmission potential. In addition, the geographical range of ticks also depends on the availability of suitable host species (i.e., deer and mice), which can also be affected by climate and weather conditions (Gubler et al., 2001).

It is likely that the ranges for these organisms will shift with global warming as the organisms spread into areas that previously were unsuitable for their survival, while they disappear from some currently endemic areas as climate conditions no longer support their survival (Gubler et al., 2001).

The people most at risk for experiencing serious effects from these diseases are the very young, the elderly, the infirm and people with compromised immune systems. Most healthy people are at little risk of serious disease from infection with these organisms (California Department of Health Services, 2004). Exposure to these organisms leads to antibody formation that persists for at least several years, however the degree and duration of protection provided by antibodies from an initial infection is unknown. These diseases are sufficiently rare that there are no data available on re-infection rates (Personal communication, California Department of Health Services).

7.2.1. Adaptations

There are no human vaccines for these diseases. Consequently the only effective mitigations include disease surveillance and vector control programs, use of window screens and air conditioning, along with public health advisories to wear clothing that provides skin coverage, use insect repellent, and remain indoors during heightened vector activity times, for example, at dusk (California Department of Health Services, 2004).

The risk of transmission of these diseases to humans is influenced by the effectiveness of surveillance and control programs, and also by human adherence to recommended behaviors. It is possible that the small number of cases of these diseases, compared to the large populations living in endemic areas, may be related to the effectiveness of these programs and recommendations (Barker et al., 2003).

California has well developed protocols involving the State, counties and cities for surveillance for these diseases. The State also has a multi-level protocol that is activated based on risk of disease transmission (California Department of Health Services, 2004; Barker et al., 2003).

7.3. Rodent-Borne Diseases

Rodent-borne diseases are usually transmitted to humans through direct contact with rodent urine, feces or other body fluids. The most common and well-known rodent-borne human disease is hanta virus, although rodents are also hosts for fleas and ticks that can spread plague and several other infectious diseases (McMichael and Githeko, 2001). The potential for human infection with hanta virus appears to be primarily related to the size of the rodent population. For example, in 1993 there was an outbreak of hanta virus in the Southwestern United States. The winter of 1992-1993 was unusually wet due to an El Niño Southern

Oscillation condition, leading to a large increase in availability of food for rodents, which led to a rodent population explosion, and increased risk and incidence of human disease. With the subsequent onset of drought conditions, both the rodent population and number of human cases of hanta virus declined considerably. The impact of climate change on rodent-borne diseases is likely to be related to relatively short cycles, for example a year or two rather than longer-term, and based primarily on the availability of food, and consequently the rodent population (Gubler et al., 2001). Five cases of hanta virus have been reported in California for the time period 2002 through 2004 (CDHS, 2004).

7.4. Food-Borne Diseases

Food-borne diseases can originate with contamination of fruits, vegetables and seafood by flooding or contaminated runoff following heavy rain or to contamination of seafood by toxic substances released by algal blooms (Rose et al., 2001). The extent to which these diseases will increase is affected by multiple inputs, including the extent to which irrigation water becomes contaminated by flooding or heavy runoff, and the frequency of toxic algal blooms. It is likely that the degree of irrigation water contamination could increase due to more rapid organism replication under future warming conditions. In addition, more frequent toxic algal blooms may occur under conditions of increased water temperature, leading to increased incidences of seafood contamination.

Most outbreaks of food-borne diseases, however, are related to improper food handling or storage. Food-borne illnesses could increase due to more rapid bacterial proliferation at warmer temperatures in food not handled correctly, or not maintained at proper storage temperatures (Colwell and Patz, 1998).

Those most at risk of experiencing serious effects from food-borne diseases are the very young, the elderly, the infirm and people with compromised immune systems. The California Department of Health Services, the counties and cities have protocols in place for surveillance for these diseases, as well as protocols that are activated when outbreaks of disease occur.

8.0 Wildfires

Wildfires can be a significant contributor to air pollution in both urban and rural areas, and have the potential to significantly impact public health primarily through their smoke. Fires also affect the economy and public safety. Various climate change scenarios project that through the 21st Century it is likely there will be an increase in the frequency, size, and intensity of wildfires. However, quantitative estimation of the public health impacts of future wildfire events is extremely difficult. The public health impacts of any fire are unique to that fire, and are influenced not only by the magnitude, intensity and duration of the fire, but also the proximity of the smoke plume to a population.

Smoke from burning vegetation includes a large quantity of particulate matter (PM), particularly less than 2.5 microns in diameter (PM2.5), but also less than 10 microns in diameter (PM10). The likelihood that smoke from wildfires can impact public health can reasonably be inferred from the extensive literature on the health impacts of PM2.5 and PM10. Most epidemiologic studies (examples of which are referenced here) investigating the health impacts of PM have reported statistically significant associations between ambient PM exposure and premature mortality (Dockery et al., 1993; Pope et al., 1995; Krewski et al., 2000; Burnett and Goldberg, 2003; Fairley, 2003; Ito, 2003), hospital admissions and emergency room visits for cardiopulmonary causes (Atkinson et al., 2003; Zanobetti and Schwartz, 2003; Sheppard, 2003), asthma exacerbation (Ostro et al., 2001; Delfino et al., 1998), and a variety of minor morbidity conditions (Ostro and Rothschild, 1989).

Because wildfires are relatively rare, and most frequently occur in sparsely inhabited areas, there are few studies evaluating the public health impacts of wildfires. Assessment of the public health impacts of wildfires is also complicated by the fact that there are usually few, if any, air quality data available for fire-impacted regions. Since this precludes development of exposure assessments and concentration-response functions, analyses of public health impacts of wildfires are generally limited to retrospective assessments of the change in incidence of health endpoints during the fire compared to that observed during a baseline time period.

The largest group of studies has examined changes in emergency room visits, or self-reported symptoms. However, because the decision to visit an emergency room is influenced by individual perceptions of risk and a decision to seek medical care is not necessarily based on objective assessment of medical need, these results are somewhat subjective. In addition, psychosomatic stress associated with wildfires and resulting air quality emergencies also can influence the decision as to whether to visit an emergency room (Mott et al., 2005). There are few studies of more objective and severe health endpoints, such as hospitalization and mortality. As noted above, this is primarily because population densities in exposed communities are rarely large enough to yield sufficient sample sizes for assessment of epidemiologic relationships between poor air quality due to fires and health endpoints, and because adequate air quality data are generally not available (Mott et al. 2005).

While not directly similar to fires that typically occur in California, several reports on health-related impacts of a series of fires that impacted Southeast Asia between April and November of 1997 suggest a worst-case scenario. In most cases air quality monitoring data

were inadequate for development of concentration-response functions, although the few air quality monitoring data available suggest that while PM10 levels varied widely during the fire period, including many days with typical PM10 concentrations, there were days on which PM10 concentrations reached alarming levels. Emmanuel (2000) investigated the impact of the fire haze on lung health in Singapore where monthly average PM10 values, typically between 30 and 50 $\mu g/m^3$, increased significantly to 60 to 100 $\mu g/m^3$ during September and October 1997. Between August and early November 1997 air quality reached the unhealthy range, based on the U.S. Environmental Protection Agency Pollutant Standards Index (PSI; values over 100 are considered unhealthy) on 12 days, with the highest PSI recorded being 138. The results showed that an increase in PM10 from 50 to 150 $\mu g/m^3$ was significantly associated with a 12% increase in upper respiratory tract illness, a 19% increase in asthma exacerbation, and a 26% increase in rhinitis. There was no significant increase in hospital admissions or in mortality.

Mott et al. (2005) evaluated the frequency distribution of hospitalizations during August 1 through October 31, 1997 compared to the same months in 1995, 1996, and 1998 in the Kuching region of the Malaysian state of Sarawak. All cause hospitalizations increased by 8% during the fire period, although the number of respiratory hospitalizations increased to a greater degree than other causes. There was also a statistically significant increase in the number of persons over 65 years of age readmitted to the hospital during the fire period. Re-hospitalization rates for exposed people resumed the pre-fire relationship once the fires ended.

Sastry (2002) found a 19% increase in mortality ($P<0.05$) in Kuala Lumpur, Malaysia on the day following days with 24-hour average PM10 measurements above 210 $\mu g/m^3$ for people 65 to 74 years of age, but not in other age groups at any PM10 concentration. The 90th percentile PM10 value was 99.4 (g/m^3, indicating that there were relatively few days during the fire period on which an increase in mortality would have been expected. The study estimated that the relative risk of mortality with a 100 $\mu g/m^3$ increase in PM10 was about 1.07. The results also suggested that displacement of deaths from the exposure to the smoke haze was short lived, although for those aged 65 to 74 there was an upward shift in death rate that lasted for a few weeks after the fires ended. Overall, the study found that mortality burden, in terms of days of life lost, was small.

Several studies have investigated the public health impacts of wildfires in the western United States. Morris et al. (2003) found that those who were not evacuated from the area impacted by smoke from the June 2002 Rodeo-Chedeski fire in Arizona reported significantly more respiratory symptoms, compared to people who were evacuated. The most commonly reported symptoms were eye irritation, itchy sore throat, and cough. Prevalence of self-reported asthma exacerbation increased 86% among people living in the non-evacuated area, compared to 39% among evacuees.

Vedal (2003) reported an increase in the mean number of daily emergency room visits for respiratory causes on two days in June of 2002 experiencing peak one-hour PM2.5 concentrations of 352 and 390 $\mu g/m^3$, respectively, consequent to a wildfire near Denver, Colorado. Vedal and Dutton (2005) also evaluated mortality related to the same fire, during which the highest measured one-hour PM10 concentration was 372 $\mu g/m^3$. However, in

spite of an exposed population of about two million people, there was no evidence for an increase in daily mortality attributable to increased PM10 levels due to the fire.

Several investigators have evaluated health effects of recent major fires in California. Duclos et al. (1990) assessed the impact of a series of fires in late August and early September 1987 that burned over 600,000 acres of California forests. A comparison of the observed number of cases compared to expected showed a 40% increase in the number of visits for asthma (120 vs. 86) and a 30% increase in visits for chronic obstructive pulmonary disease (74 vs. 57) during the period with the greatest smoke impact.

Shusterman et al. (1993) investigated the immediate health effects of an urban wildfire that burned parts of Alameda County, California in late October 1991. The analysis included review of emergency room visits to nine local hospitals, and coroner's records of mortality during the two days of the fire. There were 25 fire-related deaths, all principally due to extensive burns, although many of these patients also had smoke inhalation injury. About one-fourth of emergency room visits were for work-related injuries, particularly in firefighters. Smoke-related causes constituted about one-half of the emergency room visits during the fire, particularly for bronchospasm.

In 1999 a large wildfire burned from August 23 to November 3 near the Hoopa Valley National Indian Reservation in northern California. On 15 days the PM10 concentration on the reservation exceeded the U.S. EPA 24-hour standard of 150 $\mu g/m^3$, and on October 21 and 22, PM10 levels exceeded the U.S. EPA hazardous level of 500 $\mu g/m^3$. A survey of 26% of all tribal households on the reservation showed a 52% increase in medical visits for respiratory problems during the fire, compared to the same period of 1998. More than 60% of those surveyed reported an increase in respiratory symptoms during the smoke episode, and 20% continued to report increased respiratory symptoms two weeks after the smoke cleared (Mott et al., 2002).

Collectively, these papers provide evidence that fire smoke can increase incidence of various indices of public health, including mortality, hospitalization, emergency room visits, and respiratory symptoms, in a manner and magnitude similar to that reported for PM10 and PM2.5. However, the actual magnitude of future fire impacts can not be estimated due to the unique nature of each fire, and the necessity that the smoke plume covers an inhabited area. The literature consistently suggests that the people most at risk are those with existing cardiopulmonary disease, and that risk seems to increase with advancing age. In addition, the literature suggests that in terms of actual number of cases, wildfire impacts are likely to be modest.

8.1. Adaptations

The California Thoracic Society (1997), and the California Air Resources Board (CARB, 2003) have published fire fact sheets that describes personal actions that can minimize lung injury when exposed to a fire. In addition, the document "Wildfire Smoke: A Guide for Public Health Officials (available at http://www.arb.ca.gov/smp/progdev/pubeduc/wfgv8.pdf) describes health risks related to fire smoke inhalation, actions that can be taken to protect oneself, and also provides guidance to public health officials on assessing the level of public health risk a particular fire poses, and recommended responses. Key points are that

individuals and families should have an evacuation plan, keeping in mind that a wildfire may disrupt usual travel routes. In addition, the plan should include provisions for sheltering in place if not directed by authorities to evacuate. This plan should include food and especially water in the event utility service is disrupted by the fire.

9.0 Environmental Justice

Several studies have indicated that risk of adverse heat-related health impacts appears to be greater among the poor and ethnic minorities (O'Neill et al., 2003, 2005; Curriero et al., 2002; Michelozzi et al., 2005; Semenza et al., 1996; see also Union of Concerned Scientists, 2004 based on Hayhoe et al., 2004) who are often disproportionately represented among those living in poverty. Other identified risk factors for both heat- and cold-related death include age above 65 years, chronic cardiovascular or respiratory disease, mental impairment, and residence in an urban area (O'Neill et al., 2003; Curriero et al., 2002; Michelozzi et al., 2005), and social isolation, not leaving the home daily, and for heat-related mortality, living on the upper floors of multi-story buildings (Naughton et al., 2002). Many of these risk factors, particularly those that can be related to inadequate health care, residence in urban areas, and factors related to social isolation and lack of transportation, are common among the poor, suggesting that they may be more vulnerable to effects of extreme heat events compared to other segments of the population. Because of this, there is concern that health-related impacts of increasing ambient temperatures may be disproportionately borne by the poor and by people of color.

Multiple studies have shown that air conditioning is the single most effective mitigation for heat-related mortality (CDC, 2005a,b; Kilbourne, 2002; Kaiser et al., 2001). However, the poor often do not have access to air conditioning, or may not have the economic resources to pay for electricity to operate an air conditioner, even if one is available. This generally leads to ventilation and attempts at cooling the home via open windows and doors, or by fans, which have been shown to be ineffective in preventing heat-related mortality (Naughton et al., 2002; Kaiser et al., 2001; Bernard and McGheein, 2004). This also tends to lead people to spend more time outdoors, particularly during cooler morning and evening hours. Substandard housing, however, often lacks window screens. The combination of lack of air conditioning and window screens can lead to both increased heat exposure, as well as increased risk of infection with vector-borne diseases, such as West Nile virus. In addition, open windows during times of elevated ozone levels would lead to increased risk of adverse health impacts related to ozone, but would not likely alter risk related to PM exposure in that indoor and outdoor levels tend to be similar in the absence of air conditioning (CARB, 2002,2005).

Infectious diseases, including vector-, water- and food-borne diseases pose the greatest risk to the very young, the elderly and infirm, and those with compromised immune systems. Those with inadequate healthcare are more likely to experience poorer outcomes should they acquire these diseases than those with more extensive healthcare options. As discussed above, lack of air conditioning and window screens will increase the likelihood of infection with vector-borne diseases in environmental justice communities. Those living in poverty will also be at increased risk if they do not have access to, or means to acquire, adequate supplies of bottled water during water contamination events.

Most outbreaks of food-borne diseases are related to improper food handling or storage after the food leaves the fields or processing facilities. While food contamination could increase due to more rapid bacterial proliferation at warmer temperatures in food not handled correctly, or not maintained at proper storage temperatures (Colwell and Patz, 1998), risk of acquiring these diseases is primarily related to the handling of food once it reaches the

kitchen, rather than contamination in the field. Those most at risk of experiencing serious effects from food-borne diseases are the very young, the elderly, the infirm and people with compromised immune systems. Those with inadequate healthcare are more likely to experience poorer outcomes should they acquire food-borne diseases than those with more extensive healthcare options.

The literature suggests that the people most at risk of adverse responses to smoke from wildfires are those with existing cardiopulmonary disease (Mott et al., 2005; Sastry, 2002), and that risk seems to increase with advancing age. A further issue with relation to wildfires is that evacuations may be ordered based on level of risk to human life. People lacking transportation should evacuation be necessary would be at increased risk of adverse health impacts related to wildfires to the extent that they are unable to obtain assistance with evacuating.

Another concern in environmental justice communities is high asthma prevalence and morbidity (CDC, 2004), and potential effects of climate change on this disease burden. It is difficult to predict effects of climate change on asthma morbidity and mortality for several reasons. The most common asthma triggers are dust mites and molds, both which are higher indoors than outdoors. Both require a relatively humid environment for survival. Consequently, if the climate becomes drier, or drought periods increase, these triggers will become less important. However, both will respond to higher humidity with increased growth, and these triggers will become more significant. Many asthmatics are allergic to various plant pollens. Plants and trees typically have pollination seasons that last a few weeks per year. To the extent that pollen seasons lengthen or become more intense in response to climate change, the season for particular pollens could become longer, and lead to increased asthma exacerbation.

It is clear that those living in poverty and in inner city areas will need greater assistance in coping with various potential impacts associated with climate change than other segments of the community. The particular vulnerabilities of environmental justice communities will require consideration in development of mitigation and adaptation actions. Although there will be costs involved, the literature suggests that the most effective adaptation would be to insure that all housing units have functional air conditioners (CDC, 2005a,b; Kilbourne, 2002; Kaiser et al., 2001). This measure will reduce risk of not only heat-related mortality, but also risks from air pollution exposure and vector-borne diseases that will be associated with global warming. In addition, means to assist the poor with increased electricity costs will be required to insure that the benefit of this intervention accrues to this segment of the population. Communities should also consider developing protocols for distribution of bottled water to disadvantaged areas in the event of water contamination events to minimize human illness.

10.0 Research Needs

There are a number of difficulties in estimating the likely public health impacts of global climate change. A key issue is development and validation of downscaling methodologies such that the general circulation models can examine meteorological impacts on a scale that adequately represents local conditions. A similar need applies to air quality modeling. The material described in this report on regional air quality models is the first attempt to examine the influence of changes in meteorology on regional air quality in California. Further research in this area is critically needed to support setting and attainment of health-based ambient air quality standards. Research is also needed in development and validation of effective public health programs to mitigate the impacts of climate change, particularly heat emergency action plans. A number of American cities outside California already have such plans in place, and evaluation of their effectiveness, and methodologies to adapt them to California are also needed.

11.0 References

Abbey, D.E., N. Nishino, W.F. McDonnell, R.J. Burchette, S.F. Knutsen, W.L. Beeson, J.X. Yang. 1999. Long-term inhalable particles and other air pollutants related to death in nonsmokers. American Journal of Respiratory and Critical Care Medicine. 159:373-382.

Anderson H.R, C. Spix, S. Medina, J.P. Schouten, J. Castellsague, G. Rossi, D. Zmirou, G. Touloumi, B. Wojtyniak, A. Ponka, L. Bacharova, J. Schwartz, K. Katsouyanni. 1997. Air pollution and daily admissions for chronic obstructive pulmonary disease in 6 European cities: results from the APHEA project. European Respiratory Journal. 10:1064-1071.

Atkinson, R., H. Anderson, J. Sunyer, J. Ayres, M. Baccini, J. Vonk, A. Boumghar, F. Forastiere, B. Forsberg, G. Touloumi, J. Schwartz, K. Katsouyanni. 2003. Acute effects of particulate air pollution on respiratory admissions. In: Special Report. Revised analyses of time-series studies of air pollution and health. Health Effects Institute, Boston, MA.

Aw, J. and Kleeman, M.J. 2003. Evaluating the first-order effect of intraannual temperature variability on urban air pollution. Journal of Geophysical Research-Atmospheres. 108:D12.

Barker, C., W. Reisen, V. Kramer. 2003. California state mosquito-borne virus surveillance and response plan: a retrospective evaluation using conditional simulations. American Journal of Tropical Medicine and Hygiene. 68: 508-518.

Basu, R., F. Dominici, J. Samet. 2005. Temperature and mortality among the elderly in the United States: A comparison of epidemiologic methods. Epidemiology. 16: 58-66.

Basu, R., J. Samet. 2002. Relation between elevated ambient temp0erature and mortality: a review of the epidemiologic evidence. Epidemiologic Reviews. 24: 190-202.

Bell, M., F. Dominici, J. Samet. A meta-analysis of time-series studies of ozone and mortality with comparison to the National Morbidity, Mortality and Air Pollution Study. 2005. Epidemiology. 16: 436-445.

Bell, M.L., A. McDermott, S.L. Zeger, J.M. Samet, F. Dominici. 2004. Ozone and short-term death in 95 US urban communities, 1987-2000. Journal of the American Medical Association. 292:2372-2378.

Bernard, S., J. Samet, A. Grambsch, K. Ebi, I. Romieu. 2001. The potential impacts of climate variability and change on air pollution-related health effects in the United States. Environmental Health Perspectives. 109: 199-209.

Bernard, S., M. McGeehin. 2004. Municipal heat wave response plans. American Journal of Public Health. 94: 1520-1522.

Biscaye, P. E., F. E. Grousset, M. Revel, S. Van der Gaast, G. A. Zielinski, A. Vaars, and G. Kukla. 1997. Asian provenance of Glacial dust (stage 2) in the Greenland Ice Sheet Project 2 Ice Core, Summit, Greenland. Journal of Geophysical Research. 102:26,765– 26,781.

Bojkov, R. 1986. Surface ozone during the second half of the nineteenth century. Monthly Weather Review. 25: 353-352.

Bory, A. J. M., P. E. Biscaye, A. Svensson, and F. E. Grousset. 2002. Seasonal variability in the origin of recent atmospheric mineral dust at North GRIP, Greenland. Earth and Planetary Science Letters. 196:123–134.

Browell, E. *et al*. 2003. Ozone, aerosol, potential vorticity, and trace gas trends observed at high latitudes over North America from February to May 2000. Journal of Geophysical Research. 108(D4).

Burnett, R.T., J.R. Brook, W.T. Yung, R.E. Dales, D. Krewski. 1997. Association between ozone and hospitalization for respiratory diseases in 16 Canadian cities. Environmental Research. 72:24-31.

Burnett, R., M. Goldberg. 2003. Size-fractionated particulate mass and daily mortality in eight Canadian cities. In: Special Report. Revised analyses of time-series studies of air pollution and health. Health Effects Institute, Boston, MA.

California Air Resources Board. 2002. Staff Report: Public Hearing to Consider Amendments to the Ambient Air Quality Standards for Particulate Matter and Sulfates. Available at: http://www.arb.ca.gov/research/aaqs/std-rs/pm-final/pm-final.htm.

California Air Resources Board. 2003. Fact Sheet: Smoke Management and Public Health. Available at: http://www.arb.ca.gov/smp/progdev/pubeduc/smphfs0702.pdf.

California Air Resources Board. 2005. Review of the California Ambient Air Quality Standard for Ozone. Available at: http://www.arb.ca.gov/research/aaqs/ozone-rs/ozone-final/ozone-final.htm.

California Air Resources Board. 2001. Wildfire Smoke: A guide for public health officials. Available at: http://www.arb.ca.gov/smp/progdev/pubeduc/wfgv8.pdf.

California Air Resources Board. 2005. The California Almanac of Emissions and Air Quality, 2005 Edition. Appendix E: Natural Sources. Available at: http://www.arb.ca.gov/aqd/almanac/almanac05/pdf/appe05.pdf.

California Department of Health Services. 2004. California mosquito-borne virus surveillance and response plan. Available at: at http://www.dhs.ca.gov/ps/dcdc/pdf/cdtables/CM-DEC%202004.pdf.

California Thoracic Society. 1997. Position Paper: Disaster planning for lung health: fire fact sheet. Available at: http://www.thoracic.org/chapters/california_adobe/firefs.pdf.

CDC. 2001. Heat-related deaths – Los Angeles County, California, 1999-2000, and United States, 1979-1998. Morbidity and Mortality Weekly Report. 50: 623-626.

CDC. 2004. Asthma prevalence and control characteristics by race/ethnicity – United States, 2002. Morbidity and Mortality Weekly Report. 53: 145-148.

CDC. 2005b. Heat-related mortality – Arizona, 1993-202, and United States, 1979-2002. Morbidity and Mortality Weekly Report. 54: 628-630.

CDC. 2002. Hypothermia-related deaths – Utah, 2000, and United States, 1979-1998. Morbidity and Mortality Weekly Report. 51: 76-48.

CDC. 2005a. Hypothermia-related deaths – United States, 2003-2004. Morbidity and Mortality Weekly Report. 54: 173-175.

Charron, D., M. Thomas, D. Waltner-Toews, J. Aramini, T. Edge, R. Kent, A. Maarouf, J. Wilson. 2004. Vulnerability of waterborne diseases to climate change in Canada: a review. Journal of Toxicology and Environmental Health, part A. 67: 1667-1677.

Chestnut, L.G., W.S. Breffle, J.B. Smith, L.S. Kalkstein. 1998. Analysis of differences in hot-weather related mortality across 44 U.S. metropolitan areas. Environmental Science and Policy. 1:59-70.

Colwell, R., J. Patz. 1998. Climate, Infectious disease and health: An interdisciplinary perspective. American Academy of Microbiology.

Constable, J., A. Guenther, D. Schimel, and R. Monson. 1999. Modeling changes in VOC emission in response to climate change in the continental United States. Global Change Biology 5: 791-806.

Curriero, F., J. Patz, J. Rose, S. Lele. 2001. The association between extreme precipitation and waterborne disease outbreaks in the United States, 1948-1994. American Journal of Public Health. 91: 1194-1199.

Curriero, F., K. Heiner, J. Samet, S. Zeger, L. Strug, J. Patz. 2002. Temperature and mortality in 11 cities of the Eastern United States. American Journal of Epidemiology. 155: 80-87.

Davis, R., P. Knappenberger, P. Michaels, W. Novicoff. 2003. Changing heat-related mortality in the United States. Environmental Health Perspectives. 111: 1712-1718.

Davis, R., P. Knappenberger, W. Novicoff, P. Michaels. 2003. Decadal changes in summer mortality in U.S. cities. International Journal of Biometeorology. 47: 166-175.

Delworth, T.L., Broccoli, A.J., Rosati, A., Stouffer, R.J. *et al.* 2005. GFDL's CM2 global coupled climate models – Part 1 – Formulation and simulation characteristics. Journal of Climate. in press.

Dentener, F., D. Stevenson, J. Cofala, R. Mechler, M. Amann, P. Bergamaschi, F. Raes, and R. Derwent. 2004. The impact of air pollutant and methane emission controls on tropospheric ozone and radiative forcing: CTM calculations for the period 1990–2030. Atmospheric Chemistry and Physics Discussions. 4.

Dettinger, M.D., D.R. Cayan, M.K. Meyer, A.E. Jeton. 2004. Simulated hydrologic responses to climate variations and change in the Merced, Carson, and American River basins, Sierra Nevada, California, 1900-2099. Climatic Change. 62:283-317.

Dockery, 3rd,D.W., C.A., Pope, X. Xu, J.D. Spengler, J.H. Ware, M.E. Fay, *et al*. (1993). An association between air pollution and mortality in six U.S. cities. New England Journal of Medicine. 329:1753-1759.

Dominici, F., M. Daniels, A. McDermott, S. Zeger, J. Samet. 2003. Shape of the exposure-response relation and mortality displacement in the NMMAPS database. In: Special Report.

Revised analyses of time-series studies of air pollution and health. Health Effects Institute, Boston, MA.

Donaldson, G., W. Keatinge, S. Nayha. 2003. Changes in summer temperature and heat-related mortality since 1971 in North Carolina, South Finland, and Southern England. Environmental Research. 91: 1-7.

Duclos, P., L. Sanderson, M. Lipsett. 1990. The 1987 forest fire disaster in California: assessment of emergency room visits. Archives of Environmental Health. 45:53-58.

Dwight R., J. Semenza, D. Baker, B. Olson. 2002. Association of urban runoff with coastal water quality in Orange County, California. Water Environment Research. 74: 82-90.

Ebi, K.L., T.J. Teisberg, L.S. Kalkstein, L. Robinson, R.F. Weiher. 2004. Heat Watch/Warning Systems Save Lives: Estimated Costs and Benefits for Philadelphia 1995-1998. Bulletin of the American Meteorological Society. 85: 1067-74.

Emmanuel, S. 2000. Impact to lung health of haze from forest fires: the Singapore experience.

Evans, M.J., M.V. Fanucchi, G.L. Baker, L.S. Van Winkle, L.M. Pantle, S.J. Nishio, E.S. Schelegle, L.J. Gershwin, L.A. Miller, D.M. Hyde, P.L. Sannes, C.G. Plopper. 2003. Atypical development of the tracheal basement membrane zone of infant rhesus monkeys exposed to ozone and allergen. American Journal of Physiology: Lung, Cell and Molecular Physiology. 285:L931-939.

Fairley, D. 2003. Mortality and air pollution for Santa Clara County, California, 1989-1996. In: Special Report. Revised analyses of time-series studies of air pollution and health. Health Effects Institute, Boston, MA.

Ferris, Jr., B., I. Higgins, M. Higgins, J. Peters. 1973. Chronic nonspecific respiratory disease in Berlin, New Hampshire, 1961 to 1967. A follow-up study. American Review of Respiratory Disease. 107: 110-122.

Field, C., G. Daily, R. Gaines, P. Matson, J. Melack, N. L. Miller, R. Pitelka. 1999. Climate Change and California Ecosystems: A Report of the Union of Concerned Scientists and the Ecological Society of America. 65 pp.

Finlayson-Pitts, B., J. Pitts, Jr. 1999. Chemistry of the upper and lower atmosphere. Academic Press, San Diego, California.

Fiore, A. *et al.* 2002. Background ozone over the United States in summer: Origin, trend, and contribution to pollution episode. Journal of Geophysical Research. 107(D15).

Fiore, A. M., D. J. Jacob, B. D. Field, D. G. Streets, S. D. Fernandes, and C. Jang, 2002b. Linking ozone pollution and climate change: The case for controlling methane. Geophysical Research Letters. 29(19).

Fischer, P., B. Brunekreef, E. Lebret. 2004. Air pollution related deaths during the 2003 heat wave in the Netherlands. Atmospheric Environment. 38: 1083-1085.

Gauderman, W.J., R. McConnell, F. Gilliland, S. London, D. Thomas, E. Avol, H. Vora, K. Berhane, E.B. Rappaport, F. Lurmann, H.G. Margolis, J. Peters. 2000. Association between air pollution and lung function growth in southern California children. American Journal of Respiratory and Critical Care Medicine. 162:1383-1390.

Gent, J.F., E.W. Triche, T.R. Holford, K. Belanger, M.B. Bracken, W.S. Beckett, B.P. Leaderer. 2003. Association of low-level ozone and fine particles with respiratory symptoms in children with asthma. Journal of the American Medical Association. 290:1859-1867.

Gilliland, F.D., K. Berhane, E.B. Rappaport, D.C. Thomas, E. Avol, W.J. Gauderman, S.J. London, H.G. Margolis, R. McConnell, K.T. Islam, J.M. Peters. 2001. The effects of ambient air pollution on school absenteeism due to respiratory illnesses. Epidemiology 12:43-54.

Gordon, C., C. Cooper, C.A. Senior, H. Banks, J.M. Gregory, T.C. Johns, J.F.B. Mitchell, R.A. Wood. 2000. Climate Dynamics. 16:147-168.

Gryparis, A., B. Forsberg, K. Katsouyanni, A. Analitis, G. Touloumi, J. Schwartz, E. Samoli, S. Medina, H.R. Anderson, E.M. Niciu, H.E. Wichmann, B. Kriz, M. Kosnik, J. Skorkovsky, J.M. Vonk, Z. Dortbudak. 2004. Acute effects of ozone on death from the "air pollution and health: a European approach" project. American Journal of Respiratory and Critical Care Medicine. 170:1080-1087.

Gubler, D., P. Reiter, K. Ebi, W. Yap, R. Nasci, J. Patz. 2001. Climate variability and change in the United States: potential impacts on vector- and rodent-borne diseases. Environmental Health Perspectives. 109: 223-233.

Harkema, J.R., C.G. Plopper, D.M. Hyde, J.A. St George, D.W. Wilson, D.L. Dungworth. 1993. Response of macaque bronchiolar epithelium to ambient concentrations of ozone. American Journal of Pathololgy. 143:857-866.

Hauglustaine, D., and G. Brasseur. 2001. Evolution of tropospheric ozone under anthropogenic activities and associated radiative forcing of climate Journal of Geophysical Research. 106(D23).

Hayhoe, K., D. Cayan, *et al*. 2004. Emissions pathways, climate change, and impacts on California. Proceedings of the National Academy of Sciences. 101:12,422-12,427

Held, T., Q. Ying, A. Kaduwela, M. Kleeman. 2004. Modeling particulate matter in the San Joaquin Valley with a source-oriented externally mixed three-dimensional photochemical grid model. Atmospheric Environment, part A-General Topics. 38: 3689-3711.

Hodgkin, J.E., D.E. Abbey, G.L. Euler, A.R. Magie. 1984. COPD prevalence in nonsmokers in high and low photochemical air pollution areas. Chest. 86:830-838.

Hogrefe, C., B. Lynn *et al*. 2004. Simulating changes in regional air pollution over the eastern United States due to changes in global and regional climate and emissions. Journal of Geophysical Research. 109.

Houghton, J.T., Y. Ding, D.J. Griggs, M. Noguer, P.J. van der Linden, and D. Xiaosu (eds.). 2001. Climate Change 2001: The Scientific Basis. Contribution of Working Group I to the

Third Assessment Report of the Intergovernmental Panel on Climate Change. Cambridge, UK and New York, NY: Cambridge University Press.

Husar, R. *et al.* (28 co-authors). 2001. Asian dust events of April 1998. Journal of Geophysical Research. 106(D16).

IMPROVE - Inter-Agency Monitoring for Protected Visual Environments. USEPA/DOI network. data at: http://vista.cira.colostate.edu/improve/Data/IMPROVE/improve_data.htm.

ITCT2K2 - Intercontinental Transport and Chemical Transformation Study 2002, (NOAA), Trinidad Head aerosol data courtesy of Dr. Steven Cliff, UC Davis; *see also*: Parrish, D. *et al*. 2004. Intercontinental Transport and Chemical Transformation 2002 (ITCT 2K2) and Pacific Exploration of Asian Continental Emission (PEACE) experiments: An overview of the 2002 winter and spring intensives. Journal of Geophysical Research. 109(D23)S01.

Ito, K. 2003. Associations of particulate matter components with daily mortality and morbidity in Detroit, Michigan. In: Special Report. Revised analyses of time-series studies of air pollution and health. Health Effects Institute, Boston, MA.

Ito, K., S. De Leon, M. Lippmann. 2005. Associations between ozone and daily mortality: analysis and meta-analysis. Epidemiology. 16: 446-457.

Jacob, D., J. Logan, P. Murti. 1999. Effect of rising Asian emissions on surface ozone in the United States. Geophysical Research Letters. 26(14): 2,175-2,178.

Jaegle, L., D. Jaffe, H. Price, P. Weiss-Penzias, P. Palmer, M. Evans, D. Jacob, and L.Bey. 2003. Sources and budgets for CO and O3 in the northeastern Pacific during the spring of 2001: Results from the PHOBEA-II Experiment. Journal of Geophysical Research. 108(D20).

Jaffe, D., *et al.* 1999. Transport of Asian Air Pollution to North America. Geophysical Research Letters. 26(6): 711-714.

Jaffe, D., H. Price, D. Parrish, A. Goldstein, J. Harris. 2003b. Increasing background ozone during spring on the west coast of North America. Geophysical Research Letters. 30(12).

Jaffe, D., I. McKendry, T. Anderson, and H. Price. 2003c. Six 'new' episodes of trans-Pacific transport of air pollutants. Atmospheric Environment. 37: 391-404.

Jaffe, D., P. Weiss-Penzias, J. Dennison, L. Bertschi, D. Westphal. 2003a. Siberian Biomass Burning Plumes Across the Pacific: Impact on Surface Air Quality in the Pacific Northwest. Eos Transcripts American Geophysical Union. 84(46): Fall Meet. Suppl., Abstract A11I-02.

Jannsen, N., J. Schwartz, A. Zanobetti, H. Suh. 2001. Air conditioning and source-specific particles as modifiers of the effect of PM10 on hospital admissions for heart and lung disease. Environmental Health Perspectives. 110: 43-49.

Kaiser, R., C. Rubin, A. Henderson, M. Wolfe, S. Kieszak, C. Parrott, M. Adcock. 2001. Heat-related death and mental illness during the 1999 Cincinnati heat wave. The American Journal of Forensic Medicine and Pathology. 22: 303-307.

Kalkstein, L., J. Greene. 1997. An evaluation of climate/mortality relationships in large U.S. cities and possible impacts of a climate change. Environmental Health Perspectives. 105: 84-93.

Kalkstein, L.S. 1989. The impact of CO2 and trace gas-induced climate changes upon human mortality. In: The Potential of Global Climate Change in the United States, Appendix G, eds. Smith, J.B. and D.A. Tirpak. Washington, DC: Environmental Protection Agency.

Kalkstein, L.S. 1993. Direct impacts in cities. The Lancet. 342:1397-1399.

Kalkstein, L.S. 2003. Description of our heat/health watch-warning systems: Their nature and extent, and required resources. Final Report to U.S. EPA/Stratus Consulting Co.

Kalkstein, L.S., J.S. Greene. 1997. An evaluation of climate/mortality relationships in large US cities and the possible impacts of a climate change. Environmental Health Perspectives. 105: 84-93.

Kalkstein, L.S., K.M. Valimont. 1986. An evaluation of summer discomfort in the United States using a relative climatological index. Bulletin of the American Meteorological Society. 7: 842-848.

Kalkstein, L.S., K.M. Valimont. 1987. Climate effects on human health. In: Potential Effects of Future Climate Changes on Forests and Vegetation, Agriculture, Water Resources, and Human Health. EPA Science and Advisory Committee Monograph 25389:122-152.

Kalkstein, L.S., P.F. Jamason, J.S. Greene, J. Libby and L. Robinson, 1996. The Philadelphia Hot Weather-Health Watch/Warning System: Development and Application, Summer 1995. /Bulletin of the American Meteorological Society/, 77(7):1519-1528.

Kalkstein, L.S., R.E. Davis. 1989. Weather and human mortality: An evaluation of demographic and interregional responses in the United States. Annals of the Association of American Geographers. 79: 44-64.

Keatinge, W., G. Donaldson, E. Cordioli, M. Martinelli, A. Kunst, J. Mackenbach, S. Nayha, I. Vuori. 2000. Heat related mortality in warm and cold regions of Europe: observational study. British Medical Journal. 321: 670-673.

Keatinge, W., G. Donaldson. 2001. Mortality related to cold and air pollution in London after allowance for effects of associated weather patterns. Environmental Research, section A. 86: 209-216.

Kilbourne E.M. 2002. Heat-related illness: current status of prevention efforts. American Journal of Preventative Medicine. 22: 328-329.

Kinney, P.L., D.M. Nilsen, M. Lippmann, M. Brescia, T. Gordon, T. McGovern, H. El-Fawal, R.B. Devlin, W.N. Rom. 1996. Biomarkers of lung inflammation in recreational joggers exposed to ozone. American Journal of Respiratory and Critical Care Medicine. 154:1430-1435.

Kinney, P.L., M. Lippmann. 2000. Respiratory effects of seasonal exposures to ozone and particles. Archives of Environmental Health. 55:210-216.

Kleeman, M.J., and G.R. Cass. 2001. A 3D Eulerian source-oriented model for an externally mixed aerosol. Environmental Science and Technology. 35:4834-4848.

Kovats, R., S. Hajat, P. Wilkinson. 2004. Contrasting patterns of mortality and hospital admissions during hot weather and heat waves in Greater London, UK. Occupational and Environmental Medicine. 61: 893-898.

Krewski, D., R.T. Burnett, M.S. Goldberg, K. Hoover, J. Siemiatycki, M. Jerrett, M. Abrahamonwicz, W.H. White. 2000. Reanalysis of the Harvard Six Cities Study and the American Cancer Society Study of Particulate Air Pollution and Mortality. Special Report. Health Effects Institute, Cambridge MA.

Kunst, A., C. Looman, J. Mackenbach. 1993. Outdoor air temperature and mortality in the Netherlands: a time-series analysis. American Journal of Epidemiology. 137: 331-341.

Kunzli, N., F. Lurmann, M. Segal, L. Ngo, J. Balmes, I.B. Tager. 1997. Association between lifetime ambient ozone exposure and pulmonary function in college freshmen--results of a pilot study. Environmental Research. 72:8-23.

Kysely, J. 2004. Mortality and displaced mortality during heat waves in the Czech Republic. International Journal of Biometeorology. 49: 91-97.

Langer, J., R. Bergstrom, et al. 2005. Impact of climate change on surface ozone and deposition of sulphur and nitrogen in Europe. Atmospheric Environment. 39:1129-1141.

Last, J.A., T.R. Gelzleichter, J. Harkema, S. Hawk. 1994. Consequences of prolonged inhalation of ozone on Fischer-344/N rats: collaborative studies. Part I: Content and cross-linking of lung collagen. Research Report. Health Effects Institute :1-29; discussion 31-40.

Lawrence, M., R. von Kuhlmann, M. Salzmann, P. Rasch. 2003. The balance of effects of deep convective mixing on tropospheric ozone. Geophysical Research Letters. 30(18).

Lelieveld, J., and F. Dentener. 2000. What controls tropospheric ozone? Journal of Geophysical Research. 105(D3).

Levy, J., S. Chemerynski, J. Sarnat. 2005. Ozone exposure and mortality: an empiric Bayes metaregression analysis. Epidemiology. 16: 458-468.

Lewis, E. and S. Schwartz. 2004. Sea Salt Aerosol Production: Mechanisms, Methods, Measurements and Models – A Critical Review. Geophysical Monograph 152, American Geophysical Union, Washington, D.C..

Lindgren, E., L. Talleklint, T. Polfeldt. 2000. Impact of climatic change on the northern latitude limit and population density of the disease-transmitting European tick *Ixodes ricinus*. Environmental Health Perspectives. 108: 119-123.

Lisac, I., and V. Grubisic. 1991. An analysis of surface ozone data measured at the end of the 19th century in Zagreb, Yugoslavia. Atmospheric Environment. 25A(2): 481-486.

Louis, V., E. Russek-Cohen, N. Choopun, I. Rivera, B. Gangle, S. Jiang, A. Rubin, J. Patz, A. Huq, R. Colwell. 2003. Predictability of *Vibrio cholerae* in Chesapeake Bay. Applied and Environmental Microbiology. 69: 2773-2785.

Martens, W.J.M. Climate change, thermal stress and mortality changes. 1998. Social Science and Medicine. 46: 331-344.

McConnell, R., K. Berhane, F. Gilliland, S.J. London, T. Islam, W.J. Gauderman, E. Avol, H.G. Margolis, J.M. Peters. 2002. Asthma in exercising children exposed to ozone: a cohort study. Lancet 359:386-391.

McGeehin, M.A., M. Mirabelli. 2001. The potential impacts of climate variability and change on temperature-related morbidity and mortality in the United States. Environmental Health Perspectives. 109: 185-189.

McMichael, A.J., A. Githeko. 2001. Human health. In: Climate Change 2001: Impacts, Adaptation and Vulnerability. Contribution of Working Group II to the Third Assessment Report of the Intergovernmental Panel on Climate Change, eds. McCarthy, J.J., O.F. Canziani, N.A. Leary, et al. Cambridge, UK: Cambridge University Press, 451-485.

Michelozzi, P., F. de'Donato. L. Bisanti, A. Russo, E. Cadmum, M. DeMaria, M. D'Ovidio, G. Costa, C. Perucci. 2005. The impact of the summer 2003 heat waves on mortality in four Italian cities. Eurosurveillance. 10(7-8).

Mickley, L. J., D. J. Jacob, et al. 2004. Effects of future climate change on regional air pollution episodes in the United States. Geophysical. Research Letters. 31.

Miller, N.L., J. Jin, K. Hayhoe, M. Auffhammer, A. Sanstad. 2005. Heat Extremes and Energy Demand. Presented at Second Annual Climate Change Research Conference. September 15, 2005. Sacramento, CA.

Miller, N.L., K.E. Bashford, E. Strem. 2003. Potential impacts of climate change on California hydrology. Journal of the American Water Resources Association. 39:771-784.

Moolgavkar, S., W. Hazelton, E. Leubeck, *et al*. 2000. Air pollution, pollens and admissions for chronic respiratory disease in King County, Washington. Inhalation Toxicology. 12(Suppl. 1): 157-171.

Morris, J., A. Cronquist, J. Mott, S. Redd, V. Vaz. 2003. Prevalence of smoke-related symptoms after a major wildland fire. American Journal of Respiratory and Critical Care Medicine. 167: A498.

Mott, J., D. Mannino, C. Alverson, A. Kiyu, J. Hashim, T. Lee, K. Falter, S. Redd. 2005. Cardiorespiratory hospitalizations associated with smoke exposure during the 1997 Southeast Asian forest fires. International Journal of Hygiene and Environmental Health. 208: 75-85.

Mott, J., P. Meyer, D. Mannino, S. Redd, E. Smith, C. Gotway-Crawford, E. Chase. 2002. Wildland forest fire smoke: health effects and intervention evaluation, Hoopa, California, 1999. Western Journal of Medicine. 176: 157-165.

Mullahy, J., P.R. Portney. 1990. Air pollution, cigarette smoking, and the production of respiratory health. Journal of Health Economics. 9:193-205.

Mysliwiec, M.J., M.J. Kleeman. 2002. Source apportionment of secondary airborne particulate matter in a polluted atmosphere. Environmental Science and Technology. 36: 5376-5384.

Nakićenović, N., *et al*. 2000. IPCC Special Report on Emissions Scenarios. Cambridge, UK and New York, NY: Cambridge University Press.

National Center for Health Statistics, 2000. Standardized Micro-data Mortality Transcripts. U.S. Department of Health, Education, and Welfare.

NRC (National Research Council of the National Academies). 2001. Global Air Quality: An Imperative for Long-Term Observational Strategies. National Academy Press, Washington, DC, pp. 10-13. Available at: http://www.nap.edu/books/0309074142/html/.

NRC (National Research Council of the National Academies). 2004. Air Quality Management in the United States. National Academy Press, Washington, DC. pp. 16, 277-278. Available at: http://www.nap.edu/books/0309089328/html.

Naughton, M., A. Henderson, M. Mirabelli, R. Kaiser, J. Wilhelm, S. Kieszak, C. Rubin, M. McGeehin. 2002. American Journal of Preventative Medicine. 22: 221-227.
Newchurch, M. J., *et al.* 2003. Vertical distribution of ozone at four sites in the United States. Journal of Geophysical Research. 108(D1).

O'Dowd, C., M. Smith, I. Consterdine and J. Lowe. 1997. Marine Aerosol, Sea-salt, and the Marine Sulphur Cycle: a Short Review. Atmospheric Environment. 31(1).

O'Neill, M., A. Zanobetti, J. Schwartz. 2003. Modifiers of the temperature and mortality association in seven US cities. American Journal of Epidemiology. 157: 1074-1082.

O'Neill, M., A. Zanobetti, J. Schwartz. 2005. Disparities by race in heat-related mortality in four US cities: the role of air conditioning prevalence. Journal of Urban Health: Bulletin of the New York Academy of Medicine. 82: 191-197.

Oechsli, F.W., R.W. Buechley. 1970. Excess mortality associated with three Los Angeles September hot spells. Environmental Research. 3:277-284.

Ostro, B.D., S. Hurley, M.J. Lipsett. 1999. Air Pollution and Daily Mortality in the Coachella Valley, California: A Study of PM10 Dominated by Coarse Particles. Environmental Research A81:231-238.

Ostro, B.D., S. Rothschild. 1989. Air Pollution and Acute Respiratory Morbidity: An Observational Study of Multiple Pollutants. Environmental Research. 50:238-247.

Pochanart, P., H. Akimoto, Y. Kajii, V. Potemkin, T. Khodzher. 2003. Regional background ozone and carbon monoxide variations in remote Siberia/East Asia. Journal of Geophysical Research. 108(D1).

Pope III, C.A., M.J. Thun, M.M. Namboodiri, D.W. Dockery, J.S. Evans, F.E. Speizer, C.W. Heath Jr. 1995. Particulate Air Pollution As a Predictor of Mortality in a Prospective Study of U.S. Adults. American Journal of Respiratory and Critical Care Medicine. 151:669-674.

Pope, C. A., 3rd, R.T. Burnett, M.J. Thun, E.E. Calle, D. Krewski, K. Ito, G.D. Thurston. 2002. Lung cancer, cardiopulmonary death, and long-term exposure to fine particulate air pollution. Journal of the American Medical Association. 287:1132-1141.

Pope, V.D., M.L. Gallani, P.R. Rowntree, and R.A. Stratton. 2000. The impact of new physical parameterizations in the Hadley Centre climate model—HadCM3. Climate Dynamics. 16: 123-146.

Prather, M. J. 1996. Time scales in atmospheric chemistry: Theory, GWPs for CH4 and CO, and runaway growth. Geophysical Research Letters. 23.

Prather, M., *et al*., Fresh air in the 21st century? Research Letters. 30(2).

Prospero, J., and P. Lamb. 2003. African Droughts and Dust Transport to the Caribbean: Climate Change Implications. Science. 302.

Prospero, J., P. Ginoux, O. Torres, S. Nicholson, and T. Gill. 2002. Environmental Characterization Of Global Sources Of Atmospheric Soil Dust Identified With The Nimbus 7 Total Ozone Mapping Spectrometer (TOMS) Absorbing Aerosol Product. Review of Geophysics. 40(1).

Ramanathan, V., P.J. Crutzen, J.T. Keihl, D, Rosenfeld. 2001. Aerosols, Climate, and the Hydrological Cycle. Science. 294.

Reiser, K.M., W.S. Tyler, S.M. Hennessy, J.J.Dominguez, J.A. Last. 1987. Long-term consequences of exposure to ozone. II. Structural alterations in lung collagen of monkeys. Toxicology and Applied Pharmacology. 89:314-322.

Rose, J., P. Epstein, E. Lipp, B. Sherman, S. Bernard, J. Patz. 2001. Climate variability and change in the United States: potential impacts on water and foodborne diseases caused by microbiologic agents. Environmental Health Perspectives. 109: 211-220.

Sastry, N. 2002. Forest fires, air pollution, and mortality in Southeast Asia. Demography. 39: 1-23.

Schär, C., P.L. Vidale, D. Lüthi, C. Frei, C. Häberli, Liniger, C. Appenzeller. 2004. The role of increasing temperature variability in European summer heat waves. Nature. 427: 332-336.

Schelegle, E.S., L.A. Miller, L.J. Gershwin, M.V. Fanucchi, L.S. Van Winkle, J.E. Gerriets, W.F. Walby, V. Mitchell, B.K. Tarkington, V.J. Wong, G.L. Baker, L.M. Pantle, J.P. Joad, K.E. Pinkerton, R. Wu, M.J. Evans, D.M. Hyde, C.G. Plopper. 2003. Repeated episodes of ozone inhalation amplifies the effects of allergen sensitization and inhalation on airway immune and structural development in Rhesus monkeys . Toxicology and Applied Pharmacology. 191:74-85.

Seinfeld, J., S. Pandis. 1998. Atmospheric chemistry and physics – From air pollution to climate change. John Wiley and Sons, Inc. New York, NY.

Semazzi, F. 2003. Air quality research: Perspective from climate change modeling research. Environment International. 29:253-261.

Semenza, J., C. Rubin, K. Falter, J. Selanikio, W. Flanders, H. Howe, J. Wilhelm. 1996. Heat-related deaths during the July 1995 heat wave in Chicago. The New England Journal of Medicine. 335: 84-90.

Sheppard, L. 2003. Ambient air pollution and nonelderly asthma hospital admissions in Seattle, Washington, 1987-1994. In: Special Report. Revised analyses of time-series studies of air pollution and health. Health Effects Institute, Boston, MA.

Sheridan, S.C. and L.S. Kalkstein. 2004. Progress in Heat Watch-Warning System Technology. Bulletin of the American Meteorological Society. 85: 1931-1941.

Smoyer-Tomic, K., Rainham, D. 2001. Beating the heat: development and evaluation of a Canadian hot weather health-response plan. Environmental Health Perspectives. 109: 1244-1248.

Souch, C. C.S.B. Grimmond. 2004. Applied climatology: Heat waves. Progress in Physical Geography. 28: 599-606.

STACCATO. 2003. Influence of Stratosphere-Troposphere Exchange in a Changing Climate on Atmospheric Transport and Oxidation Capacity (STACCATO), Lehrstuhl für Bioklimatologie und Immissionsforschung, Technische Universität München, Germany, Web Report, (http://www.forst.tu-muenchen.de/EXT/LST/METEO/staccato/).

Stedman, J. 2004. The predicted number of air pollution related deaths in the UK during the August 2003 heat wave. Atmospheric Environment. 38: 1087-1090.

Tager, I.B., N. Kunzli, L. Ngo, J. Balmes. 1998. Methods development for epidemiologic investigations of the health effects of prolonged ozone exposure. Part I: Variability of pulmonary function measures. Research Report. Health Effects Institute:1-25; discussion 109-21.

Thouret, V., *et al*., Tropospheric ozone layers observed during PEM-Tropics B. 2001. Journal of Geophysical Research. 106(D23): 32,527–32,538.

Tolbert, P.E., J.A. Mulholland, D.L. MacIntosh, F. Xu, D. Daniels, O.J. Devine, B.P. Carlin, M. Klein, J. Dorley, A.J. Butler, D.F. Nordenberg, H. Frumkin, P.B. Ryan, M.C. White. 2000. Air quality and pediatric emergency room visits for asthma in Atlanta, Georgia, USA. American Journal of Epidemiology. 151:798-810.

Trickl, T., O. Cooper, H. Eisele, P. James, R. Mucke, A. Stohl. 2003. Intercontinental transport and its influence on the ozone concentrations over central Europe: Three case studies Journal of Geophysical Research. 108(D12).

Tyler, W.S., N.K. Tyler, J.A. Last, M.J. Gillespie, T.J. Barstow. 1988. Comparison of daily and seasonal exposures of young monkeys to ozone. Toxicology. 50:131-144.

U.S. EPA. 1996. Air Quality Criteria for Ozone and Related Photochemical Oxidants. Vol. 3.

Union of Concerned Scientists. 2004. Choosing Our Future: Climate Change in California. Rising Heat and Risks to Human Health. Berkeley, CA. Available at: www.ucsusa.org.

Van Curen, R. A. 2003. Asian aerosols in North America: Extracting the chemical composition and mass concentration of the Asian continental aerosol plume from long-term aerosol records in the western United States. Journal of Geophysical Research. 108(D20).

Van Curen, R. A., T.A. Cahill. 2002. Asian aerosols in North America: Frequency and concentration of fine dust. Journal of Geophysical Research. 107(D24).

Van Curen, R. and P. Lahm. 1996. Wild and Prescribed Fire Emissions in the Grand Canyon Visibility Transport Region with Resulting Aerosol Concentrations and Light Extinction at Selected Class 1 Areas on the Colorado Plateau. Grand Canyon Visibility Transport Commission, Technical Committee Report. April, 1996.

Vedal, S. Wildfire air pollution and respiratory emergency visits: a natural experiment. American Journal of Respiratory and Critical Care Medicine. 167: A974

Vedal, V., S. Dutton. 2005. Wildfire air pollution and daily mortality in a large urban area. Proceedings of the American Thoracic Society. 2:A264.

Washington, W.M., *et al*. 2000. Parallel Climate Model (PCM) Control and Transient Simulations. Climate Dynamics. 16: 755-774.

Watts, J.D., L.S. Kalkstein. 2004. The development of a warm-weather relative stress index for environmental applications. Journal of Applied Meteorology. 43: 503-513.

Weiskopf, M., H. Anderson, S. Foldy, L. Hanrahan, K. Blair, T. Torok, P. Rumm. 2002. Heat wave morbidity and mortality, Milwaukee, Wis. 1999 vs 1995: An improved response? American Journal of Public Health. 92: 830-833.

Zhang Lijun, vice minister China environmental agency (SEPA). 2005. Speech reported by *Agence France Presse*, October 25, 2005.

Appendix A

Interim Report: Impact of Climate Change on Meteorology and Regional Air Quality in California

INTERIM REPORT

Impact of Climate Change on Meteorology and Regional Air Quality in California

Contract # 04-349

Reporting Period: August – November 2005

Principal Investigators:
Michael Kleeman, UC Davis
Dan Cayan, Scripps Institution of Oceanography, UC San Diego

Prepared for:

State of California Air Resources Board
Research Division
PO Box 2815
Sacramento CA 95812

Contact Information:

Michael Kleeman
Department of Civil and Environmental Engineering
University of California
Davis, CA, 95616
(530) 752-8386

November, 2005

Disclaimer

The statements and conclusions of this Report are those of the contractor and not necessarily those of the California Air Resources Board. The mention of commercial products, their source, or their use in connection with material reported herein is not to be construed as actual or implied endorsement of such products.

Acknowledgment

This research was funded by the California Air Resources Board under Contract # 04-349. The authors gratefully acknowledge the assistance of Nehzat Motallebi (CARB) for help assembling and checking measurements of pollutant concentrations and review of the interim report. The authors also thank Mary Tyree (UCSD), Martha Coakley (UCSD), and Josh Schriffin (UCSD) for their development of the statistical downscaling method.

Summary of Preliminary Results

The goal of this project is to identify linkages between climate and air quality for major airsheds in California. In this first interim report, a detailed perturbation analysis was carried out to study the effect of meteorology on ozone and $PM_{2.5}$ concentrations during present-day air pollution events. Two air pollution episodes in the South Coast Air Basin (SoCAB) (September 7-9, 1993; September 23-25, 1996) and one air pollution episode in the San Joaquin Valley (SJV) (January 4-6, 1996) were used to span the wide range of meteorological conditions and pollutant concentrations experienced in California. Each base-case episode has been extensively validated against measured concentrations in previous studies providing a solid foundation for the perturbation analysis.

Temperature, humidity, mixing depth, and wind speed were systematically perturbed and the corresponding change in the regional distribution of 1-hr average ozone concentrations and 24-hr average $PM_{2.5}$ concentrations was calculated. The following systematic behavior was observed across all the episodes.

1. Increased wind speed reduces ozone and $PM_{2.5}$ concentrations by enhancing dilution of primary emissions.
2. Increased mixing depth reduces $PM_{2.5}$ concentrations by enhancing dilution of primary emissions. Surface NO_X concentrations are also reduced by enhanced dilution leading to an increase in surface ozone concentrations because less NO_X is available to titrate the ozone that is produced aloft and mixed to the surface.
3. Increasing temperature with constant absolute humidity increases ozone concentrations due to increased rate of photochemical reactions but reduces $PM_{2.5}$ concentrations due to increased volatilization of ammonium nitrate and reduced particle water content.
4. Increasing temperature with constant relative humidity increases ozone concentrations further because water vapor provides a source of hydroxyl radical to the system. The additional water vapor also maintains the particle water content, reducing the volatilization of ammonium nitrate at warmer temperatures. $PM_{2.5}$ concentrations in the SoCAB decrease in response to higher temperature with constant relative humidity. The magnitude of this decrease is smaller than the case with less water vapor. Higher temperatures at constant relative humidity actually increase predicted $PM_{2.5}$ concentrations in some regions of the SJV that have cool base-case temperatures and a large excess of gas-phase ammonia.

A statistical downscaling technique was also developed to relate the frequency of meteorological conditions that encourage high ozone formation to large-scale meteorological variables predicted by GCMs. The application of this statistical downscaling technique to GFDL predictions for future climate suggests one additional conclusion.

5. Climate change will lead to higher temperatures in the troposphere. Based on statistical linkages of ozone and 850 millibar temperatures, this warming results in an increased frequency of meteorological conditions that encourage the formation

of ozone in California. The incidence of days with favorable conditions for ozone formation grows as warming increases through the 21st Century. By the end of the 21st Century, assuming the same mechanisms and base conditions prevail as today, the frequency of days with favorable conditions for ozone formation increases by 25-80%, depending on the amount of warming, which presently is not clear because of uncertainties in the sensitivity of the climate system's sensitivity to greenhouse gas emissions and the future emissions pathway that will be followed by global society.

The trends identified above suggest some preliminary conclusions about the likely effect of future climate change on air quality in California. Future temperatures during stagnation events are likely to be warmer than current temperatures, leading to the conclusion that climate change will produce meteorological conditions that favor higher ozone concentrations and a greater frequency of ozone episodes. Warmer temperatures will also favor decreased $PM_{2.5}$ concentrations in the SoCAB, and constant or slightly increased $PM_{2.5}$ concentrations in the SJV.

All of the conclusions stated above are preliminary, since meteorology is only one factor that determines air pollution in California. Changes to emissions inventories through population expansion, application of emissions control programs, interaction between future temperature and future emissions, changes to background pollutant concentrations, and changes to the frequency and duration of stagnation events must also be considered. Phase II of the current project will address some of these issues using dynamically downscaled meteorology combined with detailed air quality modeling in combination with the development of a future emissions inventory for the SJV (part of a project funded by US EPA). This more detailed analysis will support more definitive conclusions about ozone and $PM_{2.5}$ response to future climate change.

Table of Contents

Table of Figures

1. Introduction

California's unique combination of large urban populations situated in confined air basins that are subject to severe air pollution events causes significant public health concerns. Ozone and airborne particulate matter are two of the main ingredients of the photochemical "smog" that can form when atmospheric mixing is low, causing pollutants to be trapped near the earth's surface. The adverse health effects of ozone and airborne particulate matter are widely acknowledged, and reducing the concentrations of these pollutants is an important objective for the State of California.

Meteorological patterns that encourage the formation of stagnation events play a significant role in the determination of air pollution concentrations in California. Measurements show that annual variability in temperature and precipitation has a large effect on ozone and $PM_{2.5}$ concentrations. Large scale meteorological patterns such as El Niño events may persist for 1 year, returning every 3-7 years, can significantly change the frequency and severity of air pollution episodes. The persistence of La Niña and El Niño events—which cause abnormal sea-surface temperatures thereby affecting worldwide weather patterns— might be part of a larger, long-lasting climate pattern.

El Niño conditions existed during 1997 and 1998, followed by La Niña conditions during 1999. Both conditions may have impacted ozone formation during this period. In southern California, during the four-month SCOS97-NARSTO field study, the peak ozone concentration observed over all of the 13 Intensive Operation Period days was 19 pphm. Ozone concentrations and photochemical activity were unusually low by comparison to past years in the South Coast Air Basin (SoCAB) throughout the entire study period. An increased frequency of positive vorticity advection and mid-atmospheric troughing just west of the Pacific Coast (associated with El Niño activity) is thought to have contributed to a deeper marine layer and better mixing than usual over the SoCAB during the summer and early fall of 1997. Similar pollution trends were observed in the San Joaquin Valley (SJV) during the El Niño event of 1997. Only thirty six days had 1hr-average ozone concentrations greater than 90ppb at Visalia (in the SJV) during 1997 compared to sixty nine days the year before.

In contrast to El Niño and La Niña events that last for 1 year, climate change refers to a sustained shift in meteorological patterns that gradually occurs over a longer time period. It is expected that climate change will significantly affect meteorological patterns in California over the next decade and longer. The implications of climate change on air quality problems in California are largely unknown.

The first step towards an understanding of how future climate will affect future air quality is to understand how present-day climate affects present-day air quality. The most direct route towards this understanding is a systematic perturbation study where one meteorological variable is changed at a time and the resulting change in air quality is calculated. These perturbation studies should be carried out for each of the characteristic types of air pollution episodes that occur in California.

The first major objective of this interim report is to present the results from a perturbation analysis for the air pollution episodes that occurred in the South Coast Air Basin (SoCAB) on September 7-9, 1993, in the SoCAB on September 23-25, 1996, and in the San Joaquin Valley (SJV) on January 4-6, 1996. The SoCAB and the SJV are the two most heavily polluted air basins in California. The air pollution episodes described above are distinctly different in character but each episode has ozone and/or $PM_{2.5}$ concentrations that greatly exceed the standards designed to protect human health. The extensive meteorological, emissions, and air quality information needed to support detailed modeling of each episode has been assembled previously, and base-case modeling studies have validated the performance of air quality models used to simulate the formation of pollutant concentrations. Table 1 summarizes the focus pollutants used in each episode and the published studies describing those episodes.

Temperature, relative humidity, mixing depth, and wind speed were uniformly perturbed by an amount that is representative of expected changes due to climate variation. The response of ozone and $PM_{2.5}$ concentrations that is induced by each perturbation was calculated, and common patterns of behavior across multiple air basins and episodes were be identified.

Table 1: Air quality episodes to be studied with sensitivity analysis.

Focus Pollutant	Location: SoCAB	Location: SJV
O_3	Date: September 7-9, 1993 References: [1, 2]	Footnote a.
PM	Date: September 23-25, 1996 References: [3-5]	Date: January 3-5, 1996 References: [6]

a. Sensitivity analysis of ozone response to climate change in the SJV is being conducted as part of a separate project funded by the US EPA at UC Berkeley. The results of this analysis will be published and made available for the current project as soon as possible, but they may not be available before the end of 2005.

The results from the expanded perturbation analysis described above have been combined with the results from previous research to produce an overall evaluation of the effect of meteorology on air pollution in California. This combination of current and previous research was necessary to meet the aggressive timeline for the current project. Sections of the current report have been extracted from the following previously published material:

M.J. Kleeman, "Assessing Changes in PM2.5 Due to Changes in Temperature", Final Report for the U.S. Environmental Protection Agency Contract # R-82824201-01.

J. Aw and M.J. Kleeman, "Evaluating the First-Order Effect of Intra-annual Temperature Variability on Urban Air Pollution", Journal of Geophysical Research-Atmospheres (108) D12, 2003.

M.J. Kleeman and G.R. Cass, "A 3D Eulerian source-oriented model for an externally mixed aerosol", Environmental Science and Technology (35) 4834-4848, 2001.

A.E. Held, Q. Ying, A. Kaduwela, and M.J. Kleeman "Modeling particulate matter in the San Joaquin Valley with a source-oriented externally mixed three-dimensional photochemical grid model", Atmospheric Environment (38), 3689-3711, (2004).

M.J. Kleeman, Q. Ying, and A. Kaduwela, "Control Strategies for the reduction of airborne particulate nitrate in California's San Joaquin Valley". Atmospheric Environment in press (2005).

All of the results from model simulations presented in the following chapters were produced specifically for the current report. The methodology used to produce these model results is partly described in the references listed above. Further updates were also made to the secondary organic aerosol (SOA) formation mechanism that was used for SoCAB simulations in this report as part of a collaboration with an ongoing US EPA project. The SOA formation mechanism was not updated for simulation of the winter SJV episode because the low photochemical activity during this episode is expected to produce minimal amounts of SOA.

The second major objective of this interim report is to describe the development of a statistical downscaling technique that can predict the frequency of meteorological events that encourage the formation of air pollution in California. The statistical downscaling technique was applied to GCM predictions through the year 2100 to predict how climate change will contribute to the frequency of air pollution episodes in California.

2. Background

Scientists at University of California, Los Angeles, have modeled the effects of climate change on parameters such as precipitation, snowpack, forest cover, and stream flow, but not air quality or human exposure [7-9]. They showed a strong increase in heat waves and extreme heat in Los Angeles and greater increases in summer temperatures as compared with winter temperatures, supporting the hypothesis of higher temperatures during the smog season (May to October) under future climate scenarios.

Previous studies have examined the effect of climate on regional air quality in the central and eastern portions of the United States [10]. These studies used output from Global Climate Models (GCMs) to study the frequency of large scale weather patterns that promote the formation of air pollution events. The GCM output can also be dynamically downscaled using regional meteorological models to simulate air pollution formation with regional air quality models. The results of these previous studies predict that the frequency of summer ozone air pollution events will increase in the future due to altered climate and increased background concentrations of ozone.

A directed study of the eastern U.S. [11] found that, around 2050, climate change would be the most important factor leading to increases in the upper quartile of 8-hour average surface ozone concentrations, whereas projected changes in anthropogenic emissions would cause increases only half as large. Moreover, estimated changes in surface conditions (e.g., vegetation cover) would have the least effect on the upper quartile of 8-hr ozone abundances. Similar conclusions were reached by Langner et al. [12] regarding future surface ozone concentrations in Europe. This research strongly suggests changing climate will be the primary driver of variations in surface ozone by 2050. Nevertheless, substantial contributions associated with changes in emissions (and surface conditions) should also be taken into account.

The analysis of climate change on regional particulate matter concentrations is less certain because air quality models for particulate matter are more complex and computationally challenging than ozone models. Sensitivity studies have been carried out to examine how regional particulate air pollution responds to direct changes in temperature, relative humidity, and mixing depth during a typical air pollution episode that occurred in SoCAB [13]. The results of this analysis suggested that increased temperature increases ozone concentration and the production of semi-volatile secondary products, but reduces the partitioning of those semi-volatile products to the particle phase.

A new aspect of the long-term concern about exposure to air pollution, and the public health consequences of that exposure, is potential impact of changes in Earth's climate associated with emissions of greenhouse gases leading to global warming. It is well known that atmospheric conditions affect photochemical smog formation, as well as emissions from vehicular and stationary sources of volatile organic compounds and oxides of nitrogen. However, while such phenomena have been studied extensively for

present climatic conditions, there is an urgent need to project air quality and exposure levels for future climate change scenarios by performing a more comprehensive analysis of the effect of climate change on air quality in California.

3. Model Description For Perturbation Analysis

Figure 3-1 illustrates the air quality modeling domains used to represent the SJV and the SoCAB in the current study. The SJV modeling region is a 54 x 72 rectangular domain with a grid size of 4km using the Lambert coordinate system. The SoCAB modeling region is an 80 x 30 rectangular domain with a grid size of 5 km using the UTM coordinate system. The SJV domain uses five vertical layers with depth of 38.5, 115.5, 154, 363 and 429 meters (which gives a total high of 1100 meters in the vertical). The SoCAB domain applied to the September 7-9, 1993 episode uses the same vertical structure. The SoCAB domain applied to the September 23-25, 1996 episode used 7 vertical layers with depths 35, 65, 100, 200, 200, 200, and 200 for a total depth of 1000m. The ~1km model depth is sufficient to resolve air pollution episodes in California since they occur in well defined air basins in the presence of temperature inversions at elevations of 0-700m.

The internally-mixed version of the UCD-CIT air quality model was used to predict the response of pollutant concentrations to changes in meteorological parameters. Previous studies [4-6, 14] have described the formulation of the UCD/CIT source-oriented air quality model, and so only those aspects that differ for the current project are discussed here.

SJV

The gas-phase chemical mechanism used to model episodes in the SJV is based on the SAPRC90 [15] mechanism with extensions to predict the formation of 10 semi-volatile organic compounds [16]. The partitioning of semi-volatile organic species to the particle phase is calculated using an absorption model calibrated using surrogate species that have representative properties for the 10 lumped model compounds [17]. The temperature dependance of the surrogate species is estimated using the Classius Clapyron equation based on a literature survey of available thermodynamic data [13]. Photochemical activity in the SJV is low during the winter months when airborne particulate matter episodes occur, leading to low predictions for SOA concentrations.

SoCAB

The gas-phase mechanism used to model episodes in the SoCAB is the Caltech Atmospheric Chemistry Model (CACM) [18, 19]. The thermodynamic data describing the partitioning of semi-volatile reaction products between the gas phase, condensed organic phase, and condensed aqueous phase [19, 20] were adapted to work with the UCD/CIT air quality model. Ethane was removed from the lumped model species ALKL and tracked as an individual species so that a more appropriate rate constant could be specified for reaction with hydroxyl radical. The model subroutines that partition inorganic and organic species between the gas and particle phases were combined so that the inorganic and organic mechanisms could be more tightly coupled. The new routines simultaneously predict the vapor pressure of semi-volatile inorganic and organic species above each particle by calculating the thermodynamic equilibrium concentration for each

species between a solid (inorganic species only), organic (organic species only) and aqueous (inorganic and organic species) phase. Activity coefficients for inorganic species are calculated using the method described by Kusik and Meissner [21]. Activity coefficients for organic species are calculated using the UNIFAC model [22]. Experimental data describing interactions between organic and inorganic species is sparse [23, 24] and so these interactions are neglected in the current study. Likewise, heterogeneous acid-catalyzed reactions leading to the formation of low-volatility organic compounds have been observed in several studies [25-27] but a comprehensive representation of these reactions suitable for use in an air quality model have not yet been formulated. In the current study, the general effect of acid catalyzed reactions is accounted for by adjusting the vapor pressures of surrogate compounds used to represent the semi-volatile organic species as discussed by Griffin et al. [19]. This procedure is applied to all particles without considering their chemical composition.

Both inorganic and organic species in the aqueous phase are used to calculate the partial vapor pressure of water above the particle surface. The exchange of all semi-volatile species (including water) between the gas phase and particles is calculated as a dynamic process using equations described by Kleeman et al. [28]. At low relative humidity, when aerosol water content becomes so small that some particles become solid, the volume available for aqueous organic species to partition into becomes negligible, reducing aqueous organic concentrations to zero. Under these conditions, the only semi-volatile species contained on particles are solid inorganic species and SOA in the condensed organic phase. Dry particles can spontaneously form a new aqueous phase when relative humidity increases.

Perturbations

Temperature perturbations to be considered in the present study include +2 K and +5 K. These values span the range of IPCC projections for global mean surface temperature rise over the next 100 years. The actual temperature rise in California is not uniform and it may differ from these values. Never-the-less, +2 K and +5 K perturbations provide a useful starting point to investigate sensitivity.

Humidity perturbations to be considered in the present study are combined with temperature perturbations to avoid artificially specifying an atmosphere with RH>100%. Each temperature perturbation will be evaluated once with constant absolute humidity and once with constant relative humidity. The likely change in humidity will occur somewhere between these limiting cases.

Perturbations in wind speed and mixing depth considered in this study were arbitrarily chosen to be +20% and +50%, respectively. These values should result in an observable effect, enabling some evaluation of the sensitivity of pollutant concentrations to these variables.

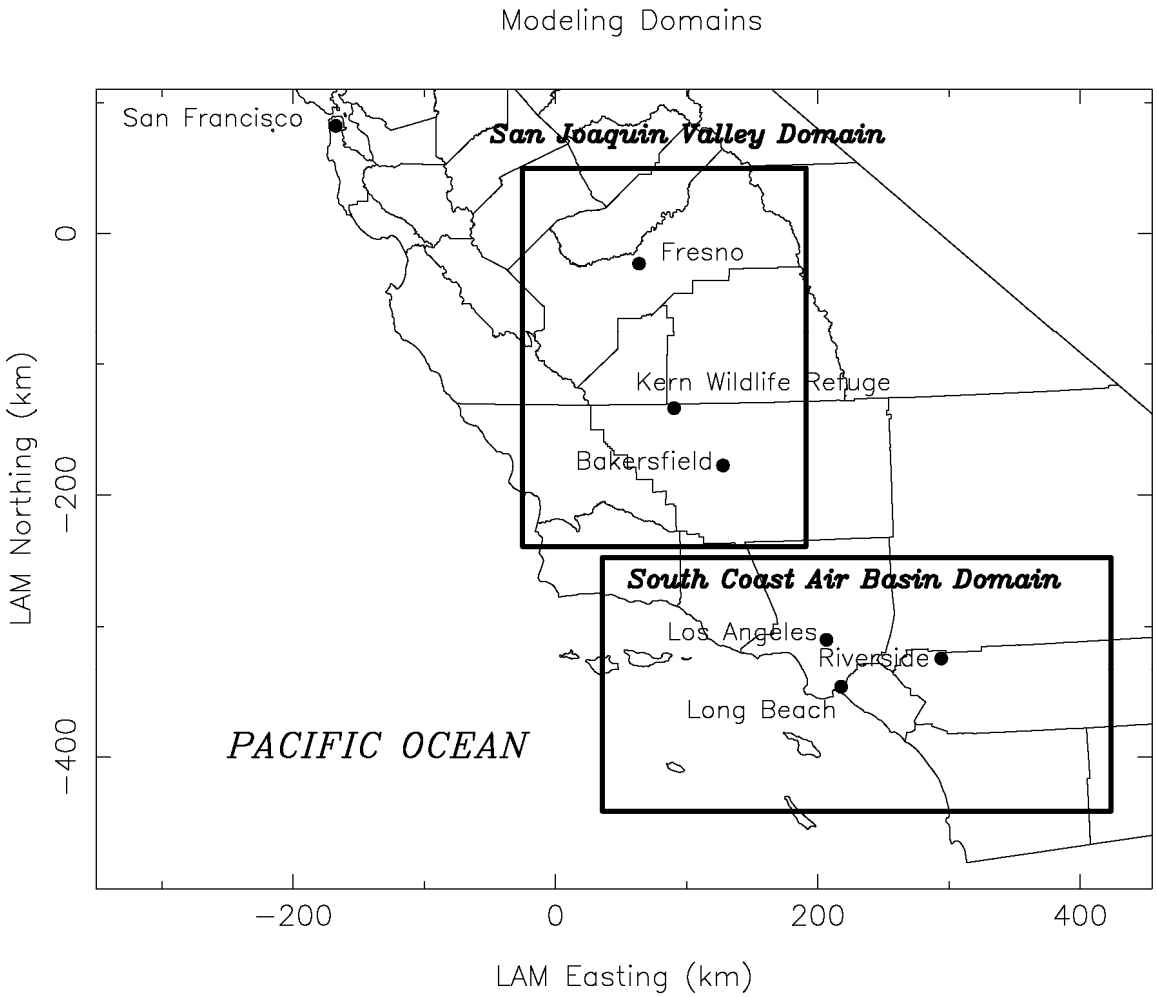

Figure 3-1: Modeling domains used for sensitivity studies in the San Joaquin Valley and the South Coast Air Basin [14].

4. Perturbation Results for Southern California on September 9, 1993

Meteorological Patterns [29]
The SoCAB is California's largest metropolitan region, which covers an area of approximately 16,700 km^2. It is bounded on the north by the San Gabriel and San Bernardino Mountains, on the east by the San Jacinto Mountains, and on the west and south by the Pacific Ocean. Elevated particulate matter concentrations usually occur in the spring and fall when photochemical reaction rates are large but temperatures are still relatively cool. Analysis indicates that the prevailing wind direction during these seasons is from the west and south over the Pacific Ocean to the inland region during the morning, switching to predominantly westerly winds by the afternoon. Intensive dairy operations in the east end of the SoCAB release large amounts of ammonia that combines with the nitric acid formed from photochemical reactions to produce high concentrations of secondary ammonium nitrate.

The severe air quality episode that occurred in the SoCAB during the period September 7-9, 1993 was characterized by daytime surface temperatures exceeding 35^oC at inland locations and a strong elevated temperature inversion. Light surface winds followed the land-sea breeze pattern with onshore flow during the day and stangation at night. Upper level winds originated from the north – north west of the modeling domain (over land), perhaps contributing to the hot daytime temperatures. This episode producted extreme ozone concentrations, even by current SoCAB standards.

Model Application
The preparation of meteorological and emissions input data needed for photochemical modeling of this episode has been described previously [1, 2] and so only a brief summary is provided here. Surface meteorological parameters were measured at 50 sites in the model region operated by the California Irrigation Management System, the South Coast Air Quality Management District, and the National Climatic Data Center. Elevated meteorological parameters were measured at West Los Angeles by the South Coast Air Quality Management District and at Claremont by the California Air Resources Board. The meteorological measurements were interpolated using a diagnostic meteorology model [30] to produce continuous meteorological fields with hourly resolution needed by the air quality simulation.

Emissions information was provided by the SCAQMD based on the emissions inventories used to support the 1997 Air Quality Management Plan along with temperature corrections for evaporative emissions based on the temperature conditions experienced on September 7-9, 1993. The emissions from the Los Angeles International Airport were updated in the current work based on the inventory developed for the summer 1997 Southern California Ozone Study (SCOS97). Biogenic emissions were represented using the biogenic inventory developed for the late August 1987 episode of the Southern California Air Quality Study (SCAQS) with appropriate temperature corrections for the conditions experienced on September 7-9, 1993. Particle-phase

emissions were speciated using measured emissions profiles [31-37] and then combined into 9 inorganic model species and 9 lumped carbonaceous model species based on chemical structure (normal alkanes, polycyclic aromatic hydrocarbons (PAH), oxygenated PAH, diacids, aliphatic acids, substituted monoaromatic compounds, cyclic petroleum biomarkers, "other organic compounds", and elemental carbon). The size distribution of particulate matter emissions from different sources was specified in 15 sections spanning 0.01 – 10 µm particle diameter based on source emission measurements [38-40]. Gas-phase organic emissions were speciated using measured emissions profiles [33-37, 41] and then combined into 24 lumped model organic species [18] based on chemical structure, reactivity, and experimentally determined SOA formation potential.

Results

Measured ozone concentrations in the SoCAB on September 9, 1993 exceeded 250 ppb, while 3-hr average $PM_{2.5}$ concentrations reached a maximum value of 90 µg m^{-3}. Model predictions have been compared to measured concentrations with good agreement [29].

Figure 4-1 (a) shows the predicted regional pattern of 1hr-average ozone concentrations on September 9, 1993 at 1500 PST. A band of high ozone concentrations is predicted to occur alone a line connecting Claremont, Riverside, and Perris, with the highest predicted concentrations reaching 290 ppb at Perris. Regional concentrations of ozone over the entire modeling domain are large during the episode, approaching 90 ppb. Predicted ozone concentrations in the region immediately downwind of Central Los Angeles are slightly lower than the regional average because they are suppressed by emissions of fresh NO_X.

Figure 4-1(b) shows the predicted increase in regional ozone concentrations at 1500 PST on September 9, 1993 when temperature is uniformly perturbed by +2 K at all times and locations. Ozone concentrations along the line connecting Claremont, Riverside, and Perris increase by approximatley 18 ppb in response to this change. Regional ozone concentrations at other locations increase by 4-5 ppb. Small regions with a ~1 ppb decrease are also observed, but these effects are minor compared to increases at other locations.

Figure 4-1(c) shows the predicted increase in regional ozone concentrations at 1500 PST on September 9, 1993 when temperature is uniformly perturbed by +5 K at all times and locations. Ozone concentrations along the line connecting Claremont, Riverside, and Perris increase by approximatley 40 ppb in response to this change. Regional ozone concentrations at other locations increase by 12-14 ppb. Small regions with a ~3 ppb decrease are also observed, but these effects are minor compared to increases at other locations.

Figure 4-2(a) shows the predicted regional pattern of 24-hr average $PM_{2.5}$ concentrations on September 9, 1993. The largest $PM_{2.5}$ concentrations 194 µg m^{-3} are predicted to occur in the region west of Riverside where ammonia concentrations are very large leading to enhanced formation of particulate ammonium nitrate. The predicted

concentration of $PM_{2.5}$ at most other locations in the inland portion of the modeling domain is 70-90 $\mu g\ m^{-3}$. Hotter temperatures suppress the formation of particulate nitrate [13]. The hot base-case temperatures during the current episode suppress the formation of large regions of particulate nitrate.

Figure 4-2(b) shows the predicted change in regional $PM_{2.5}$ concentrations on September, 1993 when temperature is uniformly perturbed by +2 K at all times and locations. $PM_{2.5}$ concentrations in the region east of Riverside decrease by 14 $\mu g\ m^{-3}$ in response to this change. The majority of this reduction is associated with the volatilzation of particulate ammonium nitrate as temperature increases. The location west of Riverside with the highest base-case concentration of particulate nitrate (see Figure 4-2(a)) does not experience the largest reduction in $PM_{2.5}$ concentrations because regions with higher excess gas-phase ammonia concentrations respond less strongly to increased temperature than regions with lower excess gas-phase ammonia [13]. Figure 4-2(b) also shows that regional average $PM_{2.5}$ concentrations are predicted to decrease by 3-5 $\mu g\ m^{-3}$ in response to the +2 K temperature perturbation. Once again, this change is caused by the partitioning of semi-volatile species to the gas phase at hotter temperatures, with particulate ammonium nitrate being the largest contributor to this effect. The region around the Long Beach harbor experiences a 0.2 $\mu g\ m^{-3}$ increase in $PM_{2.5}$ concentrations in response to a +2 K temperature perturbation. Increased temperature promotes the oxidation of SO_2 emissions in this region to form sulfuric acid. Sulfur acid is essentially non-volatile at all ambient temperatures, and so this species partitions to the particle phase regardless of temperature perturbation.

Figure 4-2(c) shows the predicted change in regional $PM_{2.5}$ concentrations on September 9, 1993 when temperature is uniformly perturbed by +5 K at all times and locations. The change in regional $PM_{2.5}$ concentrations in this case is very similar to the trends shown in Figure 4-2(b), but additional ammonium nitrate evaporates in the region east of Riverside, leading to a maxium decrease in $PM_{2.5}$ concentrations of 31 $\mu g\ m^{-3}$.

Figure 4-3(b) shows the change in predicted regional ozone concentrations at 1500 PST on September 9, 1993 when temperature is uniformly perturbed by +2 K while relative humidity is held constant. This figure can be compared to Figure 4-1(b) which applied a +2 K temperature perturbation while absolute relative humidity was held constant. The spatial distribution of increased ozone concentrations shown in Figure 4-3(b) matches that shown in Figure 4-1(b), but the magnitude of the predicted concentration increase is 30 ppb (vs. 18 ppb for the case with lower humidity). Water vapor is a source of hydroxyl radicals in urban areas, and so the increased humidity increases the reactivity of the atmosphere.

Figure 4-3(c) shows the change in predicted regional ozone concentrations at 1500 PST on September 9, 1993 when temperature is uniformly perturbed by +5 K while relative humidity is held constant. This figure can be compared to Figure 4-1(c) which applied a +5 K temperature perturbation while absolute relative humidity was held constant. Once again, the spatial pattern of the increased ozone concentration is similar, but the magnitude of the concentrations increase is enhanced by the addition of water vapor to

the system. The maximum change in ozone concentration under this condition is 67 ppb (vs. 40 ppb for the case with lower humidity).

Figure 4-4(b) shows the change in predicted regional $PM_{2.5}$ concentrations on September 9, 1993 when temperature is uniformly perturbed by +2 K while relative humidity is held constant. This figure can be compared to Figure 4-2(b) which applied a +2 K temperature perturbation while absolute humidity was held constant. Increased humidity will increase the amount of particle-phase water, leading to enhanced partitioning of soluble semi-volatile species. This effect partly counteracts the effect of increased temperature during this perturbation, which tends to force more semi-volatile material into the gas phase. The region immediate west of Riverside experiences no decrease in $PM_{2.5}$ concentrations when temperature is increased by +2 K with constant relative humdity, and one grid cell (4km x 4km area) even experiences a 2 $\mu g\ m^{-3}$ increase $PM_{2.5}$ concentrations. The area east of Riverside still experiences a decrease of $PM_{2.5}$ concentrations by approximately 7 $\mu g\ m^{-3}$, but this is reduced from the decrease of 14 $\mu g\ m^{-3}$ predicted in the case with lower humidity. The regional average $PM_{2.5}$ concentrations also show reduced response to a +2 K increase in temperature when relative humidity remains constant. Most inland regions experience a decrease in predicted $PM_{2.5}$ concentrations of 1-3 $\mu g\ m^{-3}$, with slight increases predicted in the region around the Long Beach Harbor, and the Los Angeles International Airport. The regional increases in $PM_{2.5}$ at these locations are once again associated with the enhanced production of sulfate aerosol from SO_2 emissions.

Figure 4-4(c) shows the change in predicted regional $PM_{2.5}$ concentrations on September 9, 1993 when temperature is uniformly perturbed by +5 K while relative humidity is held constant. This figure can be compared to Figure 4-2(c) which applied a +5 K temperature perturbation while absolute humidity was held constant. The trends shown in Figure 4-4(c) match the results shown in Figure 4-4(b). Peak concentrations in the region with extremely high gas-phase ammonia concentrations increase slightly in response to the temperature perturbation. Likewise, cooler coastal locations with moderate SO_2 emissions experience an increase in predicted $PM_{2.5}$ concentrations. The reduction of ammonium nitrate in other regions as temperature increases is mitigated by the effect of increased humidity. The largest reduction in $PM_{2.5}$ concentrations in response to the +5 K temperature perturbation with constant humidity is 19 $\mu g\ m^{-3}$ (vs. 31 $\mu g\ m^{-3}$ for the case with reduced humidity).

Figure 4-5(b) shows the change in predicted regional ozone concentrations at 1500 PST on September 9, 1993 in response to a uniform increase in mixing depths of +50%. The increased mixing depths increase predicted ozone concentrations in the western portion of the model domain by 75 ppb and decrease predicted ozone concentrations in the eastern portion of the model domain by 36 ppb. The location of the maximum concentration increase differs slightly from the location of the predicted ozone maxium in the base-case simulation, and so the net effect of the increased mixing depth is to slightly increase the maxium ozone concentrations predicted during the episode and to increase the size of the region experiencing those maximum concentrations. The observation that mixing depth increases ozone concentrations during severe photochemical episodes in the

SoCAB has been noted previously during simulations of the Southern California Air Quality Study (SCAQS).

Figure 4-5(c) shows the change in predicted regional ozone concentrations at 1500 PST on September 9, 1993 in response to a uniform increase in wind speed of +20%. Perturbed wind fields were produced by increasing the measured wind speed values that are used by the diagnostic meteorological model to generate continuous divergence-free wind fields. Increased wind speed reduces the concentration of pollutant emisions in ground-level cells and moves high concentration plumes to different locations. The results shown in Figure 4-5(c) show that predicted ozone concentrations in the wester portion of the model domain increase by 8 ppb in response to increased wind speeds, but the maximum predicted concentrations along the line connecting Claremont, Riverside, and Perris are decreased by 107 ppb. The net effect of the increased wind speeds is to make the predicted ozone concentrations more uniform across the model region, with an overall reduction in peak ozone concentrations during the current episode.

Figure 4-6(b) shows the change in predicted regional $PM_{2.5}$ concentrations on September 9, 1993 in response to a uniform increase in mixing depth of +50%. The maximum increase in $PM_{2.5}$ concentrations in response to this change is 5 $\mu g\ m^{-3}$ in the region that experienced the largest increase in ozone concentrations (see Figure 4-5(b)). Predicted $PM_{2.5}$ concentrations in the region to the east of Riverside are reduced by 9 $\mu g\ m^{-3}$ as the plume of enhanced nitrate is diluted by the increased mixing depth.

Figure 4-6(c) shows the change in predicted regional $PM_{2.5}$ concentrations on September 9, 1993 in response to a uniform increase in wind speed of +20%. Small increases of ~2 $\mu g\ m^{-3}$ $PM_{2.5}$ are predicted in a few locations, but the major change associated with this perturbation is a predicted reduction of 44 $\mu g\ m^{-3}$ in $PM_{2.5}$ concentrations at the location of maximum base-case $PM_{2.5}$. The majority of this effect is likely associated with reduced ammonia concentrations in the regions near the agricultural sources to the west of Riverside.

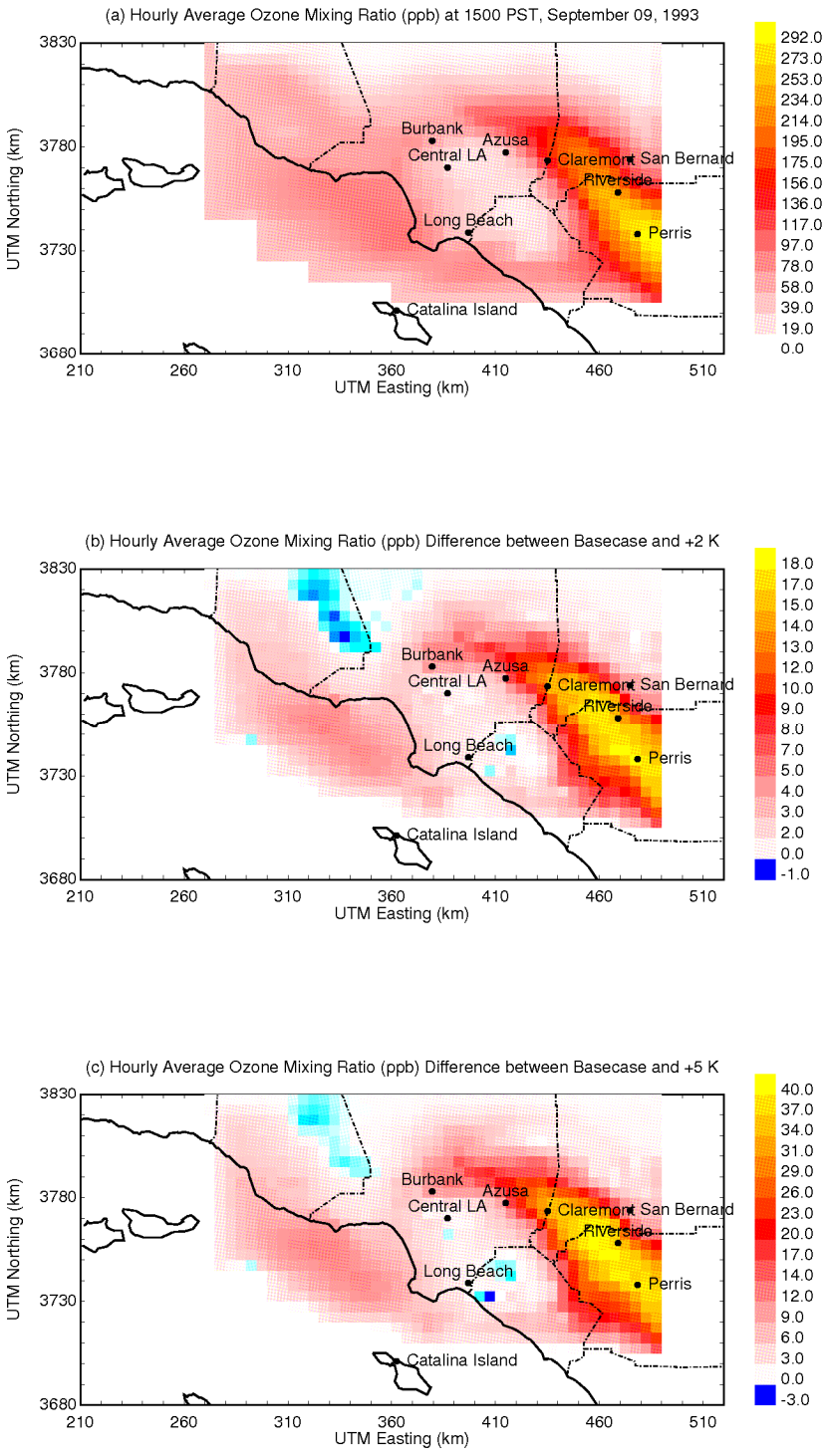

Figure 4-1: Hourly average ozone mixing ratio (panel a) and ozone mixing ratio difference in response to uniform temperature perturbations (panels b,c) at 1500 PST on September 9, 1993. Units are ppb.

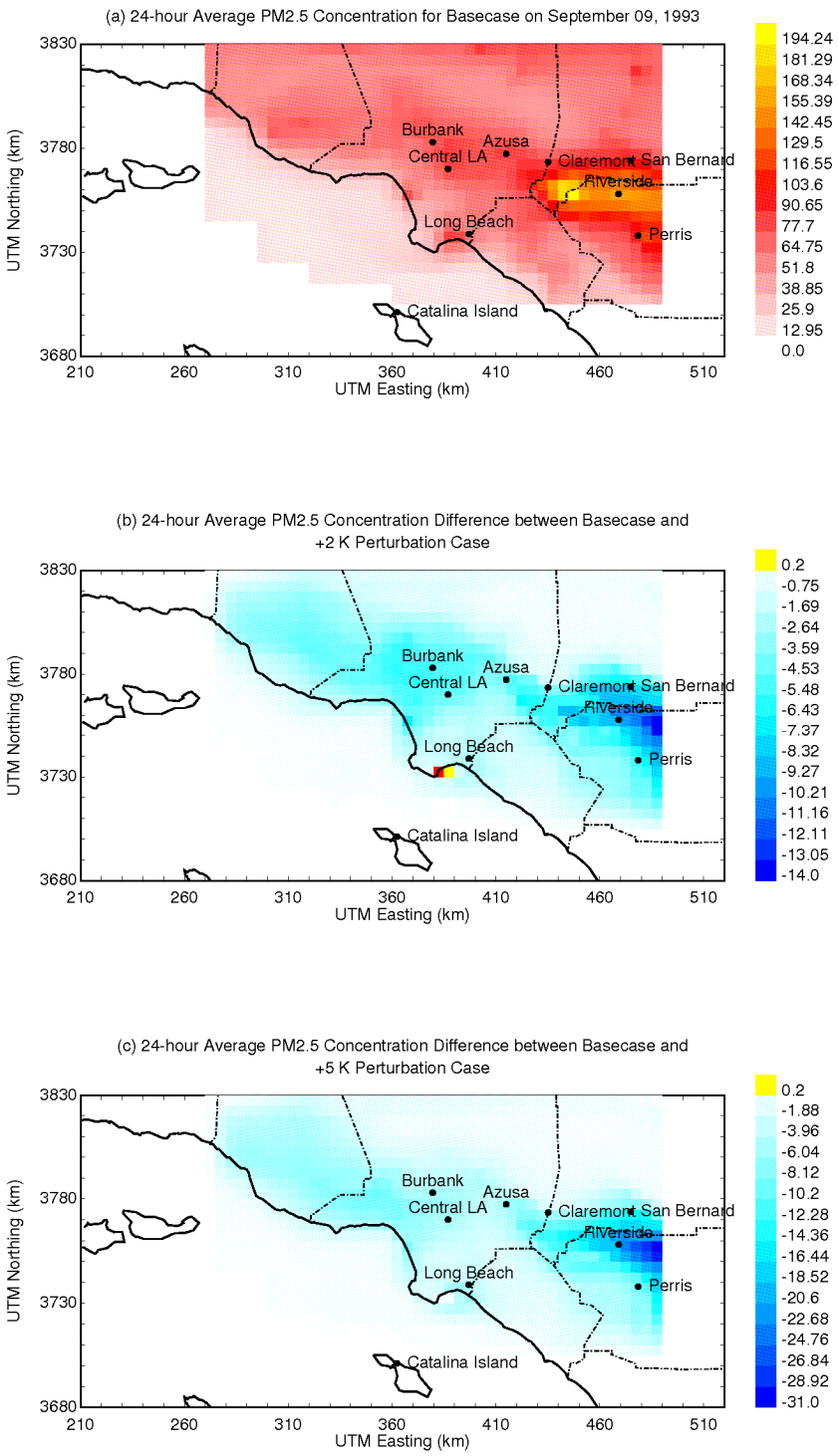

Figure 4-2: 24-hr average $PM_{2.5}$ concentration (panel a) and 24-hr average $PM_{2.5}$ concentration difference in response to uniform temperature perturbations (panels b,c) on September 9, 1993. Units are µg m^{-3}.

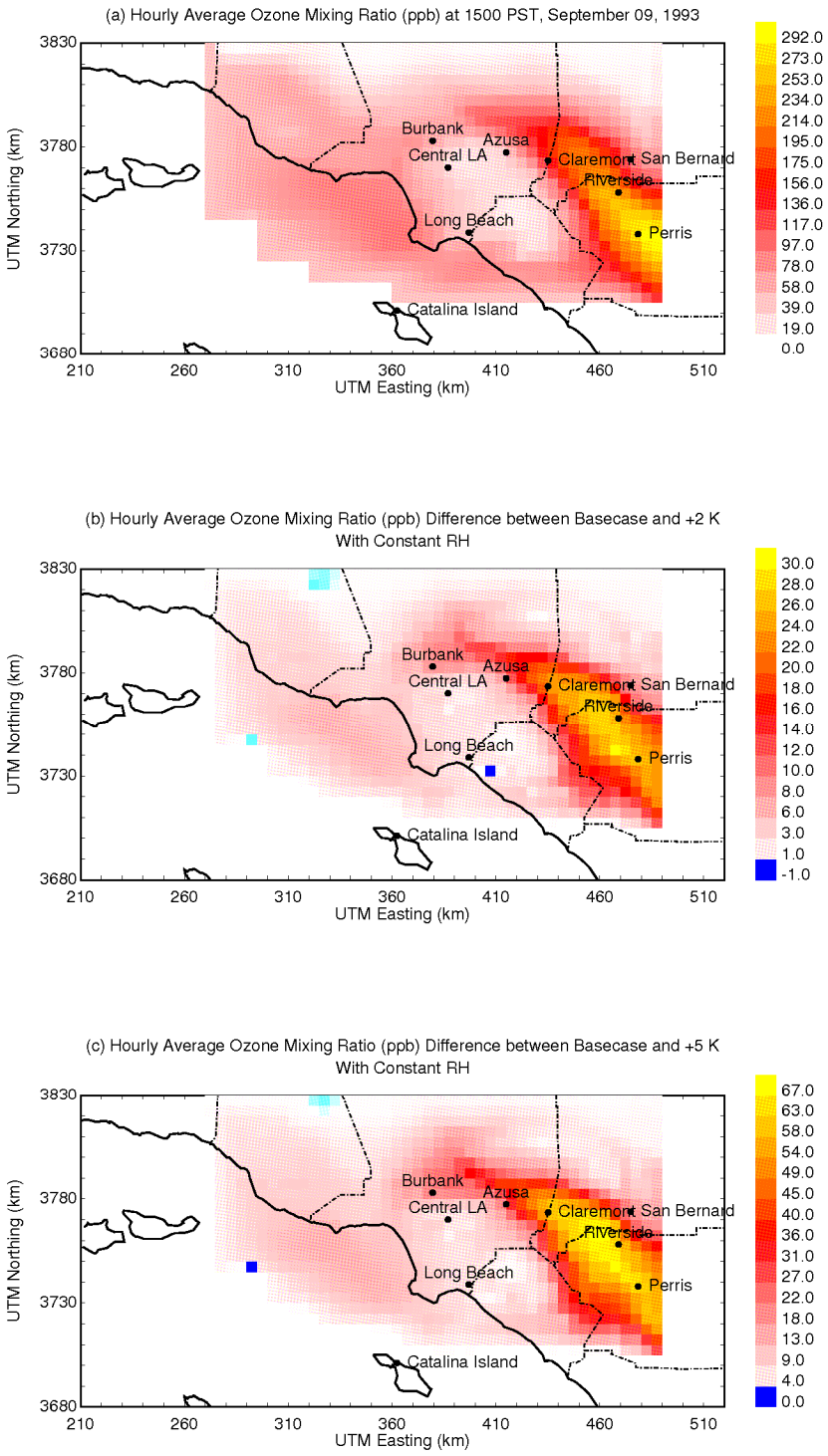

Figure 4-3: Hourly average ozone mixing ratio (panel a) and ozone mixing ratio difference in response to uniform temperature perturbations with constant relative humidity (panels b,c) at 1500 PST on September 9, 1993. Units are ppb.

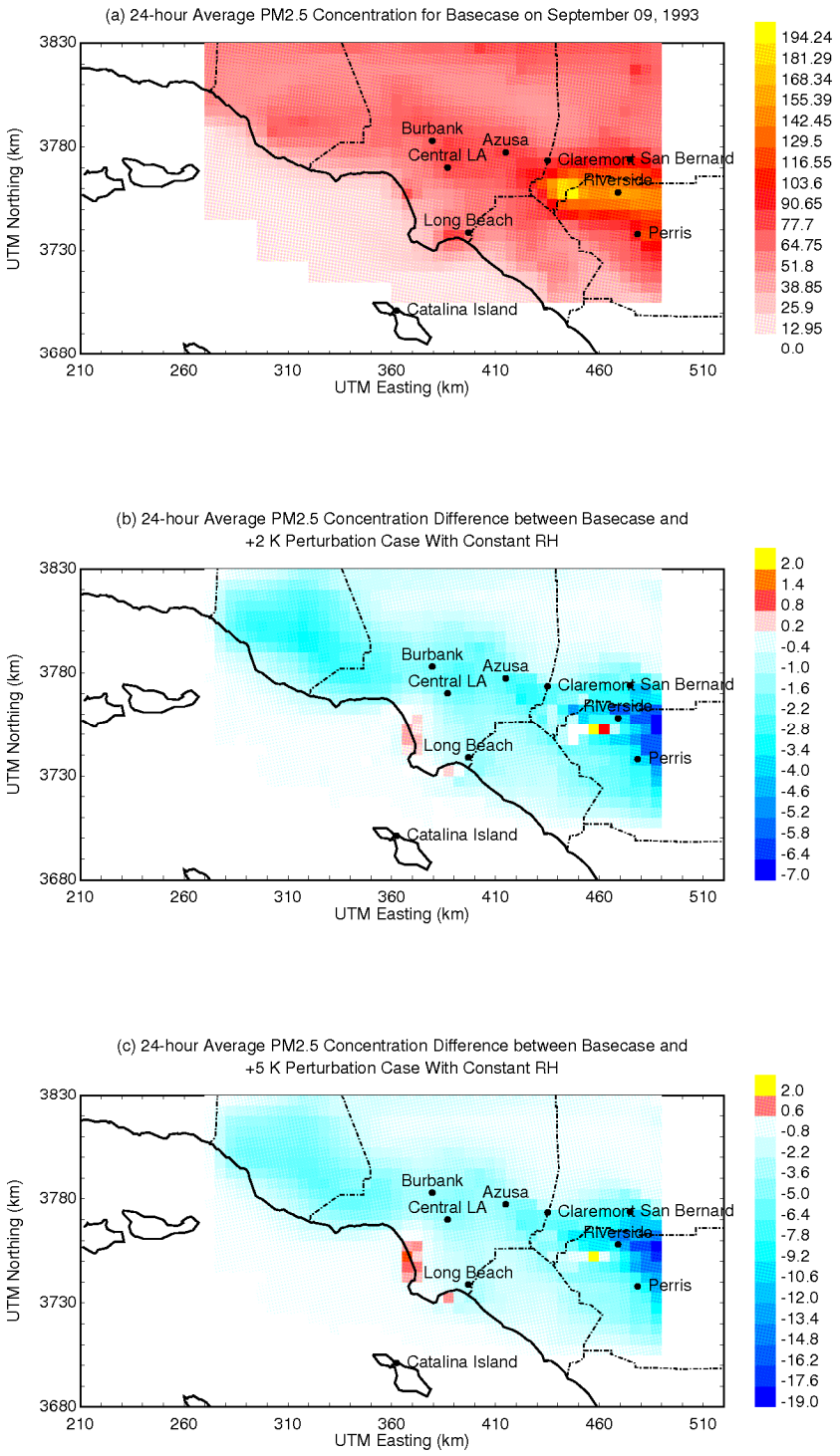

Figure 4-4: 24-hr average $PM_{2.5}$ concentration (panel a) and 24-hr average $PM_{2.5}$ concentration difference in response to uniform temperature perturbations with constant relative humidity (panels b,c) on September 9, 1993. Units are µg m-3.

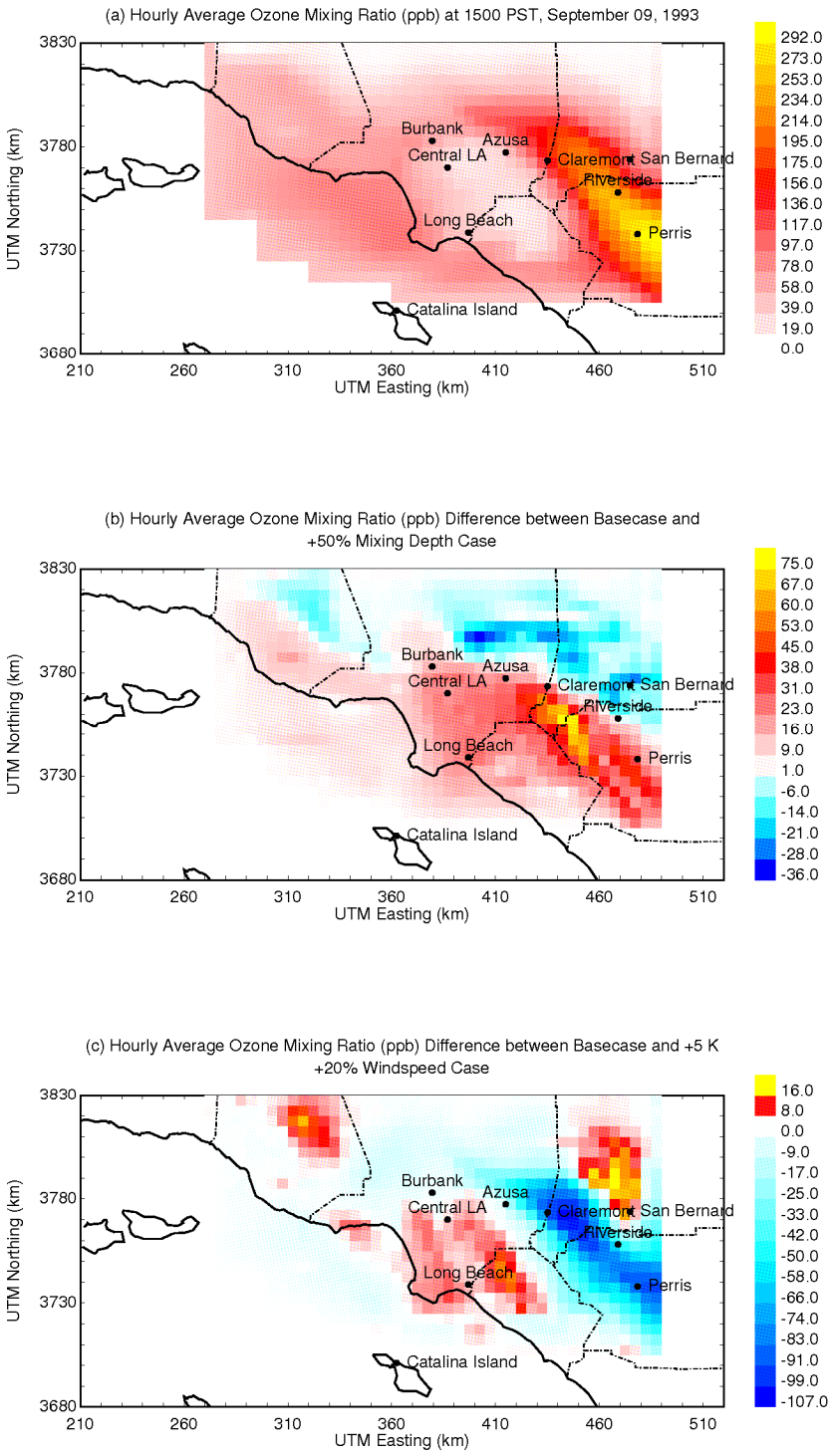

Figure 4-5: Hourly average ozone mixing ratio (panel a) and ozone mixing ratio difference in response to +50% increase in mixing depth (panels b) and +20% increase in wind speed (panel c) at 1500 PST on September 9, 1993. Units are ppb.

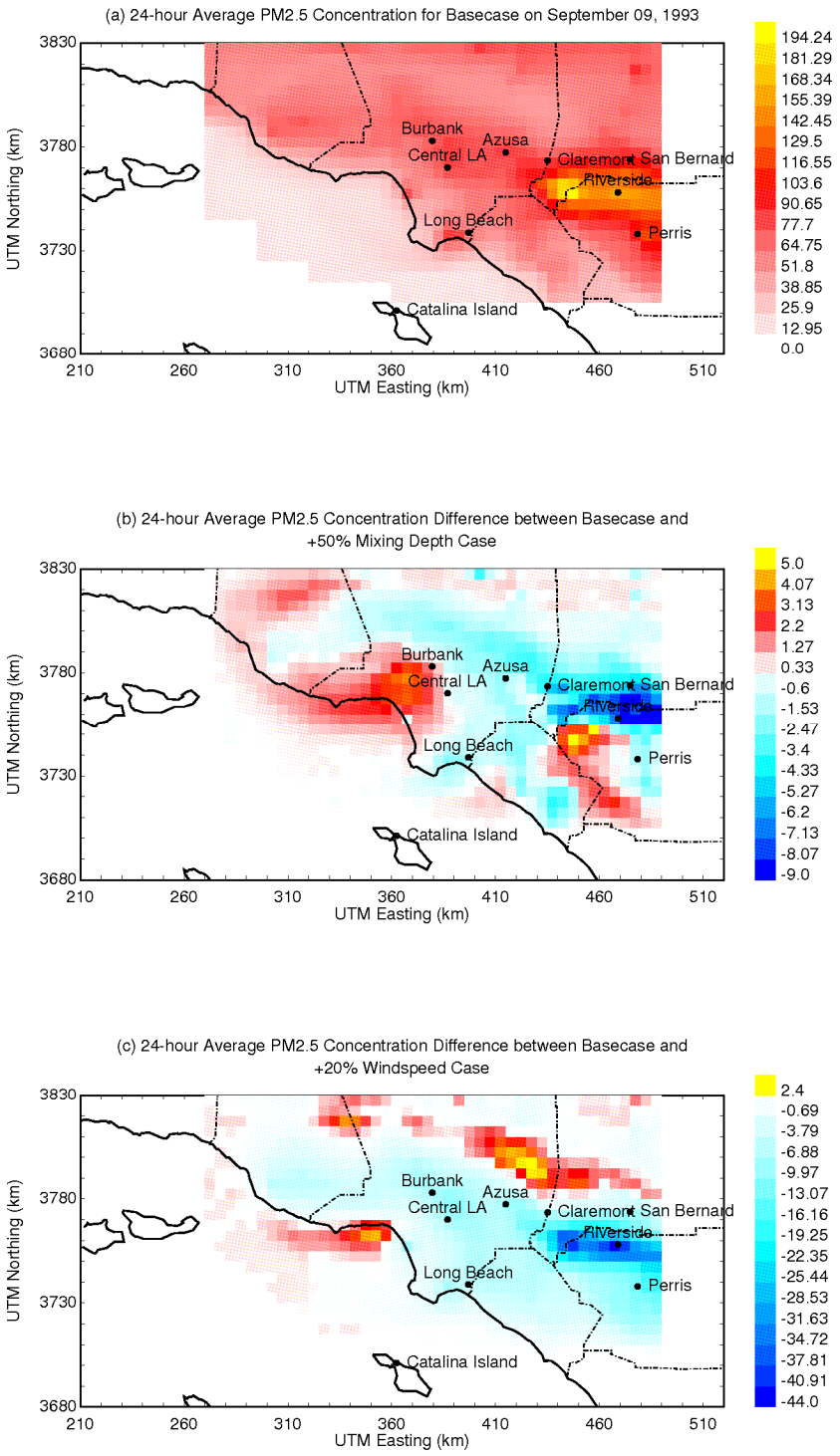

Figure 4-6: 24-hr average $PM_{2.5}$ concentration (panel a) and 24-hr average $PM_{2.5}$ concentration difference in response to +50% increase in mixing depth (panels b) and +20% increase in wind speed (panel c) on September 9, 1993. Units are µg m-3.

5. Perturbation Results for Southern California on September 25, 1996

Meteorological Patterns

Temperatures at inland locations in the South Coast Air Basin (SoCAB) were moderate on September 25, 1996, with peak daytime values reaching 25^{o}C. Winds were light onshore during the day and stagnant during the evening. The total time required for air parcels to traverse the study region from west to east was calculated to be greater than 3 days.

Model Application

Routine hourly measurements made by the SCAQMD at their monitoring sites provided the meteorological inputs for the diagnostic meteorological model used to produce continuous fields for air quality calculations. These measurements include wind speed (29 sites), temperature (10 sites), relative humidity (10 sites), total solar radiation (4 sites) and ultraviolet solar radiation (1 site). Upper level wind speed, wind direction and temperature were measured at hourly intervals using a lower atmospheric radar profiler at the Los Angeles International Airport (LAX). In the current study, wind fields were specified with high numerical accuracy to improve self-consistency and reduce wind field divergence. Atmospheric mixing depths during the simulation were constructed using Holtzworth's method [42], the interpolated surface temperature throughout the modeling domain, and the vertical temperature profile measured at LAX.

The mobile source emissions inventory was calculated with the traffic emissions model EMFAC-7G featuring a day-specific temperature correction for evaporative emissions. Area source and small point source inventories within the modeling domain were based on the 1995 average-day emissions inventory provided by SCAQMD together with measured particle size and composition profiles [39, 40]. Similarly, large point source inventories were based on the 1997 average-day emissions inventory provided by SCAQMD together with measured particle size and composition profiles [39, 40]. To reflect changes in mobile sources, fertilizer and livestock emissions, the ammonia emissions inventory for the SoCAB [43] was updated to 1996 [3].

Results

Peak ozone concentrations measured at locations around central Los Angeles on September 25, 1996 were generally less than 100 ppb. Measurements of $PM_{2.5}$ concentrations at Riverside between the hours of 1400-1700 PST exceeded 75 $\mu g\ m^{-3}$, with higher concentrations predicted during the evening hours.

Figure 5-1 (a) shows the predicted regional pattern of 1hr-average ozone concentrations on September 25, 1996 at 1500 PST. The highest predicted ozone concentration is 120 ppb in the northeast corner of the domain that is downwind of the major emissions sources during this event. Concentrations around central Los Angeles are generally moderate, with predicted values of 70-80 ppb. Concentrations immediately dowwind of central Los Angeles are once again slightly lower than the regional average because they

are suppressed by emissions of fresh NO_X.

Figure 5-1(b) shows the predicted increase in regional ozone concentrations at 1500 PST on September 25, 1996 when temperature is uniformly perturbed by +2 K at all times and locations. Ozone concentrations in the eastern portion of the air basin increase by approximately 12 ppb in response to this change, with smaller increases of 1-3 ppb over the majority of the domain.

Figure 5-1(c) shows the predicted increase in regional ozone concentrations at 1500 PST on September 25, 1996 when temperature is uniformly perturbed by +5 K at all times and locations. The area of maximum ozone increase once again occurs in the regions with the highest base-case ozone concentrations. Peak ozone values increase by 33 ppb in response to the +5 K temperature perturbation, with smaller increases of 4-6 ppb predicted over much of the domain. A minor region with a 1 ppb ozone decrease in response to the +5 K temperature perturbation is observed near Fullerton.

Figure 5-2(a) shows the predicted regional pattern of 24-hr average $PM_{2.5}$ concentrations on September 25, 1996. The largest $PM_{2.5}$ concentrations 154 $\mu g\ m^{-3}$ are predicted to occur in the region west and northeast of Riverside where ammonia concentrations are very large leading to enhanced formation of particulate ammonium nitrate. The predicted concentration of $PM_{2.5}$ most other locations in the inland portion of the modeling domain is 40-80 $\mu g\ m^{-3}$. The moderate base-case temperatures during the current episode allow for the formation of significant quantities of particulate ammonium nitrate throughout the study region.

Figure 5-2(b) shows the predicted change in regional $PM_{2.5}$ concentrations on September 25, 1996 when temperature is uniformly perturbed by +2 K at all times and locations. $PM_{2.5}$ concentrations in the region north of Fontana and south of Riverside decrease by 11 $\mu g\ m^{-3}$ in response to this change. As discussed previously, the majority of this reduction is associated with the volatilzation of particulate ammonium nitrate as temperature increases. The locations west and northeast of Riverside with the highest base-case concentration of particulate nitrate (see Figure 5-2(a)) do not experience the largest reduction in $PM_{2.5}$ concentrations because of the high gas-phase ammonia concentrations in this region under the current meteorological conditions. Figure 5-2(b) also shows that regional average $PM_{2.5}$ concentrations are predicted to decrease by 2-5 $\mu g\ m^{-3}$ in response to the +2 K temperature perturbation. Scattered locations in the coastal evivornment experience miniscule increases of 0.2 $\mu g\ m^{-3}$ in $PM_{2.5}$ concentrations in response to a +2 K temperature perturbation.

Figure 5-2(c) shows the predicted change in regional $PM_{2.5}$ concentrations on September 25, 1993 when temperature is uniformly perturbed by +5 K at all times and locations. The trends shown in Figure 5-2(c) are very similar to those shown in Figure 5-2(b), but additional ammonium nitrate evaporates in the region northeast of Riverside around the high concentration plume formed by ammonia emissions from agricultural operations. The maximum decrease in $PM_{2.5}$ concentrations in this region is 29 $\mu g\ m^{-3}$.

Figure 5-3(b) shows the change in predicted regional ozone concentrations at 1500 PST on September 25, 1996 when temperature is uniformly perturbed by +2 K while relative humidity is held constant. This figure can be compared to Figure 5-1(b) which applied a +2 K temperature perturbation while absolute relative humidity was held constant. The spatial pattern of increased ozone between these two cases is very similar, but the magnitude of the ozone increase is larger for the case with higher relative humidity. The maximum increase in ozone concentrations shown in Figure 5-3(b) is 17 ppb compared to only 12 ppb in Figure 5-1(b). As discussed previously, water vapor is a source of hydroxyl radicals in urban areas, and so the increased humidity increases the reactivity of the atmosphere.

Figure 5-3(c) shows the change in predicted regional ozone concentrations at 1500 PST on September 25, 1993 when temperature is uniformly perturbed by +5 K while relative humidity is held constant. This figure can be compared to Figure 5-1(c) which applied a +5 K temperature perturbation while absolute relative humidity was held constant. Once again, the spatial pattern of the increased ozone concentration is similar, but the magnitude of the concentrations increase is enhanced by the addition of water vapor to the system. The maximum change in ozone concentration under this condition is 46 ppb (vs. 29 ppb for the case with lower humidity).

Figure 5-4(b) shows the change in predicted regional $PM_{2.5}$ concentrations on September 25, 1996 when temperature is uniformly perturbed by +2 K while relative humidity is held constant. This figure can be compared to Figure 5-2(b) which applied a +2 K temperature perturbation while absolute humidity was held constant. The region immediately west and northeast of Riverside experiences very little decrease in $PM_{2.5}$ concentrations when temperature is increased by +2 K with constant relative humdity because the high concencentration of gas-phase ammonia in the area and the constant water content of the aerosol maintain favorable conditions for nitrate formation even when temperature is increasing. The fringe around the high concentration region experiences a decrease in predicted $PM_{2.5}$ concentrations of 6 $\mu g\ m^{-3}$ under these conditions. Most inland portions of the domain experience a regional decrease in $PM_{2.5}$ concentrations of 1-3 $\mu g\ m^{-3}$.

Figure 5-4(c) shows the change in predicted regional $PM_{2.5}$ concentrations on September 25, 1996 when temperature is uniformly perturbed by +5 K while relative humidity is held constant. This figure can be compared to Figure 5-2(c) which applied a +5 K temperature perturbation while absolute humidity was held constant. The trends shown in Figure 5-4(c) match the results shown in Figure 5-4(b). The additional water in the case with constant relative humidity mitigates the reduction of ammonium nitrate associated with increased temperature. The largest reduction in $PM_{2.5}$ concentrations in response to the +5 K temperature perturbation with constant humidity is 15 $\mu g\ m^{-3}$ (vs. 29 $\mu g\ m^{-3}$ for the case with reduced humidity).

Figure 5-5(b) shows the change in predicted regional ozone concentrations at 1500 PST on September 25, 1996 in response to a uniform increase in mixing depths of +50%. The increased mixing depth has little impact on predicted ozone concentrations in this

pollution episode because base-case mixing depths are already relatively large. Predicted ozone concentrations in the eastern portion of the domain increase by a maximum of 11 ppb, with smaller increases of a few ppb (or even slight decreases) predicted for the central portion of the study region. The difference in the behavior of the pollution episode on September 25, 1996 vs September 9, 1993 emphasizes the need to model a large number of systems to explore the full range of possible outcomes.

Figure 5-5(c) shows the change in predicted regional ozone concentrations at 1500 PST on September 25, 1996 in repsonse to a uniform increase in wind speed of +20%. Predicted ozone concentrations in the wester portion of the model domain increase by 10 ppb in response to increased wind speeds, but the maximum predicted concentrations in the far northeast of the model domain decrease by 55 ppb. It is likely that the higher ozone concentrations were simply advected out of the study region by the increased winds. along the line connecting Claremont, Riverside, and Perris are decreased by 107 ppb.

Figure 5-6(b) shows the change in predicted regional $PM_{2.5}$ concentrations on September 25, 1996 in response to a uniform increase in mixing depth of +50%. A small increase in $PM_{2.5}$ concentrations of ~0.5 $\mu g\ m^{-3}$ is predicted to occur in the area downwind of Long Beach in response to this change, while concentrations in the eastern portion of the domain are predicted to decrease by ~6 $\mu g\ m^{-3}$. .

Figure 5-6(c) shows the change in predicted regional $PM_{2.5}$ concentrations on September 25, 1996 in response to a uniform increase in wind speed of +20%. The region with the highest base-case $PM_{2.5}$ concentrations is predicted to experience a decrease in $PM_{2.5}$ concentrations of 31 $\mu g\ m^{-3}$ in response to the increased wind speed, primarily through the enhanced dilution of primary ammonia emissions.

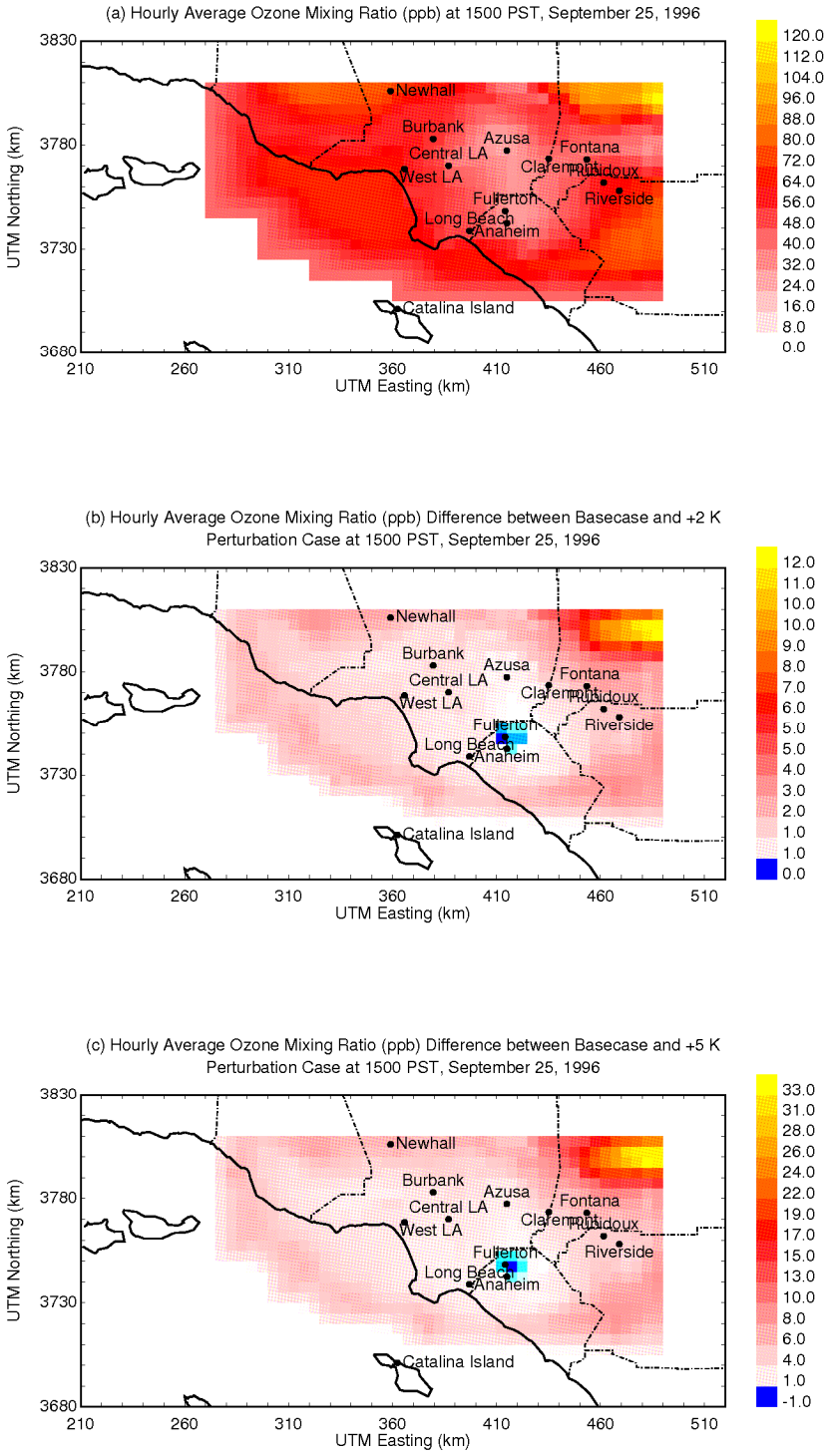

Figure 5-1: Hourly average ozone mixing ratio (panel a) and ozone mixing ratio difference in response to uniform temperature perturbations (panels b,c) at 1500 PST on September 25, 1996. Units are ppb.

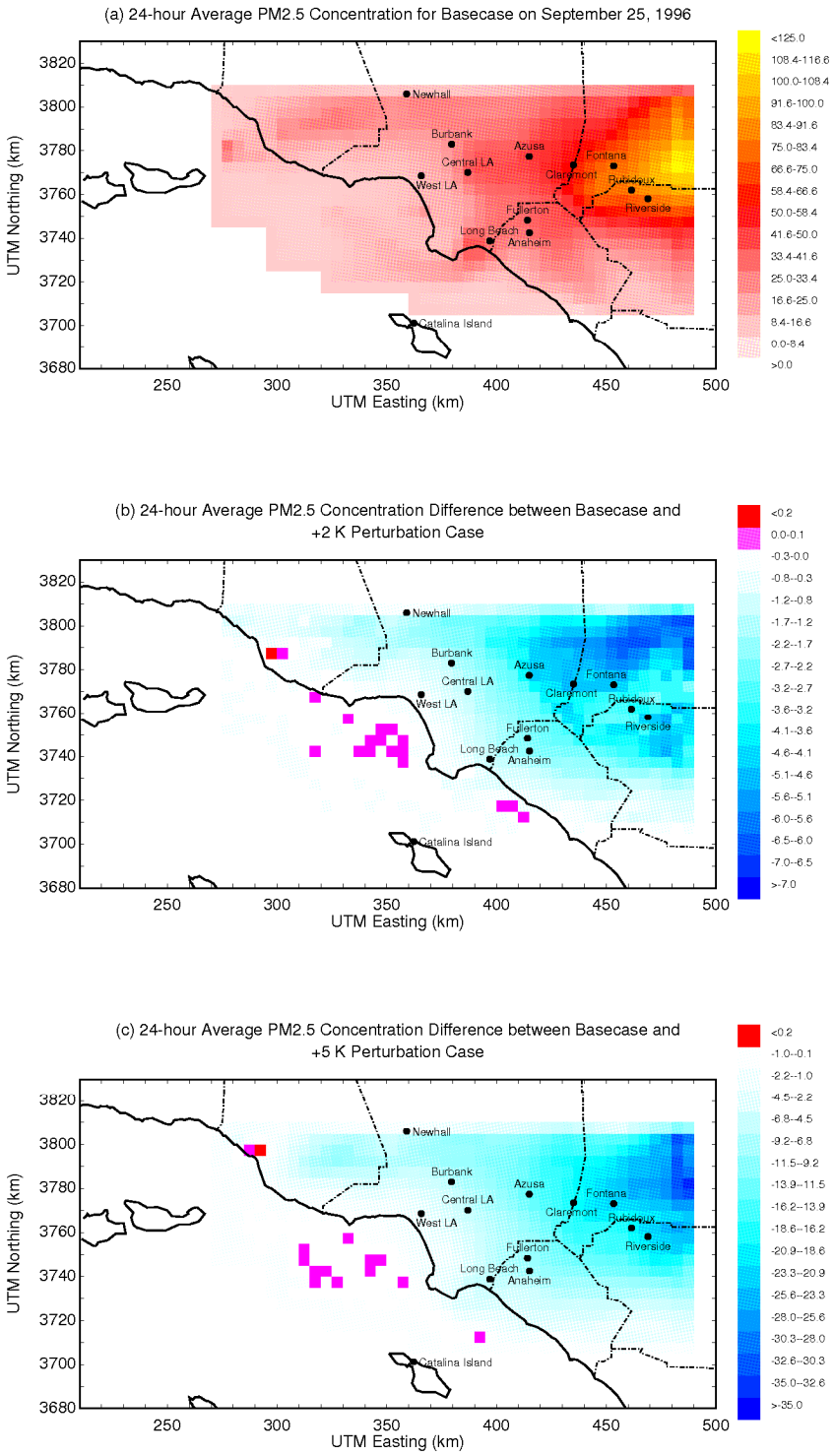

Figure 5-2: 24-hr average $PM_{2.5}$ concentration (panel a) and 24-hr average $PM_{2.5}$ concentration difference in response to uniform temperature perturbations (panels b,c) on September 25, 1996. Units are µg m-3.

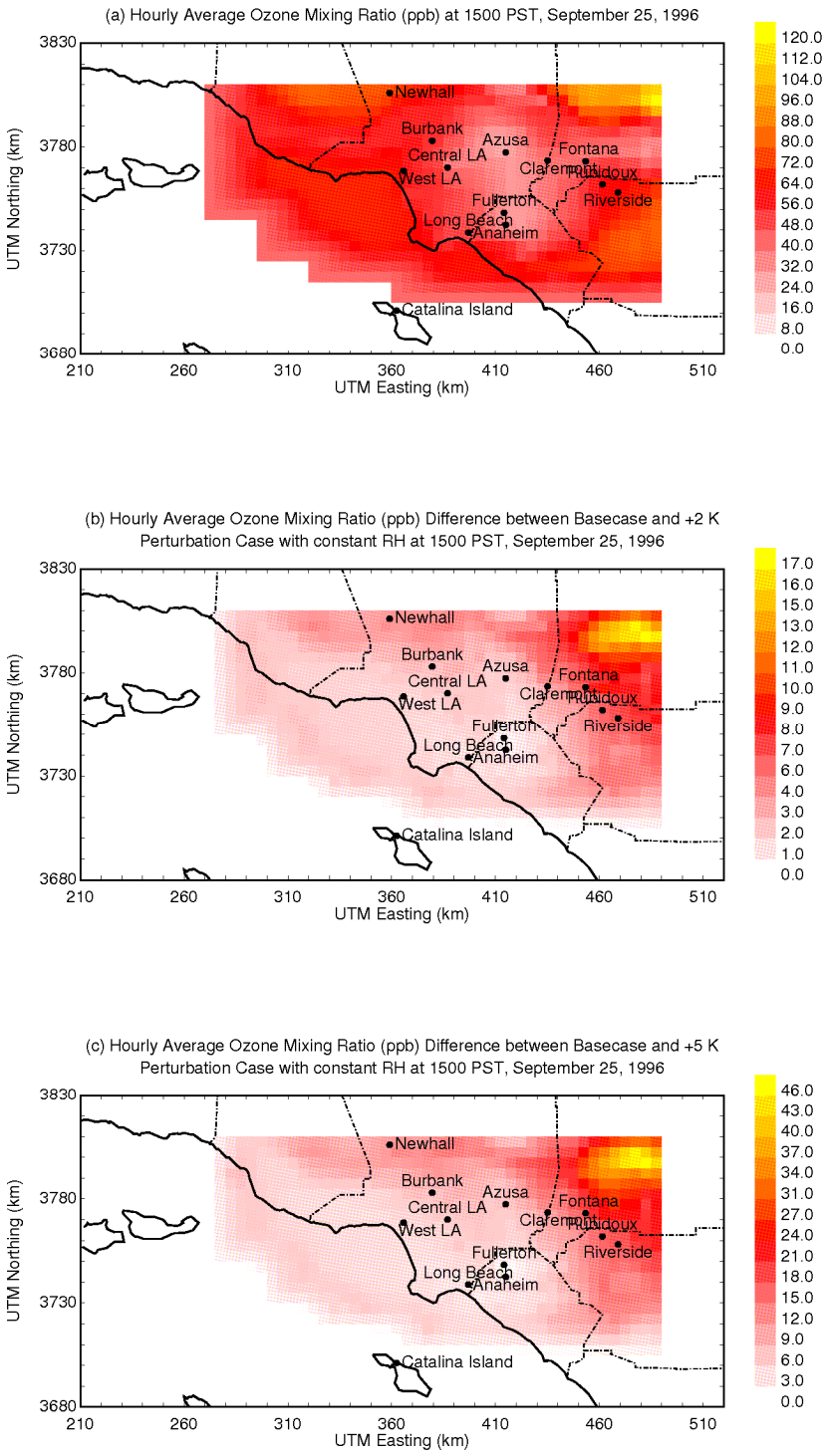

Figure 5-3: Hourly average ozone mixing ratio (panel a) and ozone mixing ratio difference in response to uniform temperature perturbations with constant relative humidity (panels b,c) at 1500 PST on September 25, 1996. Units are ppb.

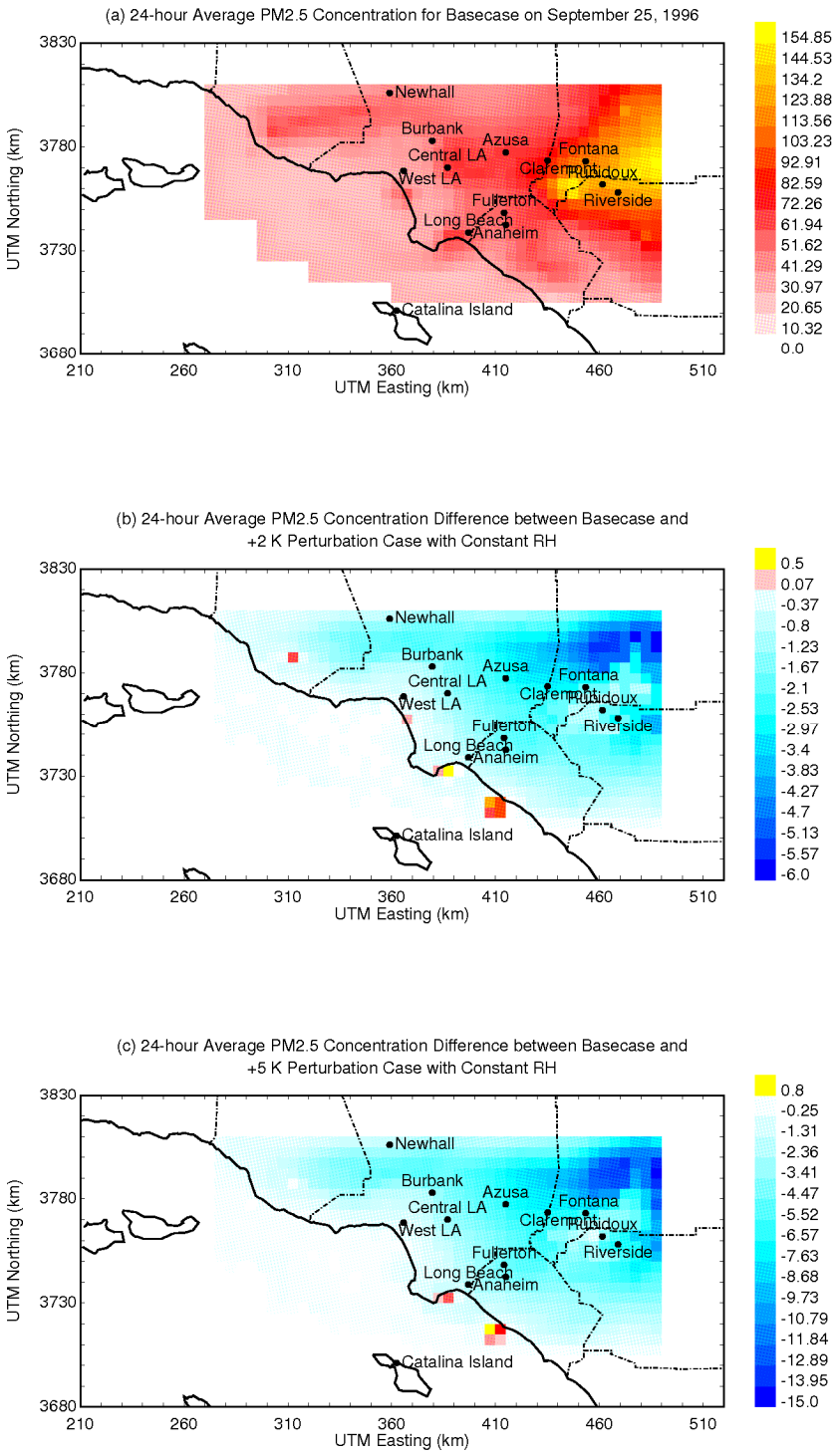

Figure 5-4: 24-hr average $PM_{2.5}$ concentration (panel a) and 24-hr average $PM_{2.5}$ concentration difference in response to uniform temperature perturbations with constant relative humidity (panels b,c) on September 25, 1996. Units are µg m-3.

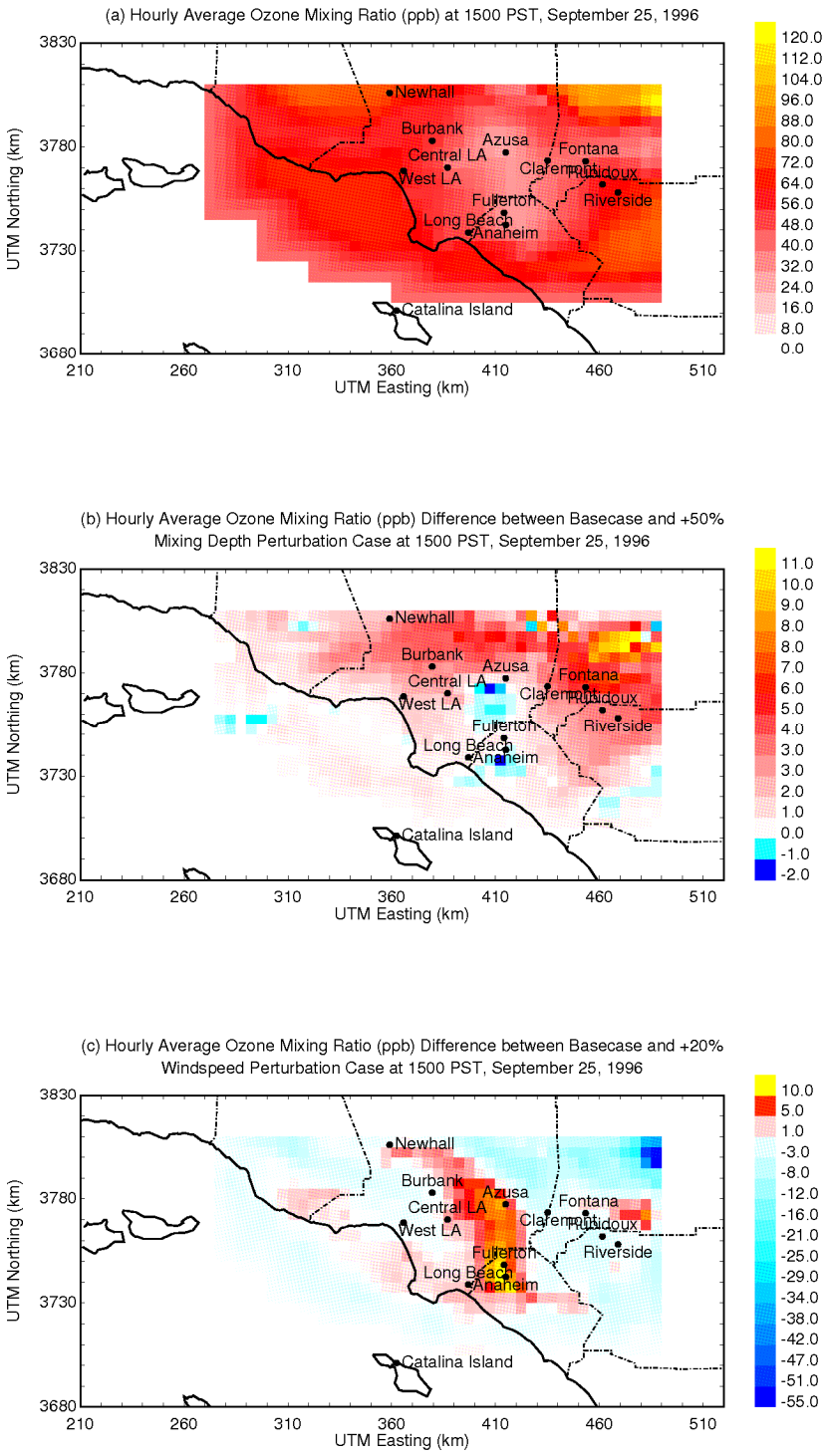

Figure 5-5: Hourly average ozone mixing ratio (panel a) and ozone mixing ratio difference in response to +50% increase in mixing depth (panels b) and +20% increase in wind speed (panel c) at 1500 PST on September 25, 1996. Units are ppb.

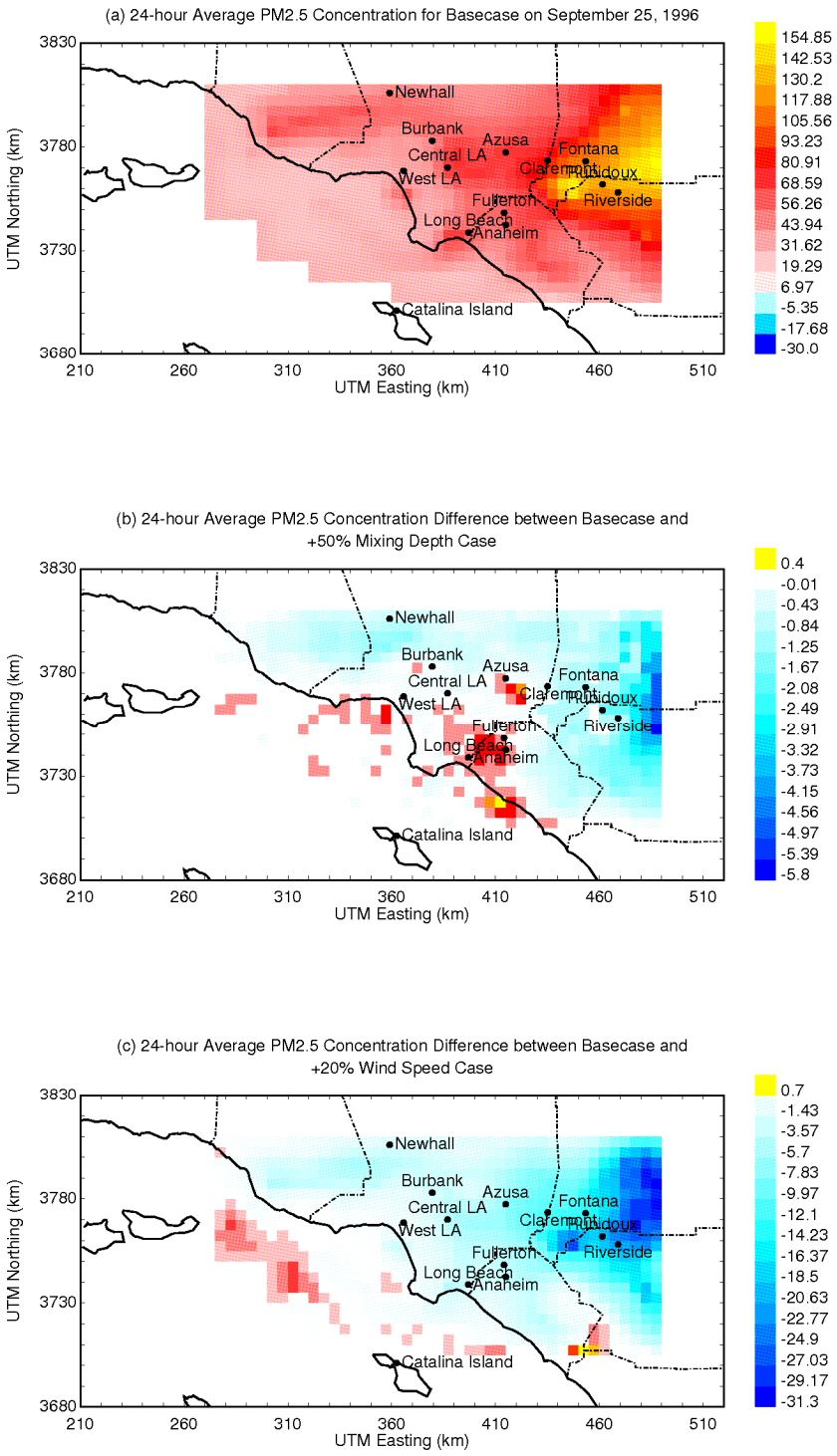

Figure 5-6: 24-hr average $PM_{2.5}$ concentration (panel a) and 24-hr average $PM_{2.5}$ concentration difference in response to +50% increase in mixing depth (panels b) and +20% increase in wind speed (panel c) on September 25, 1996. Units are µg m-3.

6. Perturbation Results for San Joaquin Valley on January 6, 1996

Meteorological Patterns

Even though the airborne particulate matter in the SJV and SoCAB has similar characteristics, each region has unique geography, emissions, and meteorological patterns. The SJV is approximately 400 km in length and 100 km in width. It is bounded on the west by the Coast Mountain range, on the east by the Sierra Nevada range and on the south by the Tehachapi Mountains. Elevated particulate matter concentrations in the SJV are usually associated with stagnant atmospheric conditions (low mixing depth and slow wind speed), which commonly occur between mid-November and mid-February. Typical meteorological patterns transport pollutants from north to south across the SJV. Temperatures during these episodes approach freezing during the night and reach a maximum value of ~15^{o}C during the day.

Model Application [6]

Surface meteorological conditions within the study domain were measured by monitoring stations operated by CARB, the National Climatic Data Center (NCDC), and the California Irrigation Management System (CIMIS). Measured values of solar radiation (19 sites), relative humidity (70 sites), temperature (70 sites), wind speed (18 sites), wind direction (18 sites), and fog (10 airports) were used to specify surface meteorological conditions throughout the study region based on Goodin's interpolation procedure [30]. Reductions of the surface UV irradiants due to cloud cover were estimated using the empirical equation described by [44]. The surface fields were augmented with upper elevation measurements to create interpolated 3D fields for certain meteorological variables. Rawinsonde measurements collected near Fresno and Bakersfield provide vertical profiles of temperature and humidity in the domain. Rawinsonde and radar profiler measurements collected at six sites were used to interpolate the upper layer wind speed and wind direction. Transport was generally stagnant with low wind-flows from the northwest to the southeast during the study period. Based on the rawinsonde data, the Holtzworth method [42] was used to generate interpolated mixing depth fields that were verified and improved upon by detailed inspection of the temperature profiles. Calculated mixing depths were all well below 1000m during the 3 day simulation period, with a typical afternoon maximum mixing depth of approximately 700 m. Thus, the modeled column depth of 1100m encompasses the entire turbulent boundary layer during the modeling period.

The air pollutant emission rates in the SJV are the second largest in the state of California (preceded only by the SoCAB). Inventories describing the emissions of total organic gases (TOG), oxides of nitrogen (NO_X), oxides of sulfur (SO_X), ammonia (NH_3) and total suspended particulate matter (TSP) were compiled by CARB for the IMS95 study. All major area, point, and mobile source emissions within the study region were included in the inventory with a spatial resolution of 4 km and a temporal resolution of 1 h. Individual emissions records included a source classification category (SCC) number that could be used to assign detailed chemical speciation profiles to TOG and TSP emissions.

TOG and TSP profiles used in this study were based on previous emissions source tests [31-41, 45-47].

Models for the emission of airborne particulate matter from mobile sources are relatively new and often contain large sources of uncertainty. In the current study, the spatial and temporal distribution of TSP emissions for each mobile source category (diesel, non-catalystequipped gasoline, catalyst-equipped gasoline) was retained, but the emissions were scaled to match the product of vehicle miles traveled (VMT) and measured emissions factors [33, 36] appropriate for that category. This procedure increased the TSP emission rate from mobile sources (tailpipe+tire dust) in the study region from 5030 to 8460 kg day^{-1}.

Previous Analysis

The direct effect of temperature on ozone and particulate matter concentrations for the episode that occurred in the SoCAB on September 23-25, 1996 was examined previously by Aw and Kleeman [13]. The results of this analysis show that increased temperatures promote the formation of ozone and suppress the partitioning of semi-volatile species into the particle phase. Decreased relative humidity lowered both the ozone concentration and the concentration of semi-volatile particulate matter. Pollutant concentrations were not strongly sensitive to small variations in atmospheric mixing depths, likely because mixing depths were relatively large (100m – 1000m) during this study period. The results presented below repeat this analysis using the updated model described in Section 2.

Results

Measured ozone concentrations on January 6, 1996 were less than 40 ppb, reflecting the low photochemical activity during winter pollution events in the SJV. Particulate nitrate concentrations over the entire region built up to high levels during the stagnation event. Local emissions of carbonaceous aerosol also develop around urban areas where fuel combustion is used for home heating. Measured PM10 concentrations during the episode reached 150 $\mu g\ m^{-3}$ during the evening hours, with the majority of that material in the $PM_{2.5}$ size range.

Figure 6-1(a) shows the regional distribution of 1hr-average ozone concentrations in the SJV at 1500 PST on January 6, 1996. Peak ozone concentrations are 41 ppb across a wide portion of the study domain except in regions with large NO_X emissions where the ozone concentrations is titrate to very low values. The ozone suppression associated with the Highway 99 transportation corridor connecting Fresno, Visalia, and Bakersfield is clearly visible in this plot.

Figure 6-1(b) shows the regional distribution of 24-hr average $PM_{2.5}$ concentrations in the SJV on January 6, 1996. Peak $PM_{2.5}$ values reach 95 $\mu g\ m^{-3}$ around the urban locations of Fresno and Bakersfield due to the accumulation of wood smoke and other combustion particles combined with a regional background of ammonium nitrate particles.

Figure 6-1(c) shows the predicted increase in regional ozone concentrations at 1500 PST

on January 6, 1996 in the SJV when temperature is uniformly perturbed by +2 K at all times and locations. Ozone concentrations in the eastern portion of the air basin increase by only 4 ppb in response to this change, with smaller increases of ~2 ppb over the majority of the domain.

Figure 6-1(d) shows the predicted decrease in regional $PM_{2.5}$ concentrations on January 6, 1996 in the SJV when temperature is uniformly perturbed by +2 K at all times and locations. $PM_{2.5}$ concentrations in the band between Fresno and Visalia decrease by ~7 $\mu g\ m^{-3}$ in response to the increased temperature as ammonium nitrate partitions back to gas-phase ammonia and nitric acid.

Figure 6-1(e) shows the predicted increase in regional ozone concentrations at 1500 PST on January 6, 1996 in the SJV when temperature is uniformly increased by +5 K at all times and locations. Ozone concentrations in most locations increase by 7-8 ppb in response to this temperature increase except in the vicinity of Bakersfield where no change is observed. Fresh emissions of NO_X in the Bakersfield area titrate all ozone in this region to near zero. Previous studies have noted that the excess NO_X in the emissions inventory around Bakersfield appears to contradict measured concentrations in the region. Results in the area around Bakersfield are likely incorrect, but results for the remainder of the domain agree well with measurements and should be accurate.

Figure 6-1(f) shows the predicted decrease in regional $PM_{2.5}$ concentrations on January 6, 1996 in the SJV when temperature is uniformly perturbed by +5 K at all times and locations. $PM_{2.5}$ concentrations in the band between Fresno and Visalia decrease by ~15 $\mu g\ m^{-3}$ in response to the increased temperature as ammonium nitrate partitions back to gas-phase ammonia and nitric acid. The region immediately south of Visalia does not experience a large decrease in $PM_{2.5}$ concentrations because ammonia emissions in this region are very large, reducing the sensitivy of ammonium nitrate to temperature.

Figure 6-2(b) shows the change in predicted regional ozone concentrations at 1500 PST on January 6, 1996 when temperature is uniformly perturbed by +2 K while relative humidity is held constant. This figure can be compared to Figure 6-1(b) which applied a +2 K temperature perturbation while absolute humidity was held constant. The maximum increase in ozone concentrations in response to a +2 K temperature perturbaiton is +4 ppb in both cases, but the pattern of the increased concentrations changes slightly, with more production in the center of the SJV at higher humidity vs. around the edges of the SJV at lower relative humidity.

Figure 6-2(c) shows the change in predicted regional $PM_{2.5}$ concentrations on January 6, 1996 when temperature is uniformly perturbed by +2 K while relative humidity is held constant. This Figure can be compared to Figure 6-1(c) which applied a +2 K temperature perturbation while absolute humidity was held constant. The increased humidity offsets the tendancy of ammonium nitrate to partition to the gas phase. In the region immediately south of Visalia, a 3.7 $\mu g\ m^{-3}$ increase in $PM_{2.5}$ concentrations is predicted to occur when temperature increases by 2K. This region has large emissions of ammonia, which offsets the effect of increased temperature on ammonium nitrate

volatility. The base temperature is also low in the winter conditions during the current study, further reducing the sensitivity of ammonium nitrate to temperature increases. The increase of temperature in this region increases the formation rate of nitric acid faster than it increases the volatility of ammonium nitrate aerosol, leading to slightly higher predicted $PM_{2.5}$ concentrations. It should be noted that the location of the maximum increase is slightly south of the maximum base-case concentrations. The net effect of this temperature increase is to expand the region of maximum $PM_{2.5}$ concentrations during the current study. Other locations in the study region with lower amounts of excess gas-phase ammonia experience a decrease in $PM_{2.5}$ concentrations of 4.6 $\mu g\ m^{-3}$ in response to a +2 K temperature perturbation even when relative humidity remains constant.

Figure 6-2(d) shows the change in predicted regional ozone concentrations at 1500 PST on January 6, 1996 when temperature is uniformly perturbed by +5 K while relative humidity is held constant. This figure can be compared to Figure 6-1(d) which applied a +5 K temperature perturbation while absolute humidity was held constant. The maximum increase in ozone concentrations in response to this change in temperature is 11 ppb at higher relative humidity (vs. 8 ppb increase for the lower humdity case).

Figure 6-2(e) shows the change in predicted regional $PM_{2.5}$ concentrations on January 6, 1996 when temperature is uniformly perturbed by +5 K while relative humidity is held constant. This Figure can be compared to Figure 6-1(e) which applied a +5 K temperature perturbation while absolute humidity was held constant. The trends illustrate in Figure 6-2(e) match those noted previously for Figure 6-2(c), with a maximum increase in $PM_{2.5}$ concentrations of 8 $\mu g\ m^{-3}$ in the area south of Visalia, and a maximum decrease of 4.6 $\mu g\ m^{-3}$ around the edges of the model domain where gas-phase ammonia concentrations are predicted to be lower.

Figure 6-3(c) shows the change in predicted regional ozone concentrations at 1500 PST on January 6, 1996 in response to a uniform increase in mixing depths of +50%. Ozone concentrations increase at all locations in the modeling domain in response to this change except for a few boundary cells at the extreme southern end. The maximum increase is 9 ppb along the transportation corridor connecting Fresno and Visalia, and in other regions of the domain where fresh NO_X emissions titrated ozone concentrations. The increased mixing depth reduces NO_X concentrations close to the ground, leading to higher surface ozone concentrations.

Figure 6-3(d) shows the change in predicted regional $PM_{2.5}$ concentrations on January 6, 1996 in response to a uniform increase in mixing depths of +50%. Predicted $PM_{2.5}$ concentrations immediately north of Bakersfield increase by +4.6 $\mu g\ m^{-3}$ in response to the increased mixing depth because the dilluted NO_X concentrations form more nitric acid which interacts with the ammonia plume just north of that location. As noted previously, the high NO_X emissions in the Bakersfield region are an artifact of the emissions inventory used in the current study, and so this increase in concentrations is likely also an artifact. $PM_{2.5}$ concentrations at locations farther north in the domain are predicted to undergo slight decreases or increases associated with the enhanced mixing of pollutants aloft to the surface.

The results of ozone and $PM_{2.5}$ predictions associated with an increase in wind speed are not available at the present time. These data will be added at a later date.

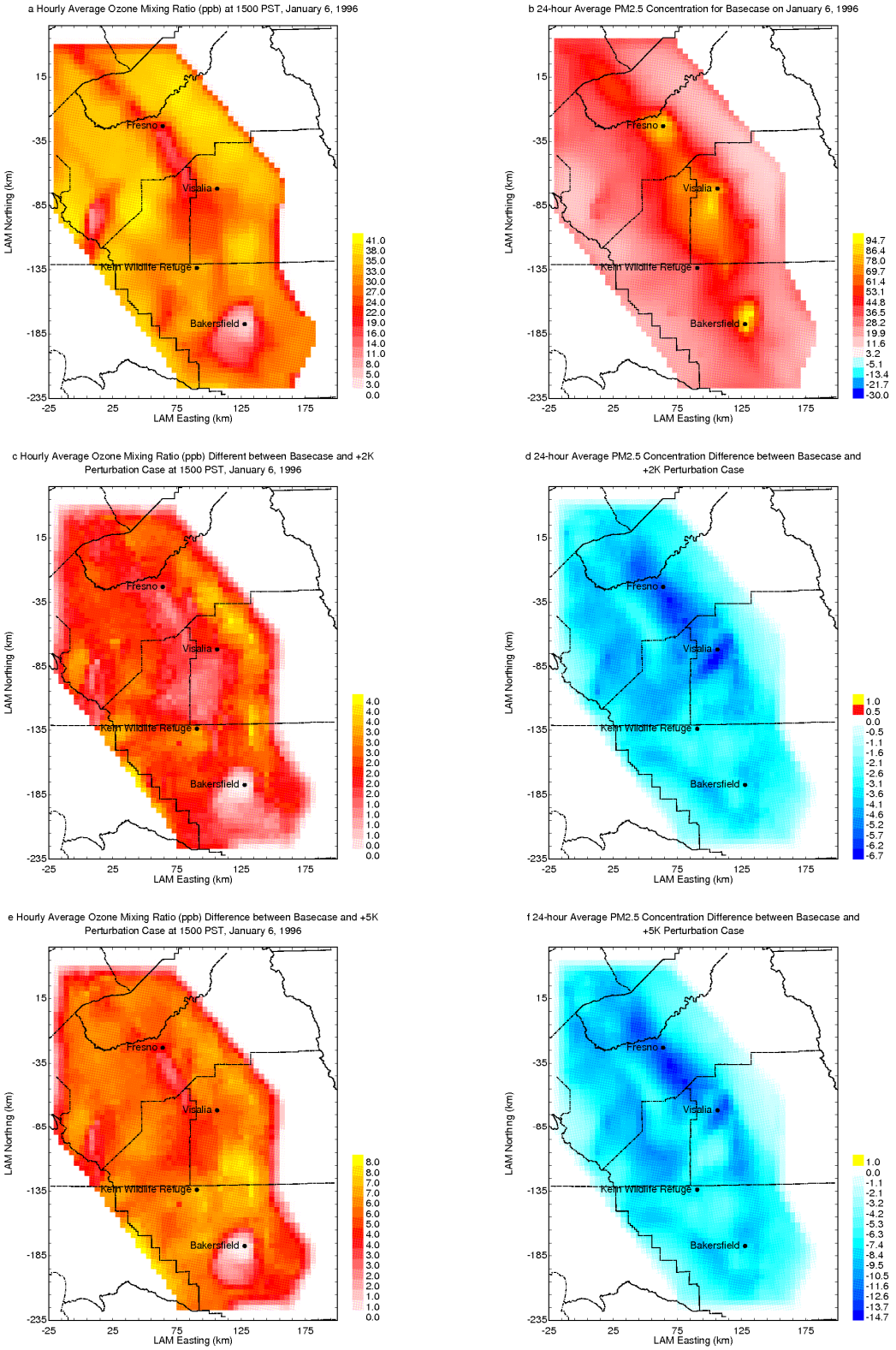

Figure 6-1: Pollutant concentrations in the San Joaquin Valley on January 6, 1996. (a) Hourly-average ozone mixing ratio (ppb) and (b) 24-hr average $PM_{2.5}$ concentration (μg m^{-3}). Panels (c-f) show the change in pollutant concentrations caused by a +2 K and +5 K temperature perturbation.

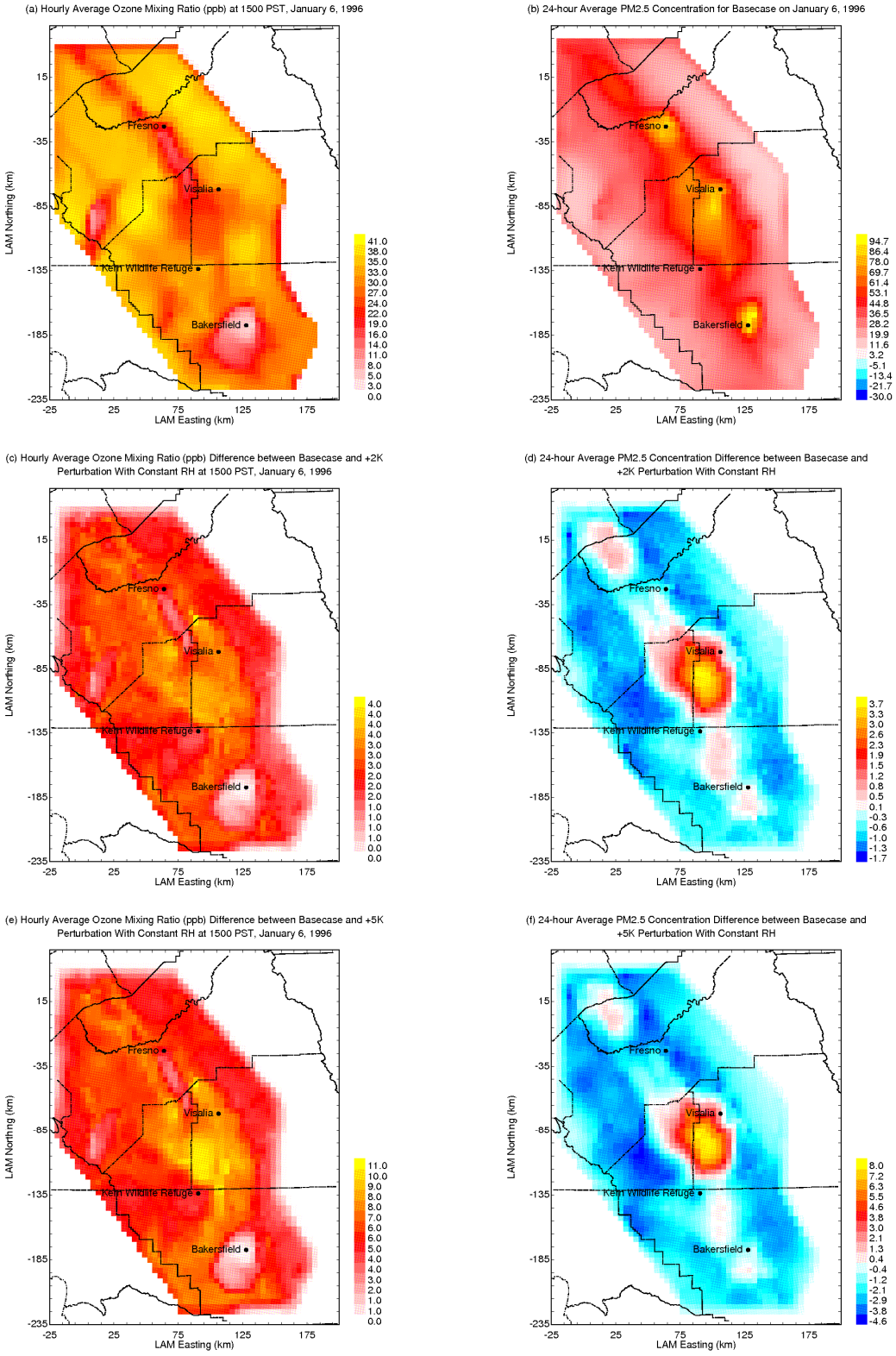

Figure 6-2: Pollutant concentrations in the San Joaquin Valley on January 6, 1996. (a) Hourly-average ozone mixing ratio (ppb) and (b) 24-hr average $PM_{2.5}$ concentration (μg m^{-3}). Panels (c-f) show the change in pollutant concentrations caused by a +2 K and +5 K temperature perturbation with constant relative humidity.

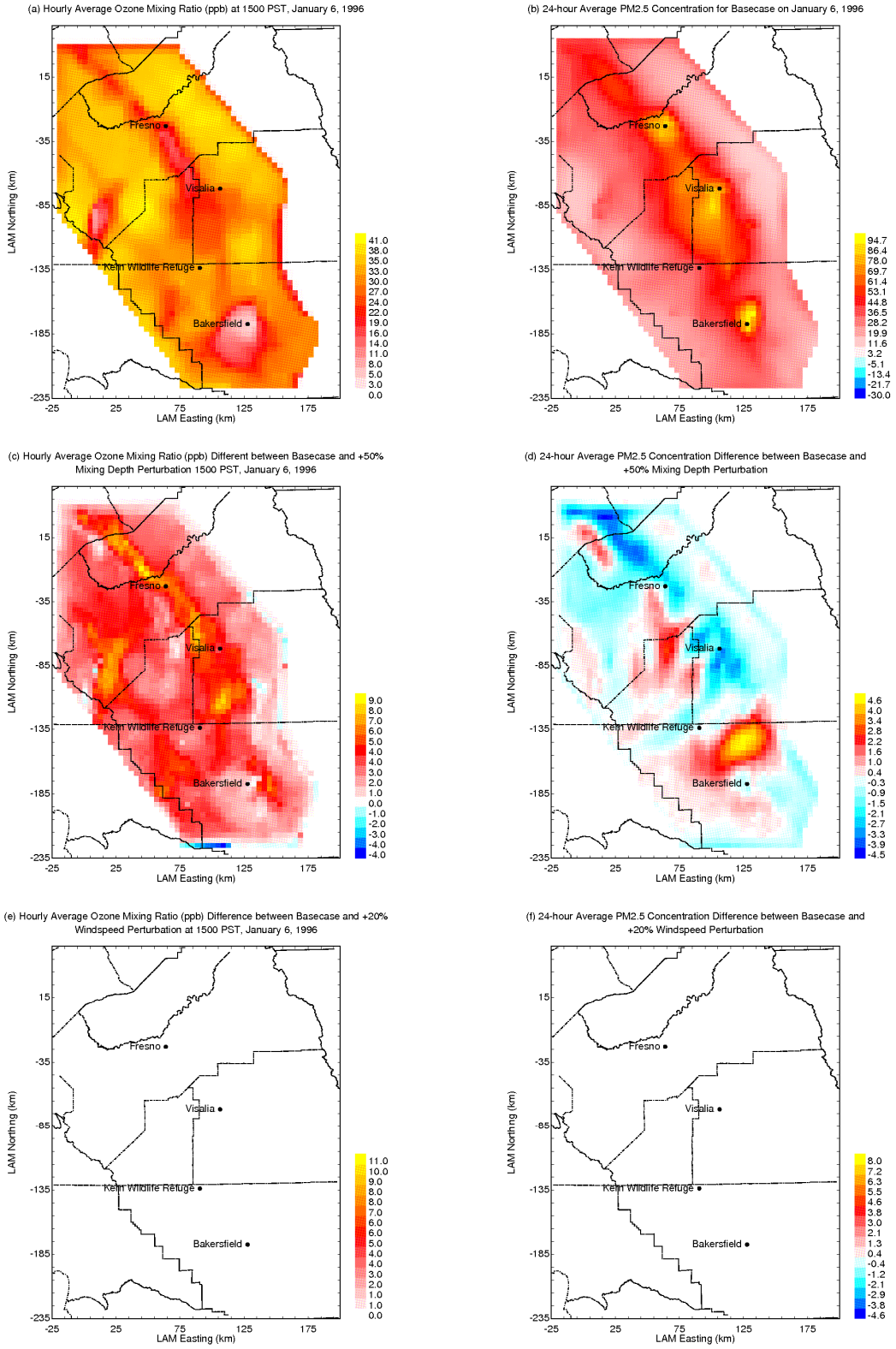

Figure 6-3: Pollutant concentrations in the San Joaquin Valley on January 6, 1996. (a) Hourly-average ozone mixing ratio (ppb) and (b) 24-hr average $PM_{2.5}$ concentration (µg m^{-3}). Panels (c-d) show the change in pollutant concentrations caused by a +50% increase in mixing depth.

7. Frequency of Future Stagnation Events

A large body of previous work, and the sensitivity studies above, indicate that frequency of atmospheric stagnation events and possibly the occurrence of warm synoptic events plays a significant role in determining the number of days with unhealthy air quality each year in California. Each of the pollution episodes studied in the preceding Sections 3-5 was driven by an atmospheric stagnation event. High pressure systems situated just off the coast of California produced warm temperatures aloft that encouraged elevated temperature inversions and weak winds. Climate change will affect the frequency and severity of atmospheric stagnation events in California. A method is needed to asses how this will influence air quality problems.

One method to quantitatively investigate the effect climate on the frequency of atmospheric stagnation events in California is to develop a simple linear statistical downscaling technique that relates large-scale meteorological information to air quality in the SJV and SoCAB. As part of the current project, linear regressions were calculated between meteorological information from the NCEP/NCAR Reanalysis Model output and ozone concentrations at Visalia (SJV) and Riverside (SoCAB) over the historical period 1980-2005. The NCEP/NCAR output has the same approximate spatial scale as GCM predictions (~200km horizontal). Linear regressions relating pollutant concentrations and large-scale atmospheric measures in the NCEP/NCAR output provide a statistical method to investigate the tendancy of future meteorology to encourage or discourage future air pollution events.

Correlations were investigated between daily maximum 1-hr average ozone concentrations and the following meteorological variables: temperature at 850 millibars (T850), temperature at 925 millibars (T925), temperature at 1000 millibars (T1000), wind speed at 850 millibars (wsp850), wind speed at 925 millibars (wsp925), and wind speed at 1000 millibars (wsp1000). Lagged versions of each variable were also considered in the multivariate statistical analysis. The most significant variable associated with daily maximum 1-hr average ozone concentrations measured at locations in both the SJV and the SoCAB was found to be temperature at 850 millibars (T850) on the same day.

The slope of the linear regression relating ozone and T850 changes as a function of the time period that was considered. Years prior to 1992 have a somewhat steeper regressions coefficient (slope) between ozone and T850 than years after 1996 for locations in both the SJV and SoCAB. This change in behavior likely results from the introduction of reformulated gasoline in California in the early-mid 1990's. The slope of the linear correlation curve relating ozone and T850 also changes as a function of month. August has the steepest linear relationship between ozone and T850, that is, ozone concentration changes in August are most responsive to changes in lower tropospheric temperature. Lesser slopes are observed for May – July, and September. This behavior is likely related to changes in biogenic emissions, absolute temperature, and possibly the length of day, but these hypotheses warrant future investigation to determine what mechanisms lie behind these statistical linkages.

Global Climate Models are best suited to characterize large scale patterns and, hopefully, long-term trends, and less so for shorter term variability on fine (hourly) time scales. The statistical correlations identified in the daily maxium 1-hr average ozone concentrations should not be used with GCM output to predict future daily maximum 1-hr average ozone concentrations, but the GCM output does not generally provide information at time intervals shorter than one day and their spatial resolution is coarse, of order 200-250km, so it may be more appropriate if longer averaging times are used. One method that appears to yield useful insight is to apply longer averaging times is to consider the relationship between monthly average T850 in the SJV and SoCAB vs. the number of days per month that exceeded the threshold of 90 ppb.

It is important to determine if the time averaging methodology can be shown to operate in the historical record. Figure 7-1 shows the number of days each month with 1-hr average ozone greater than 90 ppb vs. monthly average T850 at Riverside (SoCAB) and Visalia (SJV) for May – October during the years 1996-2003. Both locations exhibit a correlation slope between 0.7 – 0.75 and a correlation coefficient (R^2) of approximately 0.55. The correlations illustrated in Figure 7-1 can also be observed in the data prior to 1992, but the regression coefficients (slopes) are different as discussed above. The relationships illustrated in Figure 7-1 will be used to predict the degree to which future climate will encourage the formation of higher ozone concentrations.

Figure 7-2 shows the predicted number of days each year that would have 1-hr average ozone concentrations greater than 90 ppb at Riverside if the emissions and upwind boundary conditions for the SoCAB remained unchanged between the years 2000 – 2100. The exceedence days shown in Figure 7-2 are not intended to predict actual conditions in the future, since the climate model temperature are only a small subset of possible future climate in the California regiona, and future emissions and upwind boundary conditions will change in response to population growth, control programs, and new technology. Rather, the trends illustrated in Figure 7-2 illustrate the degree to which future meteorology will encourage a greater frequency of high ozone events relative to present day conditions. Figure 7-2 was construced using GCM predictions from the GFDL model for monthly average T850 over the indicated time period, combined with the correlations illustrated in Figure 7-1. The GFDL simulations were performed using both the SREAS A2 and B1 scenarios, representing medium-high and low, respectively, greenhouse gas (GHG) emissions scenario, prescribed by the IPCC; see http://www.grida.no/climate/ipcc_tar/wg1/474.htm. All of the trends illustrated in Figure 7-2 are positive, indicating that climate warming will tend to produce an increased frequency of high ozone days in the SoCAB in the future. The A2 emissions scenario (higher GHG emissions case) has a greater upward trend after the year 2050 than the B1 emissions scenario (lower GHG emissions case).

Figure 7-3 shows the predicted number of days each year that would have 1-hr average ozone concentrations greater than 90 ppb at Visalia if the emissions and upwind boundary conditions for the SJV remained unchanged between the years 2000 – 2100. Once again, this figure is designed to show the tendancy for future meteorology to

encourage ozone formation relative to present conditions (not predict future ozone concentrations). The GFDL simulations combined with the statistical downscaling technique once again predict a greater tendancy for future meteorology to encourage an increased frequency of high ozone days, with more exceedences associated with the A2 emissions scenario.

The results shown in Figures 7-2 and 7-3 were constructed using predictions from the GFDL Global Climate Model. A variety of other climate models could also be used for this analysis, but most current models predict some warming of the toposphere in the coming century. It is important to know that the GFDL model is among the class of models that is more resonsive to changes in GHG forceing—it produces a higher degree of warming, though not the highest, than other models to a prescribed change in atmospheric CO2 concentrations. Thus, the broad trends illustrated in Figure 7-2 and 7-3 are likely similar to those that would be predicted by any GCM, although the rate of change associated with each model and each GHG emissions scenario may differ slightly.

Downscaling techniques such as those illustrated in figure 7-1 to 7-3 were also investigated for airborne particulate matter, but no robust association could be found. Work is continuing to develop a statistical downscaling technique for $PM_{2.5}$. One possible outcome of this analysis is that increased temperatures could lower $PM_{2.5}$ concentrations during the early fall period that has historically experienced the highest $PM_{2.5}$ concentrations in the SoCAB, but $PM_{2.5}$ concentrations later in the year could increase as temperatures rise during the winter months. However, the sense of these changes are still not very clear, because it is necessary to determine whether vertical temperature gradients, including inversions will increase or decrease and how wind speeds and directions will be affected as California's regional climate changes. Dynamically downscaled regional atmospheric simulations may be necessary to augment and clarify the larger scale indications from the GCMs. Thus, climate change may not lower the peak $PM_{2.5}$ concentration experienced during the year, and climate change may alter the length of the $PM_{2.5}$ season in unforseen ways. These questions will be investigated in the second phase of the project.

One obvious correlation between future meteorology and $PM_{2.5}$ concentrations that can be investigated at the current time is the effect of rainfall. Rain events remove particles from the atmosphere with great efficiency. More frequent precipitation events will reduce airborne particulate matter concentrations, while less frequent precipitation events will allow for the possibility that airborne particulate matter concentrations will increase.

Figure 7-4 shows the number of predicted fall days each year with precipitation greater than 0.02mm in the SoCAB over the time period 2000 – 2100. Fall days (in the months of September – November) were chosen because these months historically have the highest $PM_{2.5}$ concentrations in the SoCAB. Predictions of precipitation were taken from GFDL simulations. No clear trends are apparent in the precipitation frequency for either the A2 or B1 GHG emissions scenario.

Figure 7-5 shows the number of predicted winter days each year with precipitation

greater than 0.02mm in the SJV over the time period 2000 – 2100. Winter days (in the months of December – February) were chose because these months historically have the highest $PM_{2.5}$ concentrations in the SJV. Again, no clear trend is obvious in Figure 7-5.

The lack of a clear precipitation trend is consistent with the observation that GCM's do not predict consistent trends for the frequency of future precipitation. There is likely a large amount of uncertainty associated with the results shown in Figures 7-4 and 7-5. As a result, no conclusions about the effect of precipitation on $PM_{2.5}$ concentrations can be made at this time.

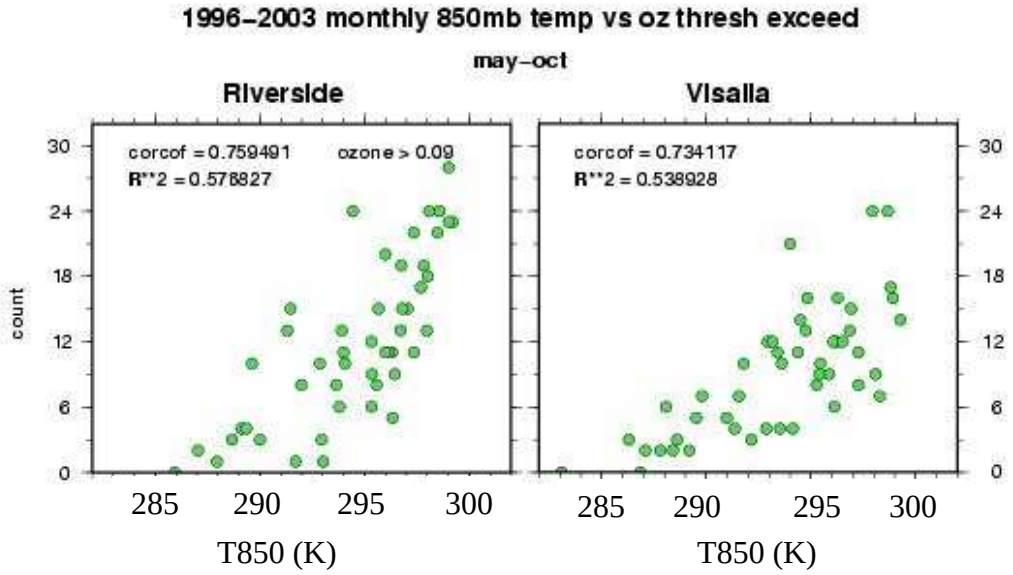

Figure 7-1: Number of days each month with 1-hr average ozone greater than 90ppb vs. monthly average T850 at Riverside (SoCAB) and Visalia (SJV) for May – October during the years 1996-2003.

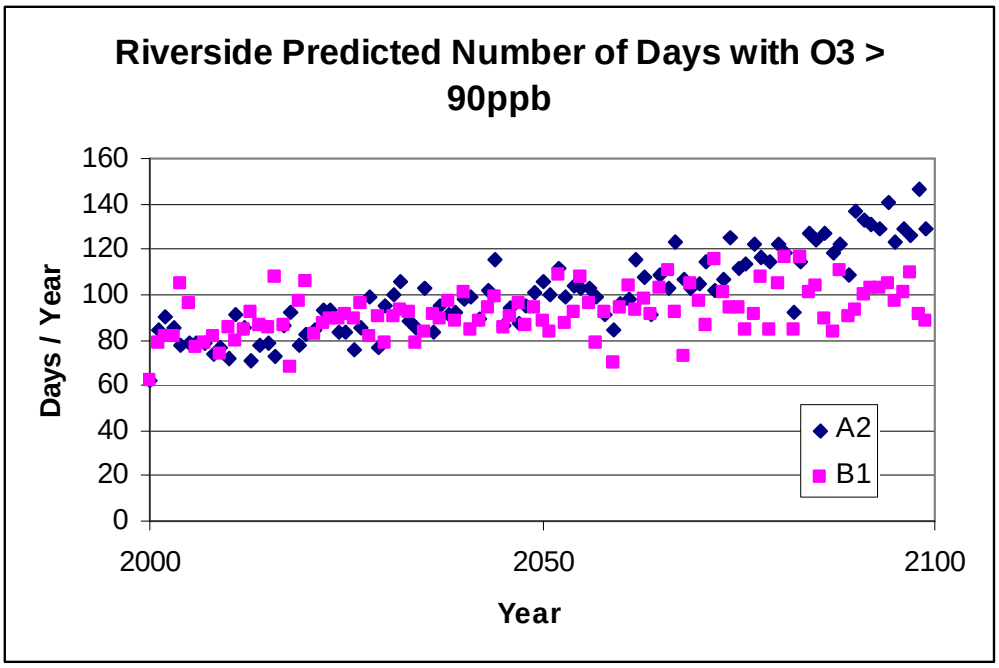

Figure 7-2: GFDL predictions for monthly mean 850 millibar temperatures in the SoCAB converted to estimates of the number of days each year with ozone greater than 90 ppb at Riverside. The results assume that emissions in the SoCAB remain constant while global emissions follow IPCC projections. Global emissions scenario A2 has higher global CO2 emissions than scenario B1.

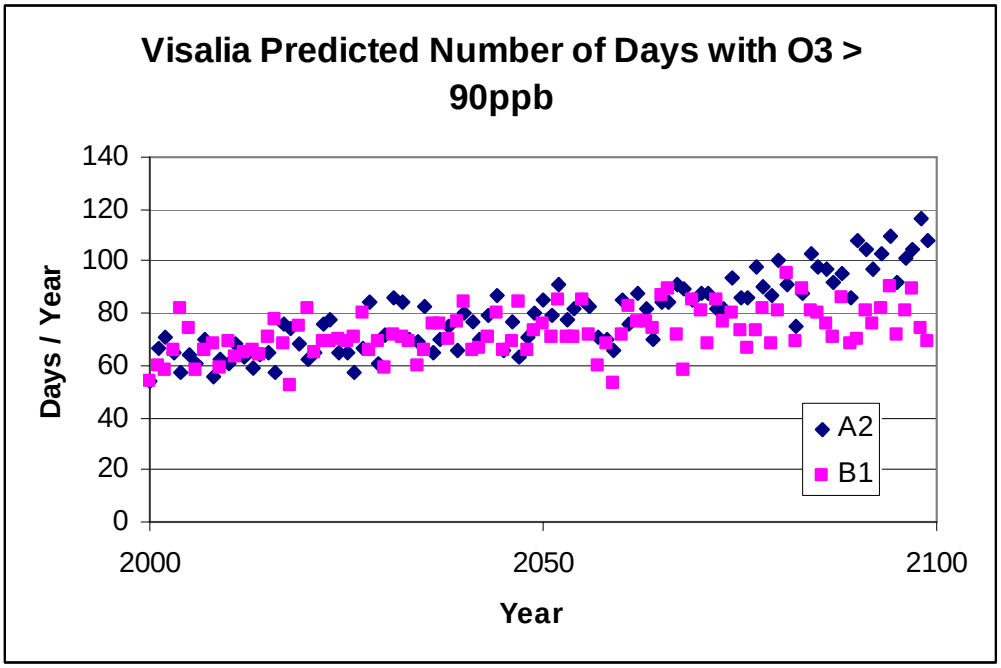

Figure 7-3: GFDL predictions for monthly mean 850 millibar temperatures in the SJV converted to estimates of the number of days each year with ozone greater than 90 ppb at Visalia. The results assume that emissions in the SJV remain constant while global emissions follow IPCC projections. Global emissions scenario A2 has higher global CO2 emissions than scenario B1.

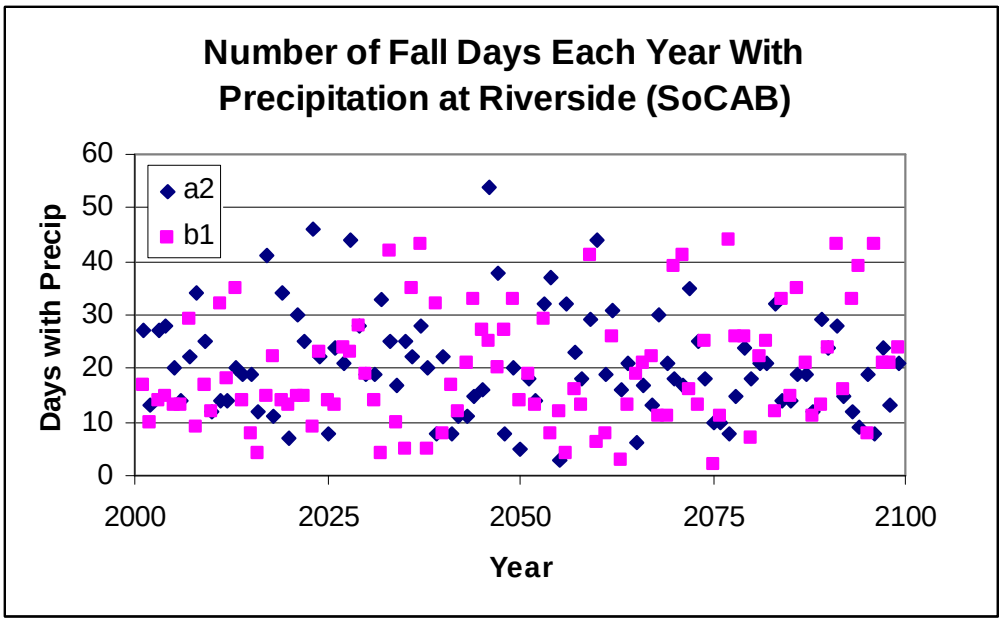

Figure 7-4: GFDL predictions for the number of fall days each year with precipitation > 0.02mm in the SoCAB at Riverside. Fall corresponds to the historical period with the highest $PM_{2.5}$ concentrations in the SoCAB. Increased precipitation greatly reduces airborne particulate matter concentrations.

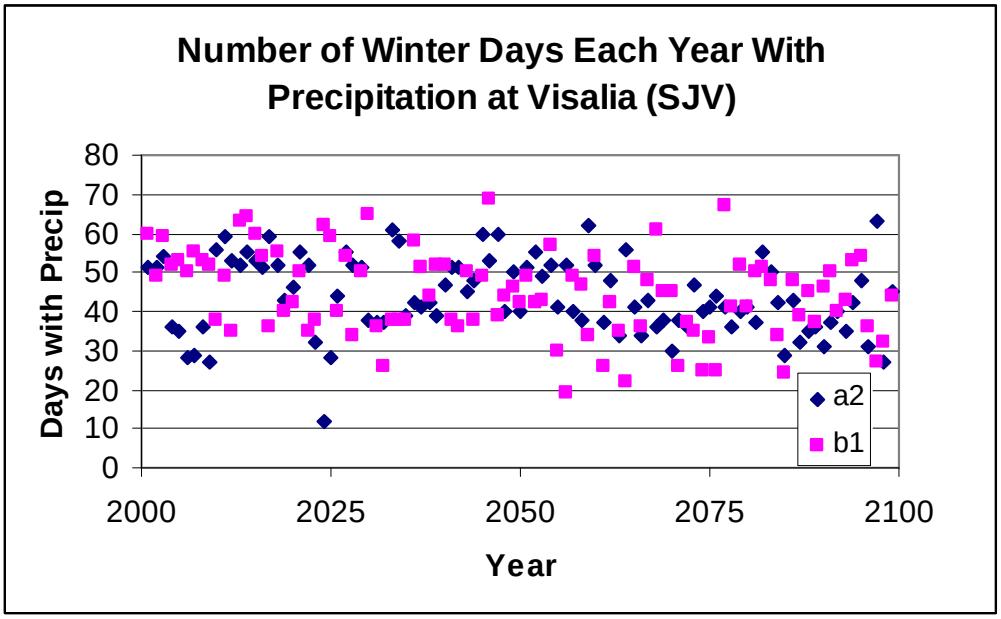

Figure 7-5: GFDL predictions for the number of winter days each year with precipitation > 0.02mm in the SJV at Visalia. Winter corresponds to the historical period with the highest $PM_{2.5}$ concentrations in the SJV. Increased precipitation greatly reduces airborne particulate matter concentrations.

8. Conclusions

Figure 8-1 summarizes the range of changes in predicted ozone and $PM_{2.5}$ concentrations resulting from all the perturbations studied in the current project. The bars shown in Figure 8-1 illustrate the largest change in pollutant concentrations predicted anywhere in the domain, while the circles illustrate the change in the maximum concentrations. When the circles are located close to the extreme values of the bars, it shows that the greatest change in concentration occurs at the location of maximum concentration.

Figure 8-1 illustrates that increasing wind speed results in the greatest decrease in ozone and $PM_{2.5}$ concentrations in the SoCAB during both the September 7-9, 1993 episode and the September 23-25, 1996 episode. These reductions occur at the location of maximum base-case concentrations except for the case of ozone in the SoCAB on September 25, 1996 when maximum ozone concentrations are not significantly affected by wind speed.

Figure 8-1 also shows that increasing temperature at constant absolute humidity generally increases peak ozone concentrations and decreases peak $PM_{2.5}$ concentrations in all the episodes studied. Part of this temperature effect on $PM_{2.5}$ concentrations may be caused by reduced particle water content, since relative humidity decreases as temperature increases and absolute humidity remains constant.

Increasing temperature at constant relative humidity increases predicted ozone concentrations even further due to the enhanced production of hydroxyl radical. The increased absolute humidity also mitigates the reduction in $PM_{2.5}$ concentrations, and even increases $PM_{2.5}$ concentrations in the SJV in regions with large excesses of gas-phase ammonia.

Figure 8-1 generally shows that increasing mixing depths usually increases surface ozone concentrations because the extra volume allows for increased dilution of fresh NO_X emissions, reducing the titration of surface ozone concentrations. This effect may not be significant at the location of maximum ozone concentration. The increased mixing depth usually also reduces primary $PM_{2.5}$ concentrations through increased dillution. This trend generally holds true in the SoCAB, but isolated regions in the SJV may experience slight increases in $PM_{2.5}$ concentrations in response to increased mixing depth.

The trends illustrated in Figure 8-1 provide a mechanistic understanding of the likely impacts of climate change on air quality in California and suggest some preliminary conclusions. Temperatures will almost certainly rise in future air pollution episodes, leading to increased ozone concentrations. Particulate nitrate concentrations are likely to decrease slightly in the SoCAB as temperatures rise, but they may stay constant or even increase slightly in the SJV depending on the corresponding change to humidity. A regional meteorological model will be used to dynamically downscale representative stagnation episodes in the future during the second phase of this project to support a more detailed analysis of how future meteorology will change pollutant concentrations.

GCM predictions from the GFDL model suggest that climate change will increase the frequency of warm synoptic events that encourage ozone formaton in both the SJV and the SoCAB. Global emissions scenarios that have higher carbon emissions appear to encourage this trend. Future emissions reduction and the adoption of new technology will need to offset this tendancy for the formation of ozone pollution episodes in order to protect the public health of California residents.

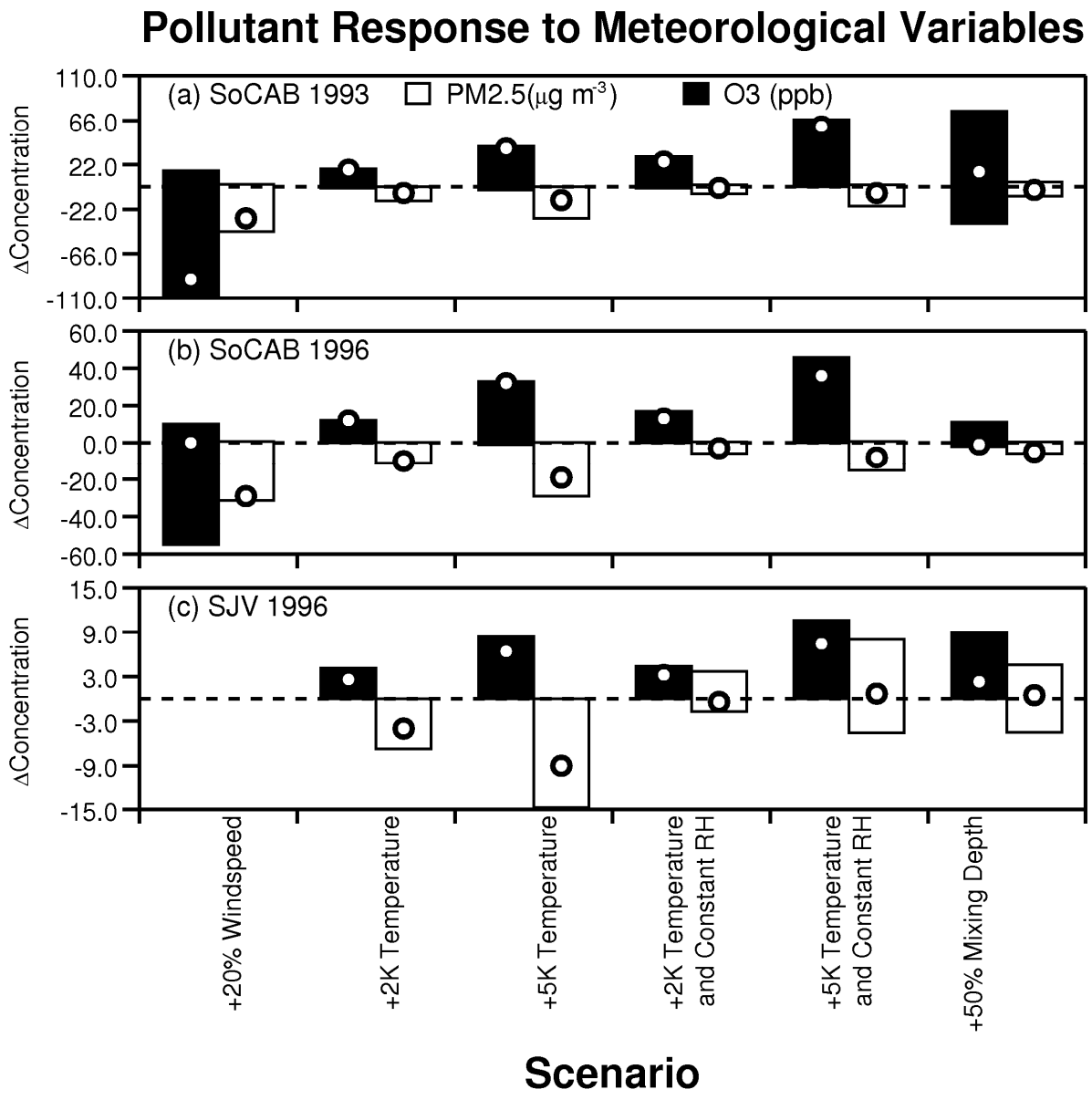

Figure 8-1: Summary of pollutant response to meteorological perturbations during pollution episodes that occurred in (a) Southern California September 9, 1993, (b) Southern California September 25, 1996, and (c) the San Joaquin Valley January 6, 1996. The bars represent the range of concentration change at any location in the modeling domain in response to the indicated perturbation. The circles represent the concentration change at the location of the maximum concentration for each pollutant.

9. References

1. Fraser, M.P., M.J. Kleeman, J.J. Schauer, and G.R. Cass, *Modeling the atmospheric concentrations of individual gas-phase and particle-phase organic compounds.* Environmental Science & Technology, 2000. **V34 N7**(APR 1): p. 1302-1312.
2. Griffin, R.J., D. Dabdub, M.J. Kleeman, M.P. Fraser, G.R. Cass, and J.H. Seinfeld, *Secondary organic aerosol - 3. Urban/regional scale model of size- and composition-resolved aerosols.* Journal of Geophysical Research-Atmospheres, 2002. **107**(D17): p. art. no.-4334.
3. Kleeman, M.J., L.S. Hughes, J.O. Allen, and G.R. Cass, *Source contributions to the size and composition distribution of atmospheric particles: Southern California in September 1996.* Environmental Science & Technology, 1999. **33**(23): p. 4331-4341.
4. Kleeman, M.J. and G.R. Cass, *A 3D Eulerian source-oriented model for an externally mixed aerosol.* Environmental Science & Technology, 2001. **35**(24): p. 4834-4848.
5. Mysliwiec, M.J. and M.J. Kleeman, *Source apportionment of secondary airborne particulate matter in a polluted atmospbere.* Environmental Science & Technology, 2002. **36**(24): p. 5376-5384.
6. Held, T., Q. Ying, A. Kaduwela, and M. Kleeman, *Modeling particulate matter in the San Joaquin Valley with a source-oriented externally mixed three-dimensional photochemical grid model.* Atmospheric Environment Part a-General Topics, 2004. **38**(22): p. 3689-3711.
7. Hayhoe, K., D. Cayan, C.B. Field, P.C. Frumhoff, E.P. Maurer, N.L. Miller, S.C. Moser, S.H. Schneider, K.N. Cahill, E.E. Cleland, L. Dale, R. Drapek, R.M. Hanemann, L.S. Kalkstein, J. Lenihan, C.K. Lunch, R.P. Neilson, S.C. Sheridan, and J.H. Verville, *Emissions pathways, climate change, and impacts on California.* PROCEEDINGS OF THE NATIONAL ACADEMY OF SCIENCES OF THE UNITED STATES OF AMERICA, 2004. **101**(34): p. 12422-12427.
8. Kim, J., *A projection of the effects of the climate change induced by increased CO2 on extreme hydrologic events in the western U.S.* Climate Change, 2005. **68**: p. 153-168.
9. Kim, J., *A nested modeling study of elevation-dependent climate change signals in California induced by increased atmospheric CO2.* Geophysical Research Letters, 2001. **28**: p. 2951-2954.
10. Mickley, L.J., D.J. Jacob, B.D. Field, and D. Rind, *Effects of future climate change on regional air pollution episodes in the United States.* Geophysical Research Letters, 2004. **31**(24).
11. Hogrefe, C., B. Lynn, K. Civerolo, J.Y. Ku, J. Rosenthal, C. Rosenzweig, R. Goldberg, S. Gaffin, K. Knowlton, and P.L. Kinney, *Simulating changes in regional air pollution over the eastern United States due to changes in global and regional climate and emissions.* Journal of Geophysical Research, 2004. **109**(D22).
12. Langner, J. and R. Bergstrom, *Impact of climate change on surface ozone and deposition of sulphur and nitrogen in Europe.* Atmospheric Environment, 2005.

39: p. 1129-1141.
13. Aw, J. and M.J. Kleeman, *Evaluating the first-order effect of intraannual temperature variability on urban air pollution.* Journal of Geophysical Research-Atmospheres, 2003. **108**(D12).
14. Ying, Q. and M.J. Kleeman, *Source contributions to the regional distribution of secondary particulate matter in California.* Atmospheric Environment, 2005. **Accepted for publication**.
15. Carter, W.P.L., *A Detailed Mechanism for the Gas-Phase Atmospheric Reactions of Organic-Compounds.* Atmospheric Environment Part a-General Topics, 1990. **24**(3): p. 481-518.
16. Pandis, S.N., R.A. Harley, G.R. Cass, and J.H. Seinfeld, *Secondary Organic Aerosol Formation and Transport.* Atmospheric Environment Part a-General Topics, 1992. **26**(13): p. 2269-2282.
17. Odum, J.R., T. Hoffmann, F. Bowman, D. Collins, R.C. Flagan, and J.H. Seinfeld, *Gas/particle partitioning and secondary organic aerosol yields.* Environmental Science & Technology, 1996. **30**(8): p. 2580-2585.
18. Griffin, R.J., D. Dabdub, and J.H. Seinfeld, *Secondary organic aerosol - 1. Atmospheric chemical mechanism for production of molecular constituents.* Journal of Geophysical Research-Atmospheres, 2002. **107**(D17).
19. Griffin, R.J., D. Dabdub, and J.H. Seinfeld, *Development and initial evaluation of a dynamic species-resolved model for gas phase chemistry and size-resolved gas/particle partitioning associated with secondary organic aerosol formation.* Journal of Geophysical Research, 2005. **110**(D5).
20. Pun, B.K., R.J. Griffin, C. Seigneur, and J.H. Seinfeld, *Secondary organic aerosol - 2. Thermodynamic model for gas/particle partitioning of molecular constituents.* Journal of Geophysical Research-Atmospheres, 2002. **107**(D17).
21. Kusik, C.L. and H.P. Meissner, *Electrolyte activity coefficients in inorganic processing.* Fundamental Aspects of Hydrometallurgical Processes AIChE Symposium Series, 1978. **74**: p. 14-20.
22. Fredenslund, A., J. Gmehling, and P. Rasmussen, *Vapor-liquid equilibrium using UNIFAC*. 1977, New York: Elsevier.
23. Clegg, S.L., J.H. Seinfeld, and E.O. Edney, *Thermodynamic modelling of aqueous aerosols containing electrolytes and dissolved organic compounds. II. An extended Zdanovskii-Stokes-Robinson approach.* Journal of Aerosol Science, 2003. **34**(6): p. 667-690.
24. Clegg, S.L., J.H. Seinfeld, and P. Brimblecombe, *Thermodynamic modelling of aqueous aerosols containing electrolytes and dissolved organic compounds.* Journal of Aerosol Science, 2001. **32**(6): p. 713-738.
25. Czoschke, N.M., M. Jang, and R.M. Kamens, *Effect of acidic seed on biogenic secondary organic aerosol growth.* Atmospheric Environment, 2003. **37**(30): p. 4287-4299.
26. Jang, M.S., B. Carroll, B. Chandramouli, and R.M. Kamens, *Particle growth by acid-catalyzed heterogeneous reactions of organic carbonyls on preexisting aerosols.* Environmental Science & Technology, 2003. **37**(17): p. 3828-3837.
27. Kalberer, M., D. Paulsen, M. Sax, M. Steinbacher, J. Dommen, A.S.H. Prevot, R. Fisseha, E. Weingartner, V. Frankevich, R. Zenobi, and U. Baltensperger,

Identification of polymers as major components of atmospheric organic aerosols. Science, 2004. **303**(5664): p. 1659-1662.
28. Kleeman, M.J., G.R. Cass, and A. Eldering, *Modeling the airborne particle complex as a source-oriented external mixture.* Journal Of Geophysical Research-Atmospheres, 1997. **102**(SEP 20): p. 21355-21372.
29. Kleeman, M.J., *Changes in PM2.5 Due to Changes in Temperature*. 2004, Final Report for the U.S. Environmental Protection Agency Contract # R-82824201-01.
30. Goodin, W.R., G.J. McRae, and J.H. Seinfeld, *A comparison of Interpolation Methods for Sparse Data: Application to Wind and Concentration Fields.* Journal of Applied Meteorology, 1979. **18**: p. 761-771.
31. Cooper, J.A., D.C. Redline, L.N. Sherman, L.M. Valdovinos, L.C. Scavone, and C. Badgett-West, *Final appendix V-G, PM10 source composition library for the South Coast Air Basin, technical report*. 1989, South Coast Air Quality Management District: Diamond Bar, California.
32. Taback, H.J., A.R. Brienza, J. Macko, and N. Brunetz, *Fine particle emissions from stationary and miscellaneous sources in the South Coast Air Basin, technical report*. 1979, California Air Resources Board; KVB Incorporated; Research-Cottrell: Tustin, California.
33. Schauer, J.J., M.J. Kleeman, G.R. Cass, and B.R.T. Simoneit, *Measurement of emissions from air pollution sources. 5. C-1-C-32 organic compounds from gasoline-powered motor vehicles.* Environmental Science & Technology, 2002. **36**(MAR 15): p. 1169-1180.
34. Schauer, J.J., M.J. Kleeman, G.R. Cass, and B.R.T. Simoneit, *Measurement of emissions from air pollution sources. 4. C-1-C-27 organic compounds from cooking with seed oils.* Environmental Science & Technology, 2002. **36**(FEB 15): p. 567-575.
35. Schauer, J.J., M.J. Kleeman, G.R. Cass, and B.R.T. Simoneit, *Measurement of emissions from air pollution sources. 3. C-1-C-29 organic compounds from fireplace combustion of wood.* Environmental Science & Technology, 2001. **35**(MAY 1): p. 1716-1728.
36. Schauer, J.J., M.J. Kleeman, G.R. Cass, and B.R.T. Simoneit, *Measurement of emissions from air pollution sources. 2. C-1 through C-30 organic compounds from medium duty diesel trucks.* Environmental Science & Technology, 1999. **33**(MAY 15): p. 1578-1587.
37. Schauer, J.J., M.J. Kleeman, G.R. Cass, and B.R.T. Simoneit, *Measurement of emissions from air pollution sources. 1. C-1 through C-29 organic compounds from meat charbroiling.* Environmental Science & Technology, 1999. **33**(MAY 15): p. 1566-1577.
38. Hildemann, L.M., G.R. Markowski, M.C. Jones, and G.R. Cass, *Submicrometer Aerosol Mass Distributions of Emissions from Boilers, Fireplaces, Automobiles, Diesel Trucks, and Meat- Cooking Operations.* Aerosol Science and Technology, 1991. **14**(1): p. 138-152.
39. Kleeman, M.J., J.J. Schauer, and G.R. Cass, *Size and composition distribution of fine particulate matter emitted from wood burning, meat charbroiling, and cigarettes.* Environmental Science & Technology, 1999. **33**(20): p. 3516-3523.
40. Kleeman, M.J., J.J. Schauer, and G.R. Cass, *Size and composition distribution of*

fine particulate matter emitted from motor vehicles. Environmental Science & Technology, 2000. **34**(7): p. 1132-1142.
41. Harley, R.A., M.P. Hannigan, and G.R. Cass, *Respeciation of Organic Gas Emissions and the Detection of Excess Unburned Gasoline in the Atmosphere.* Environmental Science & Technology, 1992. **26**(12): p. 2395-2408.
42. Holtzworth, G.C., *Mixing depths, wind speeds, and air pollution potential for selected locations in the United States.* Journal of Applied Meteorology, 1967. **6**: p. 1029-1044.
43. Gharib, S. and G.R. Cass, *Ammonia emissions in the South Coast Air Basin.* 1984, California Institute of Technology, Environmental Quality Laboratory Open File Report 84-2: Pasadena, CA.
44. Matthijsen, J., H. Slaper, H. Reinen, and G.J.M. Velders, *Reduction of solar UV by clouds: A comparison between satellite-derived cloud effects and ground-based radiation measurements.* Journal of Geophysical Research-Atmospheres, 2000. **105**(D4): p. 5069-5080.
45. Harley, R.A., A.G. Russell, G.J. McRae, G.R. Cass, and J.H. Seinfeld, *Photochemical Modeling of the Southern California Air-Quality Study.* Environmental Science & Technology, 1993. **27**(2): p. 378-388.
46. Hildemann, L.M., G.R. Markowski, and G.R. Cass, *Chemical-Composition of Emissions from Urban Sources of Fine Organic Aerosol.* Environmental Science & Technology, 1991. **25**(4): p. 744-759.
47. Houck, J.E., J.C. Chow, J.G. Watson, C.A. Simons, L.C. Pritchett, J.M. Goulet, and C.A. Frazier, *Determination of particle size distribution and chemical composition of particulate matter from selected sources in California, technical report*. 1989, California Air Resources Board; OMNI Environ. Service Incorporate; Desert Research Institute: Beaverton, Oregon.